Supporting Information

Catalytic Ester Metathesis Reaction and its Application to Transfer Hydrogenation of Esters

*Abhishek Dubey and Eugene Khaskin**

Okinawa Institute of Science and Technology Graduate University, 1919-1 Tancha, Onna-son, Kunigami-gun, Okinawa, Japan 904-0495; eugene.khaskin@oist.jp

Index

Figure Index:

Figure S8. Kinetics with 1.5 mg of **3** and **19**. 3.85ppm ethyl acetate α CH_2 of ethanol; 4.1ppm ethyl benzoate α CH_2 of ethanol; 4.90ppm benzyl acetate α CH_2 of benzyl alcohol; 5.13ppm benzyl benzoate α CH_2 of benzyl alcohol.

Figure S9. Appearance of α CH_2 of ethyl acetate with 1.5 mg of **3**. 50 ^oC; measurements every 5 minutes. Integration data (green) fitted to a first order integral $kt=\ln(X_o/(X_o-X'))$. k=5.66E-2. X-axis each point =5minutes

Figure S10. Appearance of α CH_2 of ethyl acetate with 3.0 mg of **3**. 50 ^oC; measurements every 5 minutes. Integration data (green) fitted to a first order integral $kt=\ln(X_o/(X_o-X'))$. k=5.58E-2. X-axis each point =5minutes

Figure S11. Appearance of α CH_2 of ethyl benzoate with 3.0 mg of **3**. 50 ^oC; measurements every 5 minutes. No reasonable fit found. Induction period for the first half hour. X-axis each point =5minutes

Figure S12. Appearance of α CH_2 of benzyl benzoate and with 3.0 mg of **3**. 50 ^oC; measurements every 5 minutes. Integration data (green) fitted to a first order integral $kt=\ln(X_o/(X_o-X'))$. k=5.50E-2. X-axis each point =5minutes

Figure S13. Kinetics with 4.0 mg of **3** and **20**. 3.85ppm ethyl acetate α CH_2 of ethanol; 4.1ppm ethyl benzoate α CH_2 of ethanol; 4.90ppm benzyl acetate α CH_2 of benzyl alcohol; 5.13ppm benzyl benzoate α CH_2 of benzyl alcohol.

Figure S14. Appearance of α CH_2 of ethyl acetate with 4.0 mg of **3**. 50 ^oC; measurements every 5 minutes.

Figure S15. Appearance of α CH2 of ethyl benzoate with 3.0 mg of **3**. 50 ^oC; measurements every 5 minutes.

Figure S16. Appearance of α CH_2 of benzyl benzoate and with 3.0 mg of **3**. 50 ^oC; measurements every 5 minutes.

Figure S17. ^1H NMR of **3**, soon after mixing with KO^tBu in C_6D_6.

Figure S18. ^1H NMR of **3**, 3 h after mixing with KO^tBu in C_6D_6 and heating at 50^oC.

Figure S19. ^1H NMR of **3** with 0.5 equiv of benzyl acetate after 10 minutes of heating at 50 ^oC. 3.90ppm quartet ethyl acetate α CH_2 of ethanol; 4.1ppm quartet of ethyl benzoate α CH_2 of ethanol; 4.95ppm benzyl acetate α CH_2 of benzyl alcohol; 5.17ppm benzyl benzoate α CH_2 of benzyl alcohol.

Figure S20. ^1H NMR of **3** with 1 equiv of benzyl acetate after 10 minutes of heating at 50^oC. 3.90ppm quartet ethyl acetate α CH_2 of ethanol; 4.1ppm quartet of ethyl benzoate α CH_2 of ethanol; 4.95ppm benzyl acetate α CH_2 of benzyl alcohol; 5.17ppm benzyl benzoate α CH_2 of benzyl alcohol.

Figure S21. ^{1}HNMR of **3** with 1 equiv. of benzyl acetate after overnight at r.t. 3.90ppm quartet ethyl acetate α CH_2 of ethanol; 4.1ppm quartet of ethyl benzoate α CH_2 of ethanol; 4.95ppm benzyl acetate α CH_2 of benzyl alcohol; 5.17ppm benzyl benzoate α CH_2 of benzyl alcohol.

Figure S22. ^{1}HNMR solution from Figure S17 after adding 5 more equiv of benzyl acetate and leaving at r.t. for 3 hours. 3.90ppm quartet ethyl acetate α CH_2 of ethanol; 4.1ppm quartet of ethyl benzoate α CH_2 of ethanol; 4.95ppm benzyl acetate α CH_2 of benzyl alcohol; 5.17ppm benzyl benzoate α CH_2 of benzyl alcohol.

Figure S23. ^{1}HNMR of **3** with 6 equiv of **20**, 15 minutes after mixing at r.t. 3.90ppm quartet ethyl acetate α CH_2 of ethanol obscured by carbon satellite of **20**; 4.1ppm quartet of ethyl benzoate α CH_2 of ethanol

Figure S24. ^{1}HNMR of **3** with 6eq. of **20**, 4.5 hours after heating. 3.90ppm quartet ethyl acetate α CH_2 of ethanol; 4.1ppm quartet of ethyl benzoate α CH_2 of ethanol; 4.95ppm benzyl acetate α CH_2 of benzyl alcohol; 5.17ppm benzyl benzoate α CH_2 of benzyl alcohol.

Figure S25. Mechanistic Figure from the main text with deuteration experiment included

General Specifications

All catalytic experiments with metal complexes were carried out via a general procedure specified in the main manuscript. Identity and distribution of the products were established on a QP2010 Ultra Shimadzu GC/MS system equipped with a SH-Rxi-1ms 30meter column. Yields were determined by NMR for stoichiometric/low substrate J-Young tube experiments. In most cases, yields were calculated from GC/FID results using a GC2014 Shimadzu system equipped with a SH-Rxi-1ms 60meter column, with mesitylene internal standard added after reaction completion. Standards of alcohol and ester products were run against the internal standard to determine conversion ratios and an average value for the conversion factor was obtained after several runs. Inert atmosphere experiments were carried out under an atmosphere of purified nitrogen in an MBraun Unilab pro glovebox. Ester substrates were purchased from Aldrich, Alfa Aesar, TCI and Ark-pharma and were used as is without purification. Deuterated solvents used in the study: C_6D_6 from Euroiso-top was transferred to the glove box, dried overnight over CaH_2 and filtered through celite. Complexes **2**, **3**, and **4** were purchased from TCI (**2**) and Aldrich (**3**,**4**). Complex **3** was also synthesized according to published procedure.[1]
^1H, ^{31}P NMR spectra were recorded at 400, and 161 MHz respectively, using a Bruker Ascend(AvanceIII) 400MHz and JEOL ECZ series 400MHz spectometers. ^1H and ^{31}P NMR chemical shifts are reported in ppm downfield from tetramethylsilane and corrected against PPh_3 (-6ppm) external standard respectively.

Experimental Procedures

General Procedure for ester metathesis

The catalyst (1 mg, 0.0016 mmol) and KO^{t}Bu (0.9 mg, 0.008 mmol) were mixed together in a 11 mL screwcap vial in the glove box. 3 mL of toluene solvent was added and stirred for 5 min, after which the ester (equivalents given in Tables 1 and 2, but typically 500 equiv or 0.8 mmol) was added. The screw top vial was closed and the cap was wrapped with electric tape to prevent atmosphere exchange. The vial was taken out of the glove box and heated in an oil bath for 16 hours at 80 ^{o}C while the contents were being stirred. At the end of the reaction, 100 equiv of mesitylene internal standard were added based on the catalyst and the mixture was analyzed by GC/FID. Standards of pure symmetrical products were available in most cases and were earlier calibrated against the internal standard on the same GC/FID system and under the same run conditions/column. The symmetrical metathesis product had the same conversion factor as its starting material isomer. Information for standard conversion factors is given under each relevant GC trace (Figures S26-S59).

General Procedure for ester hydrogenation

The catalyst (1 mg, 0.0016 mmol) and KO^{t}Bu (0.9 mg, 0.008 mmol) were mixed together in a 11 mL screwcap vial in the glove box. 2 mL of toluene solvent was added and stirred for 5 min, after which the ester (amounts vary in Table 3 from 100 to 500 equiv, but typically 500 equiv or 0.16 mmol; 0.16 mmol for Table 4) and ethanol (20 equiv) was added before the vial was sealed. The screw top vial was closed and the cap was wrapped with electric tape to prevent atmosphere exchange. The vial was taken out of the glove box and heated in an oil bath for 16 hours at 80 ^{o}C while the contents were being stirred. At the end of the reaction, 100 equiv of mesitylene internal standard were added based on the catalyst and the mixture was analyzed by GC/FID. Standards of pure alcohol products were available and were earlier

calibrated against mesitylene on the same GC/FID system under the same run conditions/column.

Experimental

NMR experiment with ethyl hexanoate 10 and complex 2.

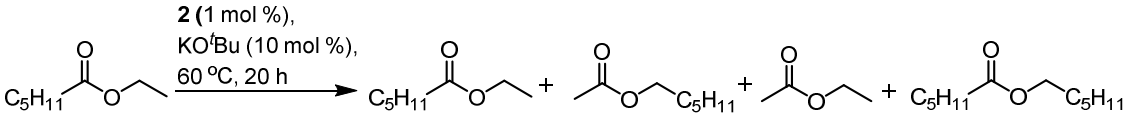

Base, catalyst and ester were mixed together in a J-Young NMR tube in C_6D_6, heated at 60 °C, and the reaction was checked the next day. Although lower catalyst loadings than (0.5 mol %) were viable for the reaction in the case of **2**, the reaction was only consistently reproducible when a 1 mol % loading was used. Based on the integration of the α CH_2 in hexanol moieties and β CH_2 in hexanoate moieties, the metathesis proceeded to at least 98% completion. Ethyl ethanoate, which is not observed by GC/FID or GC/MS, is easily detected here and in all subsequent NMR experiments.

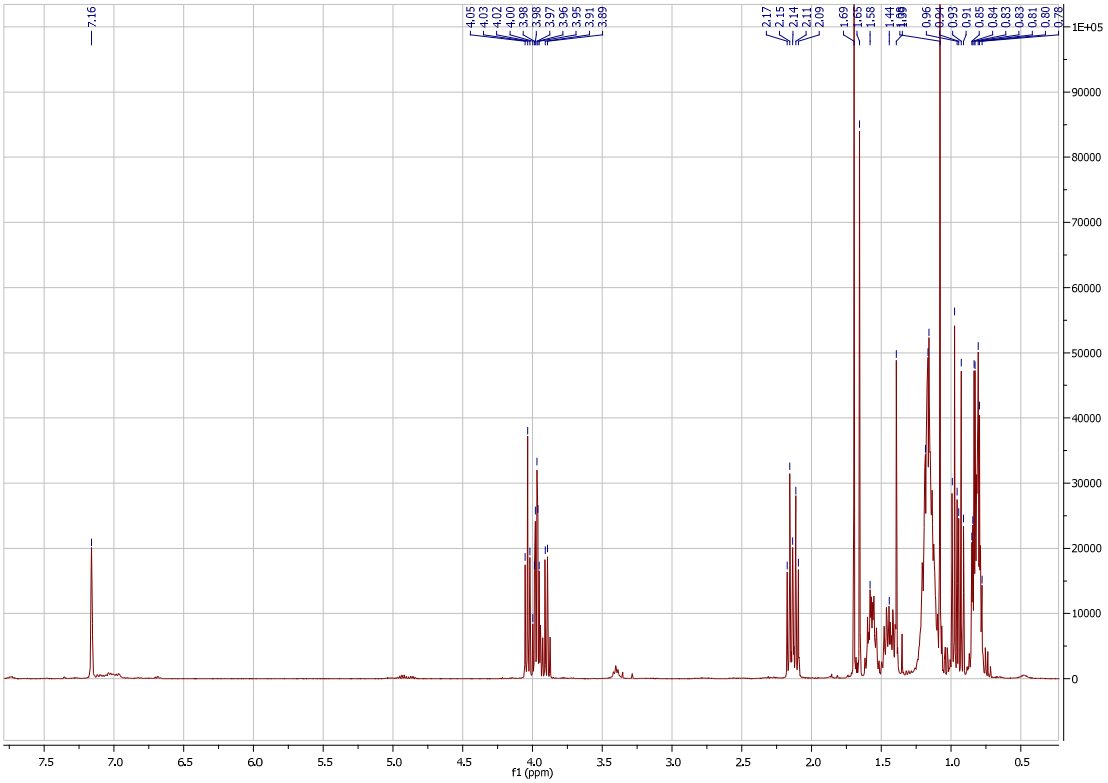

Figure S1. ^{1}HNMR of ethyl hexanoate **10** metathesis with catalyst **2**.

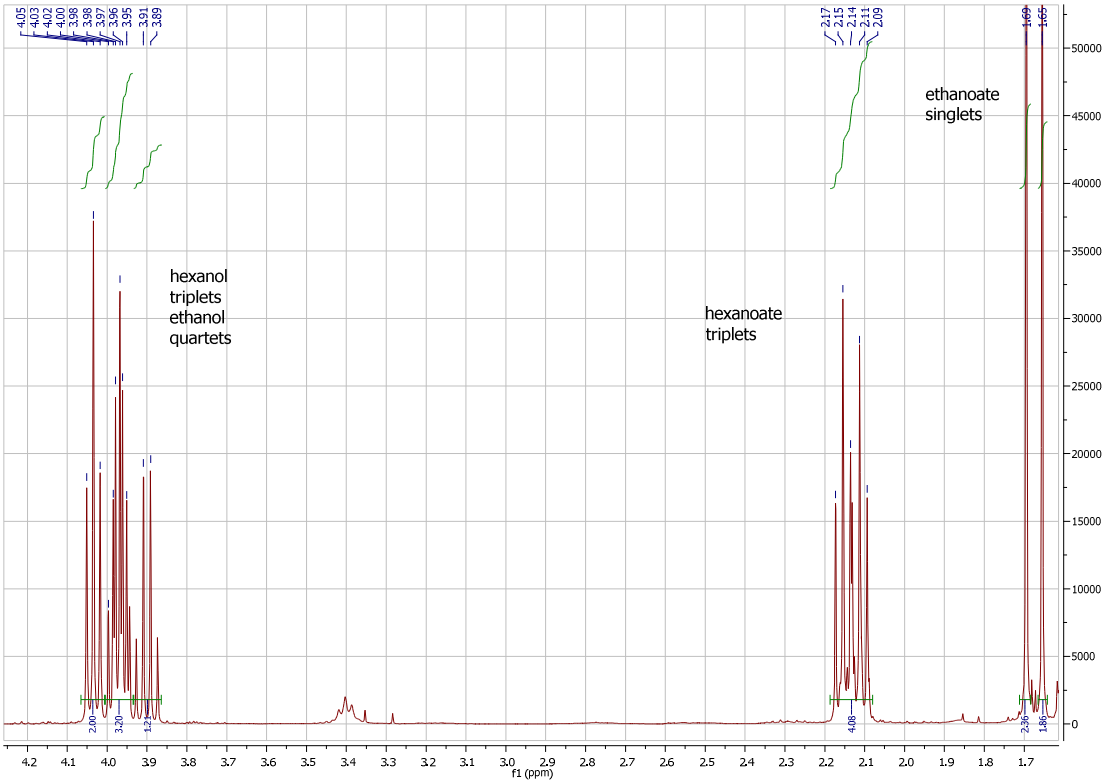

Figure S2. Expansion of ^{1}HNMR of ethyl hexanoate **10** reaction with **2**.

Synthesis of D_2benzylhexanoate 46 and subsequent scrambling experiment.

Synthesis of D_2 benzylic alcohol (Procedure adapted from earlier work)[2]

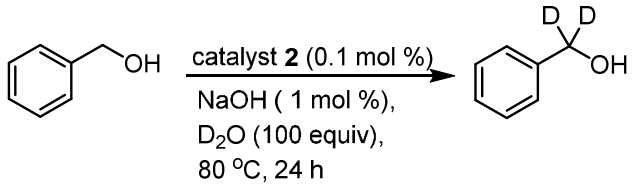

Under an argon atmosphere, 1 mL of benzyl alcohol was mixed with 100 equiv of deuterated water (18.5 mL) in a Schlenk tube, and 1 mol % of NaOH (~4 mg) and 0.1 mol % of RuMACHO catalyst (5.4 mg) were added. The tube was closed and heated at 80 ^{o}C for 24 h, with periodic shaking in order to remove condensation from walls. After one day, the product was extracted with ether (2 x 20 mL), washed with water, concentrated $NaHCO_3$, and concentrated NaCl solution, dried over anhydrous $MgSO_4$, filtered and concentrated to obtain pure D_2-benzylalcohol which was used in the next step after NMR confirmation.

Synthesis of D_2 benzyl hexanoate 46:

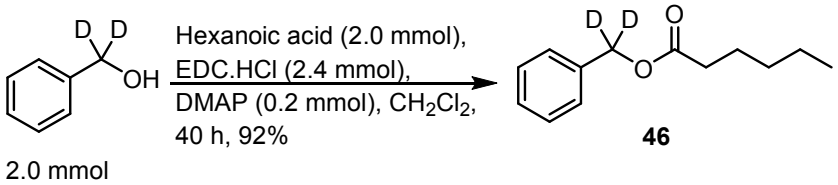

To a solution of hexanoic acid (232.3 mg, 2.0 mmol), EDC.HCl (460 mg, 2.4 mmol), and DMAP (24.4 mg, 0.2 mmol) in CH_2Cl_2 (6 mL) was added benzyl alcohol (220 mg, 2.0 mmol). After 40 h, chloroform (20 mL) and water (20 mL) were added and the layers were separated. The aqueous layer was extracted with chloroform (20 mL) and the combined organic layers were washed with brine (50 mL), dried over $MgSO_4$, and concentrated under reduced pressure. The crude product was purified by column chromatography (hexane : ethyl acetate = 98 : 2) to give the product as a colorless liquid (92% yield). ^{1}H NMR (400MHz, $CDCl_3$) δ 0.87 (t, J = 6.8 Hz, 3H), 1.26-1.31 (m, 4H), 1.58-1.67 (m, 4H), 2.33 (t, J = 7.2 Hz, 2H), 7.32-7.35 (m, 5H) ^{13}CNMR (100 MHz, CDCl3) δ 13.9, 22.3, 24.6, 31.3, 34.3, 65.5, 128.1, 128.2, 128.5, 173.6.

Synthesis of benzyl hexanoate 47:[3]

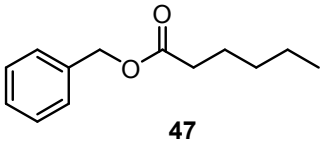

47

The title compound was prepared according to the procedure for the D_2-benzyl hexanoate. The product was obtained as a colorless liquid (96% yield). ^{1}H NMR (400MHz, $CDCl_3$) δ 0.87 (t, J = 6.8 Hz, 3H), 1.37-1.25 (m, 4H), 1.63 (quint, J = 7.6 Hz, 2H), 2.33 (t, J = 7.6 Hz, 2H), 5.10 (s, 2H), 7.28-7.37 (m, 5H).

Deuterium scrambling experiment.

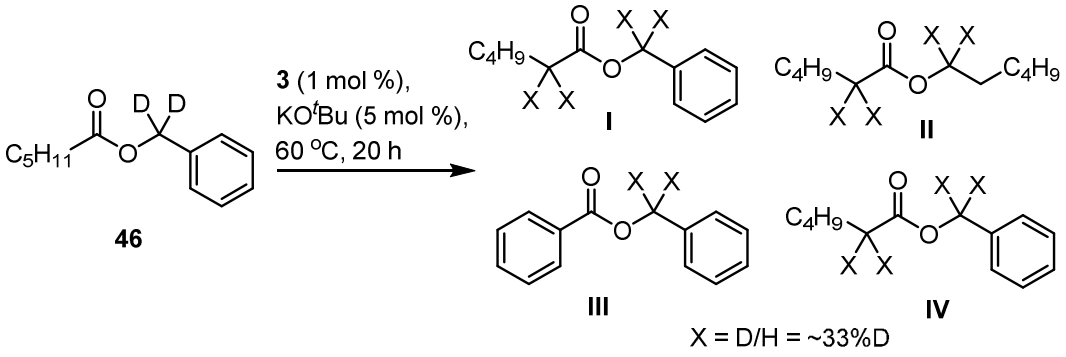

46

The experiment was done as described above for a catalytic ester metathesis except with D_2-benzyl acetate **46** and normal benzyl acetate **47** as substrates in J-Young NMR tubes. 1 mol % of catalyst **3** was used and heating was stopped after 16 hours. With the para-H peaks of benzoate products used as the standard and comparing the two reactions, the deuterated substrate showed that scrambling occurred into the β CH_2 to the same extent as onto the α CH_2 of the hexyl moieties. Although careful integration of the NMR makes it difficult to say that the scrambling is statistical, it is unambiguously present to a large extent. We argue that this is due to the presence of hexyl aldehyde, which is capable of undergoing keto-enol tautomerism and subsequent H/D scrambling through activation of the OH bond by a metal intermediate. Other hydrogen bonds, including those on the phenyl ring of the benzyl moiety, are unaffected.

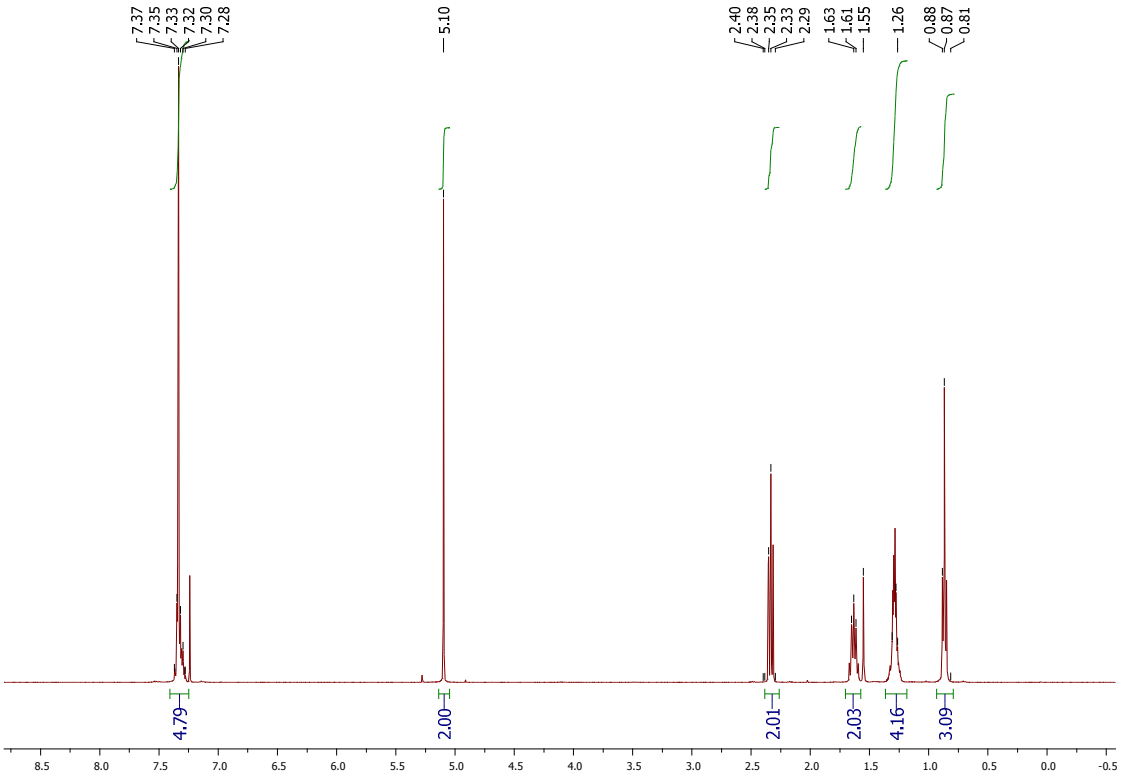

Figure S3. ^{1}H NMR of benzyl hexanoate **47**.

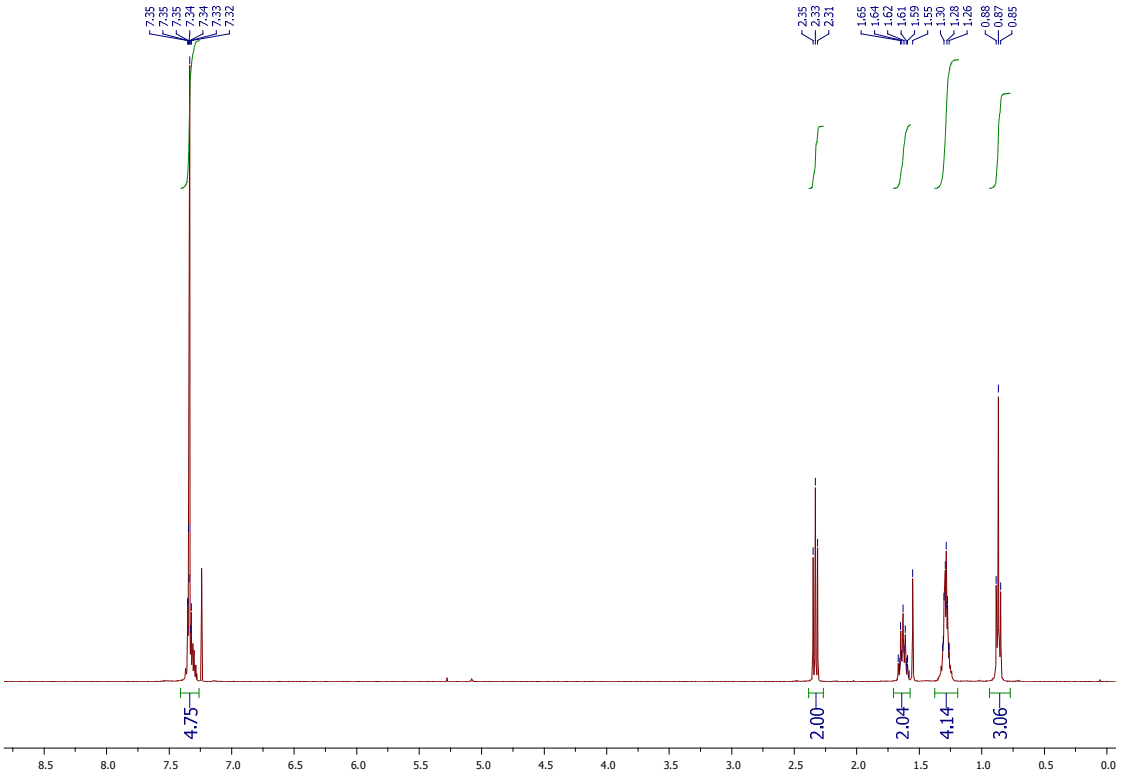

Figure S4. ^{1}H NMR of D_2-benzyl hexanoate **46**.

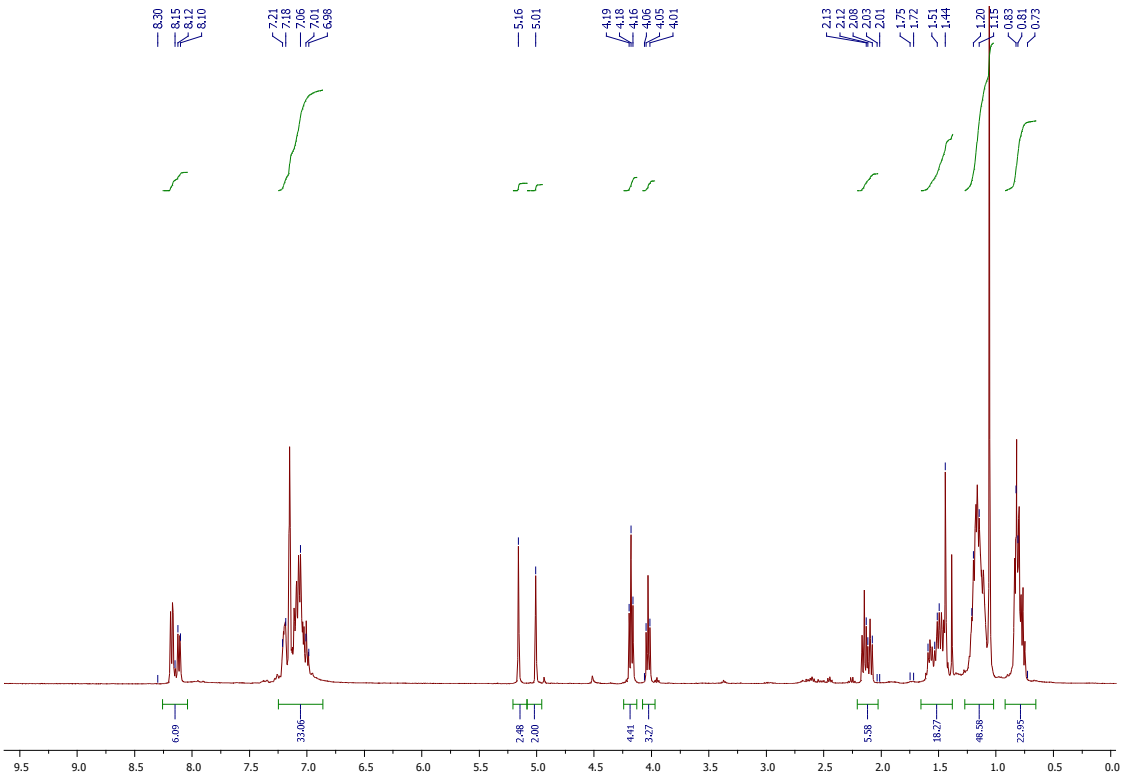

Figure S5. ^{1}H NMR of benzyl hexanoate **47** after metathesis reaction

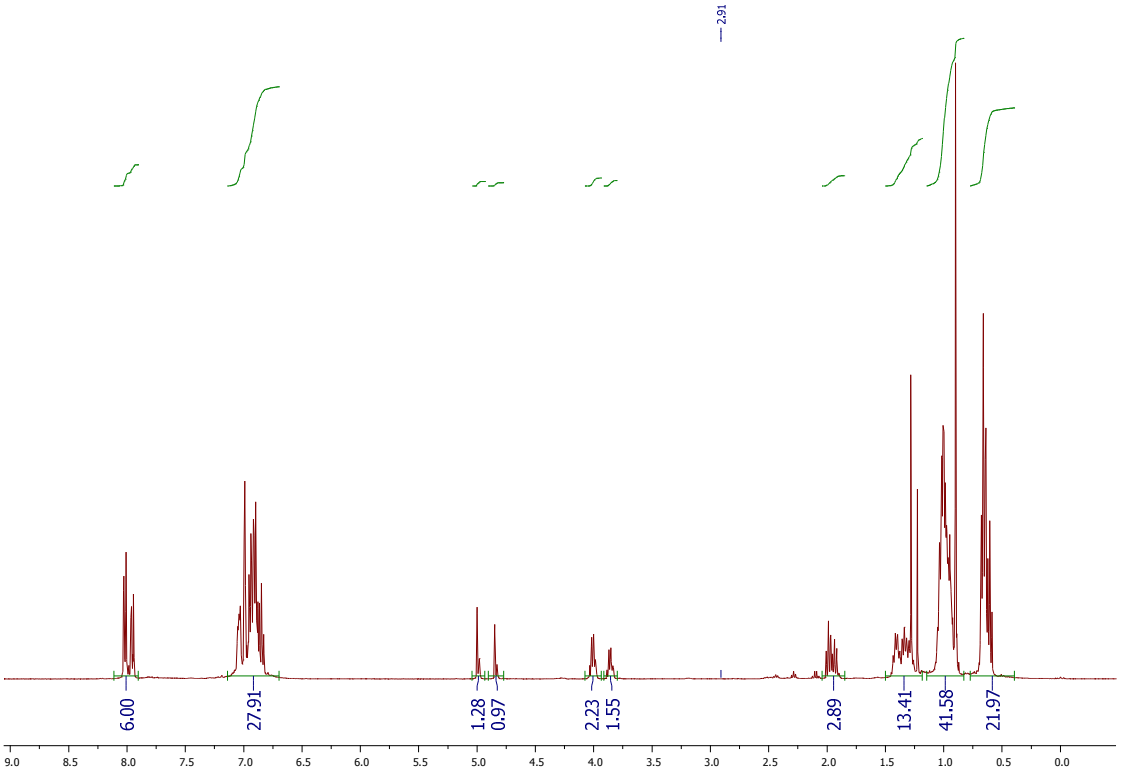

Figure S6. ^{1}H NMR of D_2-benzyl hexanoate **46** after metathesis reaction. β CH_2 of hexanol at ~1.5ppm (minor overlap with catalyst peaks) and of hexanoate at ~2.2ppm. α CH_2 of hexanol at 4.0-4.3ppm. α CH_2 of benzyl alcohol at 5.0-5.2ppm.

Kinetic NMR experiments with benzyl acetate 19

A series of reactions were set up that varied the concentration of the catalyst with a constant concentration of benzyl acetate substrate of 1.57mmol in 0.6 mL of C_6D_6 (0.26M, 223μL.). The catalyst was mixed together with 1.2 equiv. of KO^{t}Bu base in a J-Young NMR tube, solvent was added followed by the substrate. Afterwards, the kinetic experiment was started as soon as possible at 50 ^{o}C in the JEOL ECZS instrument, typically within half an hour after mixing. The reaction was followed for 4.5 hours.

The amounts of catalyst, as well as the initial reaction rate as calculated based on the appearance of ethyl acetate as the representative product, are given in the table below (Table S1). The first 50 minutes of heating were used to obtain the data. While the results are preliminary, they suggest that the rate is complex in catalyst. It increases as the concentration is increased but above 0.5 mol % catalyst to substrate, it begins to decrease. A similar effect is also seen in the stoichiometric experiments where 2:1 or 1:1 mixtures of catalyst to substrate react very sluggishly, but the rate is increased upon the addition (5 more equivalents) of substrate. The optimum amount of catalyst to substrate, as far as reaction rate is concerned, seems to be between 0.4 and 0.5 mol %.

When looking beyond initial data points, the most important finding is that the symmetrical products ethyl acetate and benzyl benzoate follow a first order rate law of appearance at the beginning of the reaction representative first order rate law curves are given below for one reaction (Figures S7-S12). In the latter parts of the reaction this cannot hold, as equilibrium kinetics become more important. The rate law for the appearance of unsymmetrical product ethyl benzoate is complex, and there is an effective induction period (Figure S11). Since this product is more thermodynamically stable than the starting material and the symmetrical isomers (see DFT results below), we conclude that the reaction is under kinetic control. Stoichiometric experiments with a lower amount of ester confirm that ethyl benzoate will be the major product after long reaction times (see Stoichiometric NMR experiments below).

The concentration of the $^-$O^{t}Bu ion which is present in a 5x excess to the catalyst, is not sufficient to cause transesterification, the base catalyzed exchange of alcohol moieties between esters, and interfere with the overall result. Even at the highest concentration, ethyl benzoate followed the same complex rate of appearance while the other products fit well within a first order curve. We can conclude that transesterification is not a significant reaction as otherwise the mixture of products would be equal or the curve for ethyl benzoate appearance would differ significantly from the curves obtained at lower concentration.

Table S1. Amounts of catalyst **3** used in kinetic experiments with initial rates calculated based on EtOAc appearance from excel's linear regression function. Integration obtained from JEOL's Delta NMR software. Reactions carried out in 0.6 mL of C_6D_6 and a constant concentration of benzyl acetate of 0.26M; heating at 50 ^{o}C with measurement intervals of 5 minutes.

Mol % Cat	Initial rate	M (cat)
0.15	2.09	0.004
0.3	2.82	0.008
0.4	7.79	0.011
0.5	8.98	0.013
0.6	4.50	0.016

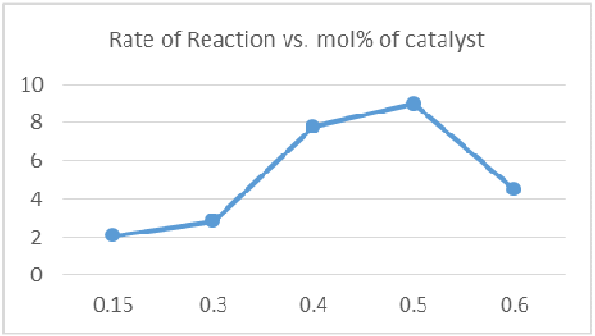

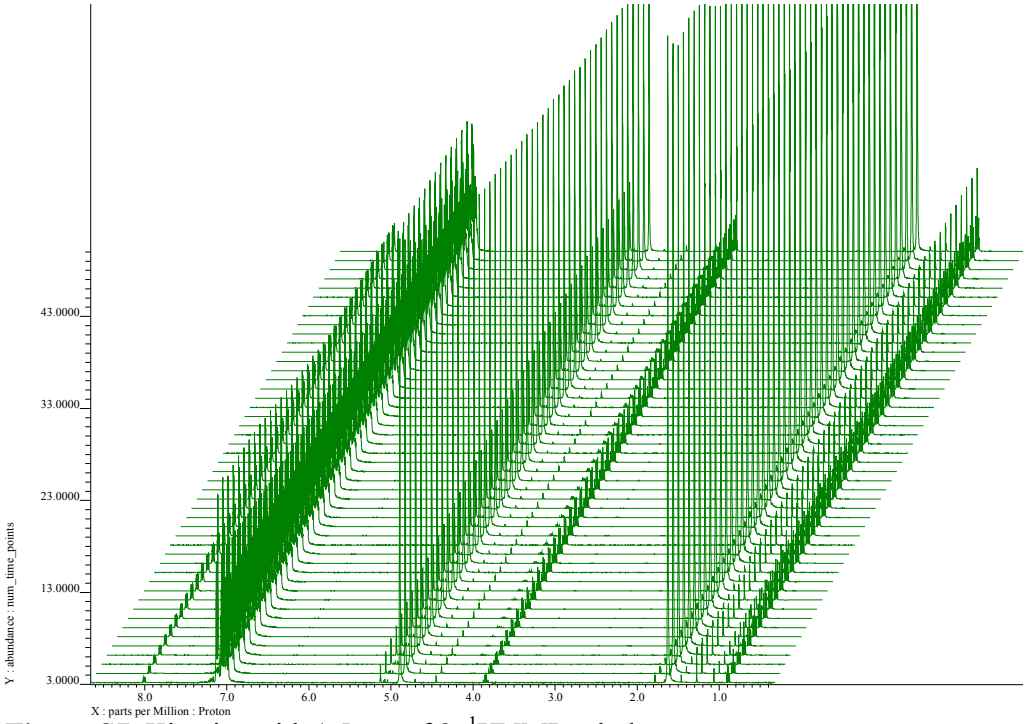

Figure S7. Kinetics with 1.5 mg of **3**. ^{1}HNMR whole spectrum.

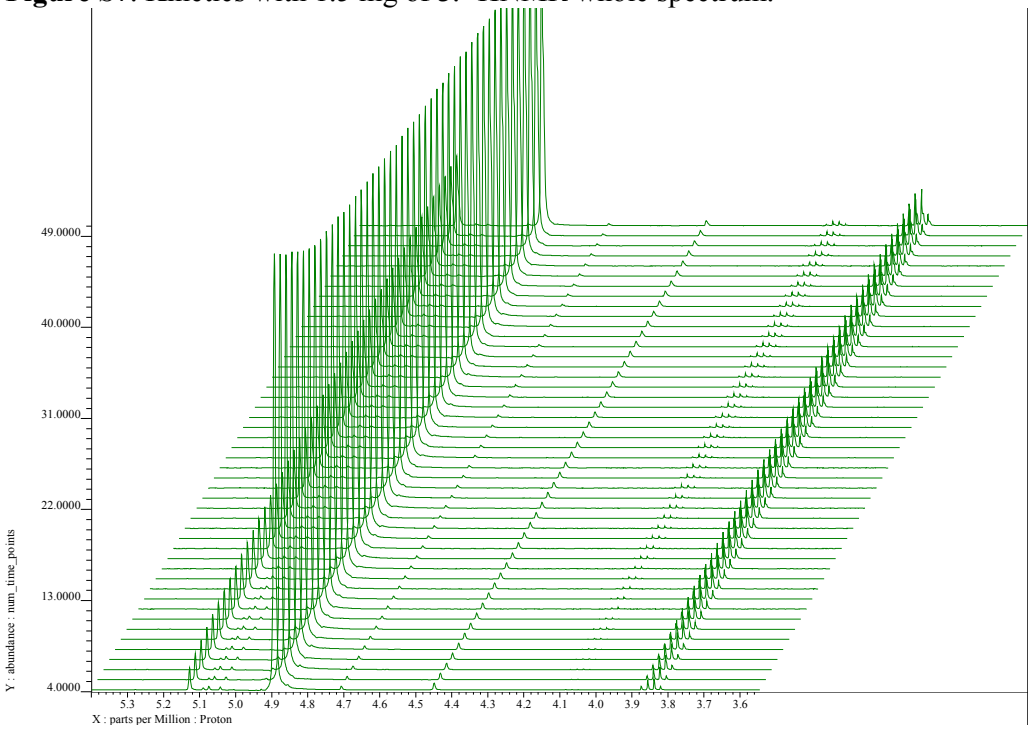

Figure S8. Kinetics with 1.5 mg of **3** and **19**. 3.85ppm ethyl acetate α CH_2 of ethanol; 4.1ppm ethyl benzoate α CH_2 of ethanol; 4.90ppm benzyl acetate α CH_2 of benzyl alcohol; 5.13ppm benzyl benzoate α CH_2 of benzyl alcohol.

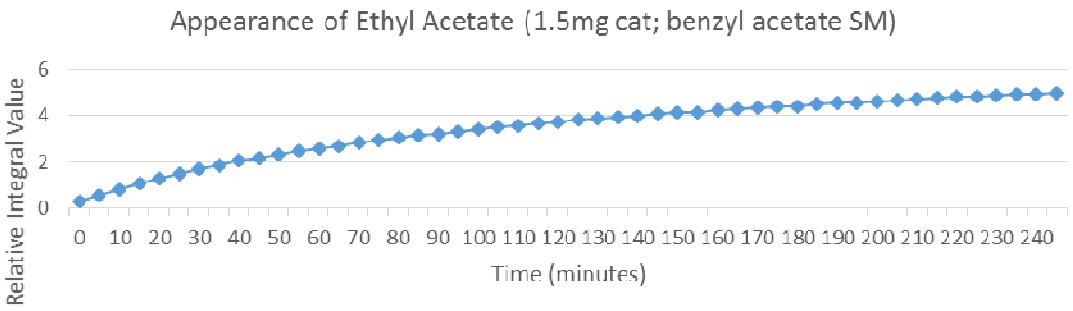

Figure S9. Appearance of α CH_2 of ethyl acetate with 1.5 mg of **3**. 50 °C; measurements every 5 minutes.

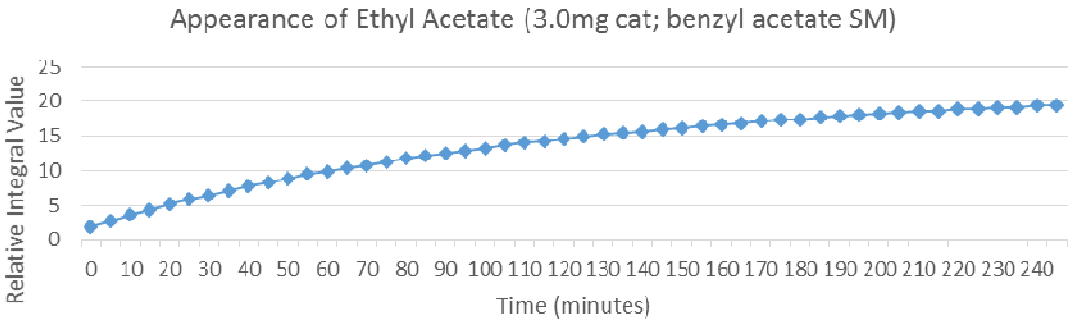

Figure S10. Appearance of α CH_2 of ethyl acetate with 3.0 mg of **3**. 50 °C; measurements every 5 minutes.

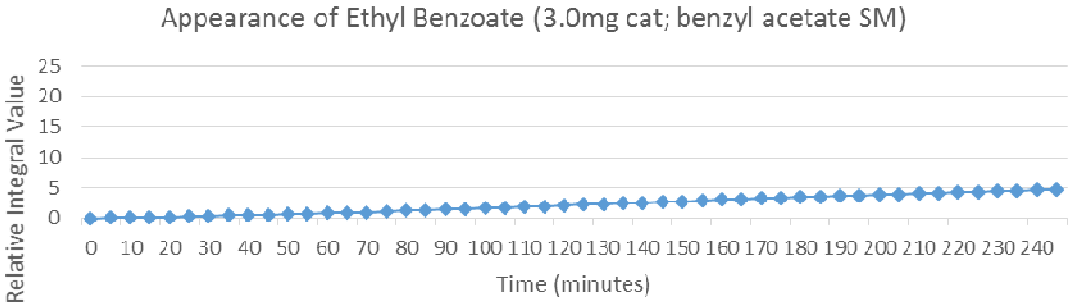

Figure S11. Appearance of α CH_2 of ethyl benzoate with 3.0 mg of **3**. 50 °C; measurements every 5 minutes.

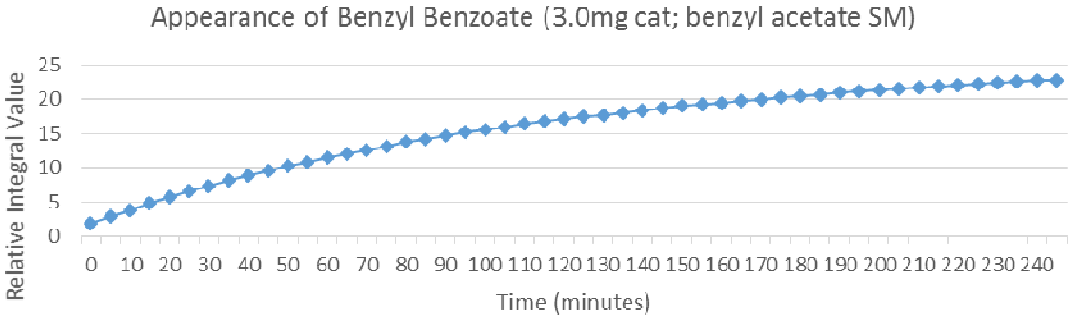

Figure S12. Appearance of α CH_2 of benzyl benzoate and with 3.0 mg of **3**. 50 °C; measurements every 5 minutes.

Kinetic NMR experiments with ethyl benzoate **20**

Only one experiment was performed with **20** in order to confirm the findings seen in the kinetic experiments performed on the mirror substrate **19**. From the experiments with benzyl acetate, it was determined that the optimum rate would be reached at ~4 mg. of catalyst in 0.6 mL of C_6D_6 with a 250 excess of ethyl benzoate (0.26M as above, 228 μL.). The reactants were mixed together with 1.2 equiv. of KO^{t}Bu (4mg) in a Young tube and the kinetics were followed every 5 minutes at 50 ^{o}C (Figure S13). We could confirm that the symmetrical products benzyl benzoate and ethyl acetate appeared at the same rate (Figures S14, S16) and the rate of appearance of the unsymmetrical **19** was significantly slower (Figure S15). The reaction was too close to equilibrium for close curve fitting after one hour. Due to the starting material **20** being more thermodynamically stable than **19** and when compared to both symmetrical products, it was the most abundant compound present at the end of the reaction; as can be seen from the slowed rate for appearance of **19** after ~3h. This situation would persist indefinitely.

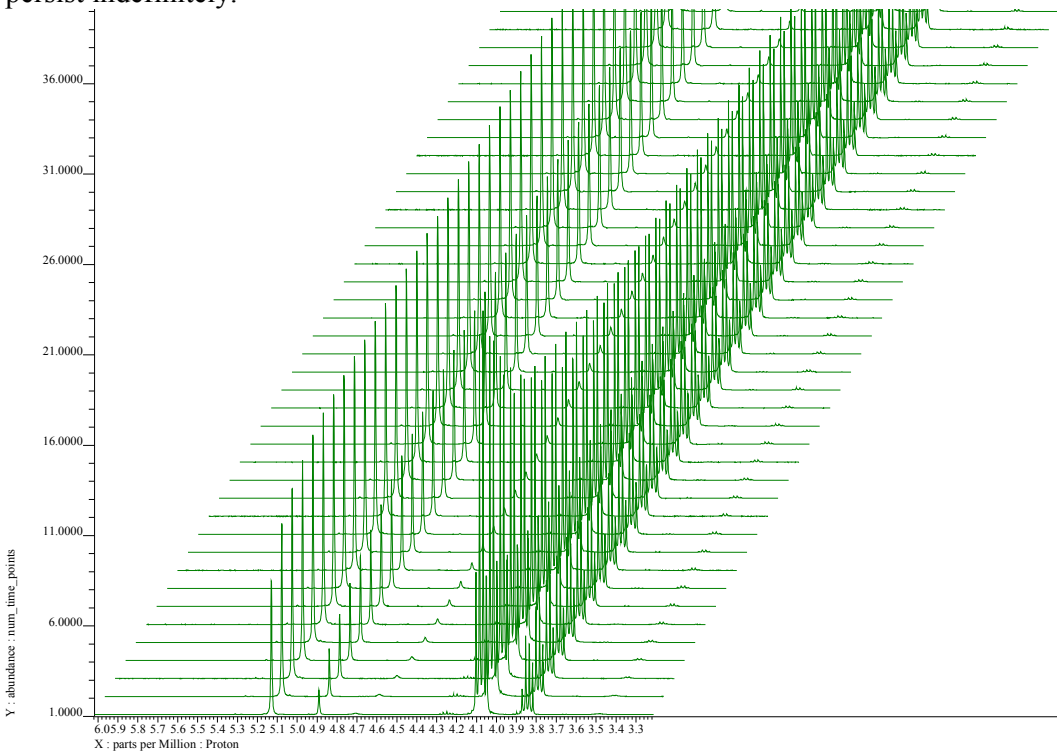

Figure S13. Kinetics with 4.0 mg of **3** and **20**. 3.85ppm ethyl acetate α CH_2 of ethanol; 4.1ppm ethyl benzoate α CH_2 of ethanol; 4.90ppm benzyl acetate α CH_2 of benzyl alcohol; 5.13ppm benzyl benzoate α CH_2 of benzyl alcohol.

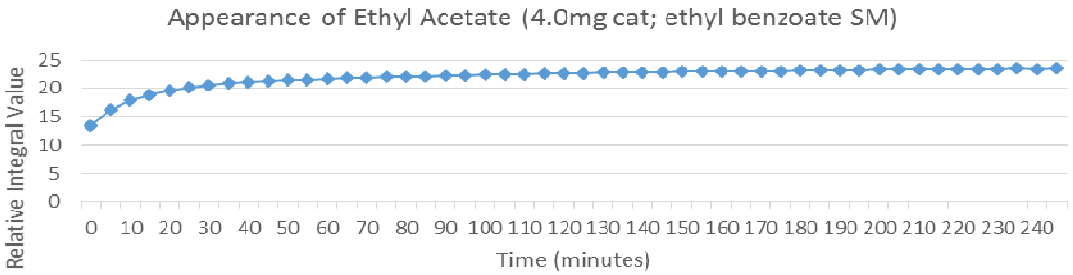

Figure S14. Appearance of α CH_2 of ethyl acetate with 4.0 mg of **3**. 50 ^{o}C; measurements every 5 minutes.

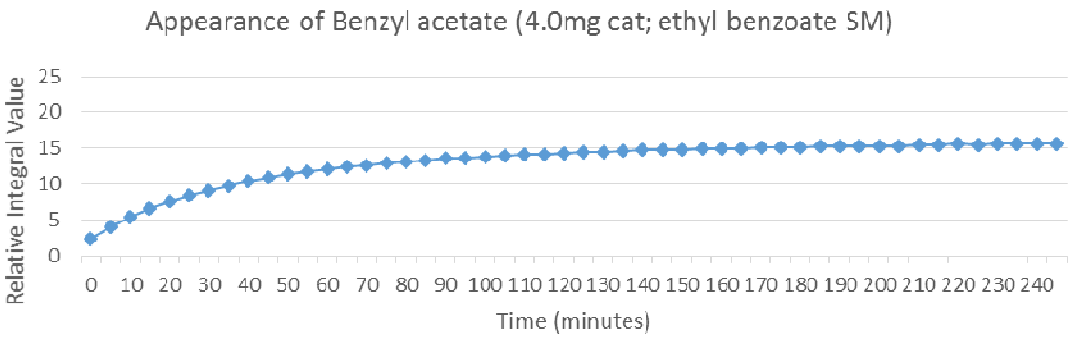

Figure S15. Appearance of α CH_2 of benzyl acetate with 4.0 mg of **3**. 50 ^{o}C; measurements every 5 minutes.

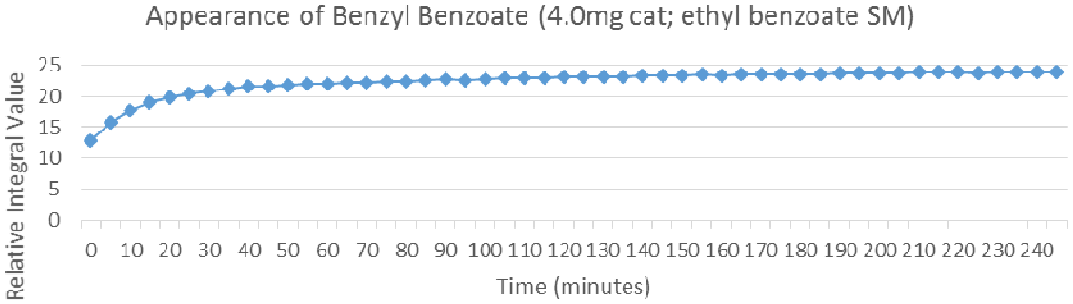

Figure S16. Appearance of α CH_2 of benzyl benzoate and with 4.0 mg of **3**. 50 ^{o}C; measurements every 5 minutes.

Stoichiometric NMR experiments

1) Activation of the pre-catalyst complex **3**

10 mg of **3** (0.016 mmol) was mixed together with 2 mg of KO^{t}Bu (0.018 mmol) in a J-Young NMR tube. 0.6 mL of C_6D_6 was added. The mixture turned a light green color and a complex mixture of complexes is observed (Figure S17). After heating for 3 hours at 50 ^{o}C, the mixture turns a dark brown and most of the signals broaden (Figure S18). There are several trace hydrides at ~ -15ppm.

It's not surprising that the NMR pattern is complex, since **3** is known to be a mixture of isomers.[2] After deprotonation by base, the Cl^- ligand is lost leading to the possibility of forming dimeric complexes and possibly complex equilibria. However, experiments described below allow us to conclude that the minor hydrides that we do see are side-products that are not active in the metathesis reaction. Addition of substrates to either the early green solution or the brown solution, does not change the outcome or the rate of these reactions.

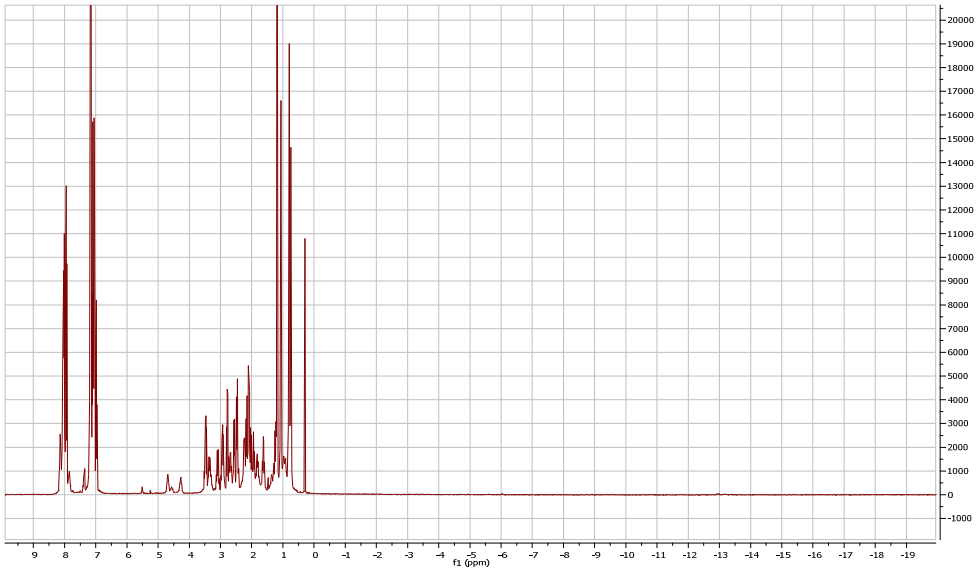

Figure S17. ^{1}H NMR of **3**, soon after mixing with KO^{t}Bu in C_6D_6.

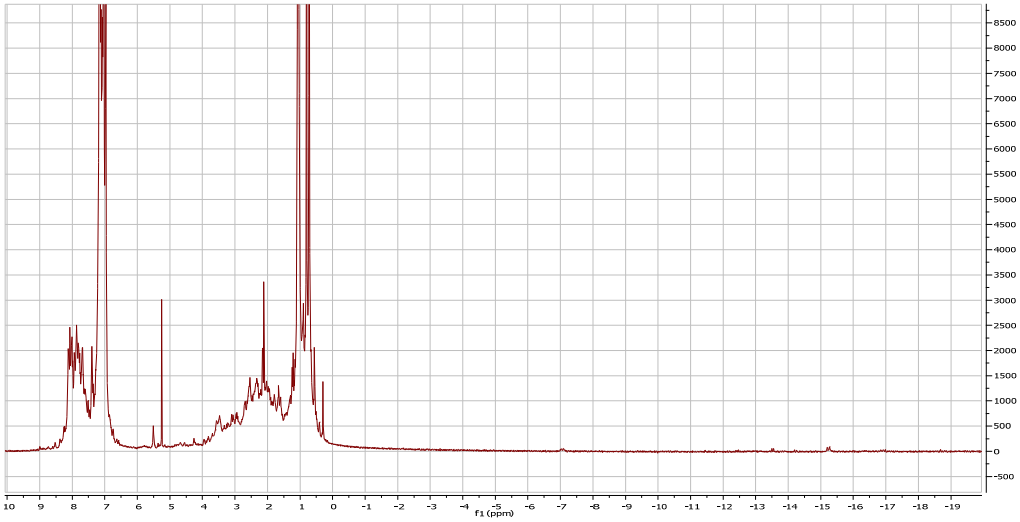

Figure S18. ^{1}H NMR of **3**, 3 hours after mixing with KO^{t}Bu in C_6D_6 and heating at 50 ^{o}C.

2) Reaction of activated **3** with benzyl acetate **19**

Adding 0.5 equiv. of benzyl acetate **19** to activated complex **3** (10 mg in 0.6 mL of C_6D_6 activated with 2 mg of KO^{t}Bu) surprisingly does not lead to a fast metathesis reaction. Even after standing for three hours at room temperature and ten minutes of heating at 50 ^{o}C, a very small amount of metathesis is seen (Figure S19). Adding the ester substrate to the brown mixture, does not affect the hydride pattern, but does lead to metathesis. In case of the green mixture, a new minor hydride pattern is generated upon addition of ester, but the metathesis reaction still occurs without a change in that second pattern. This does not prove that hydrides are not involved in metathesis, but along with them being present as trace species, makes it highly unlikely. The slow rate of metathesis when only 0.5 equiv. of **19** are used can be contrasted with the kinetic experiments where at the higher concentration of catalyst, already a few TONs are observed at room temperature (~200 equiv. of substrate) before reaction heating is started. Adding another 0.5 equiv. of benzyl acetate does not increase the slow

reaction rate, however it can be verified that the ester is not affected by the complexes, as the intensity of the signals of the ester changes by two times with respect to C_6D_6. It is thus unlikely that decomposition of the ester as a sacrificial substrate is necessary to generate the active species for metathesis (Figure S20).

After letting this mixture stand for 12 hours overnight at ambient temperature, NMR shows that complete metathesis has taken place. The major ester present is ethyl benzoate **20**, which is the thermodynamic product (Figure S21). After adding 5 more equivalents of benzyl acetate and letting the solution stand at r.t. for three hours, complete metathesis is seen, although the product distribution is more equal (Figure S22). This can be contrasted to using only 0.5 equiv. of ester, where three hours at r.t. resulted in a very slow reaction. Increasing the ester concentration when ester concentration is initially close to that of the catalyst, thus increases the rate of catalysis. Heating the reaction with now 6 equivalents of ester total for another 2 hours at 50 ^{o}C, regenerates the distribution pattern where **20** is the major product.

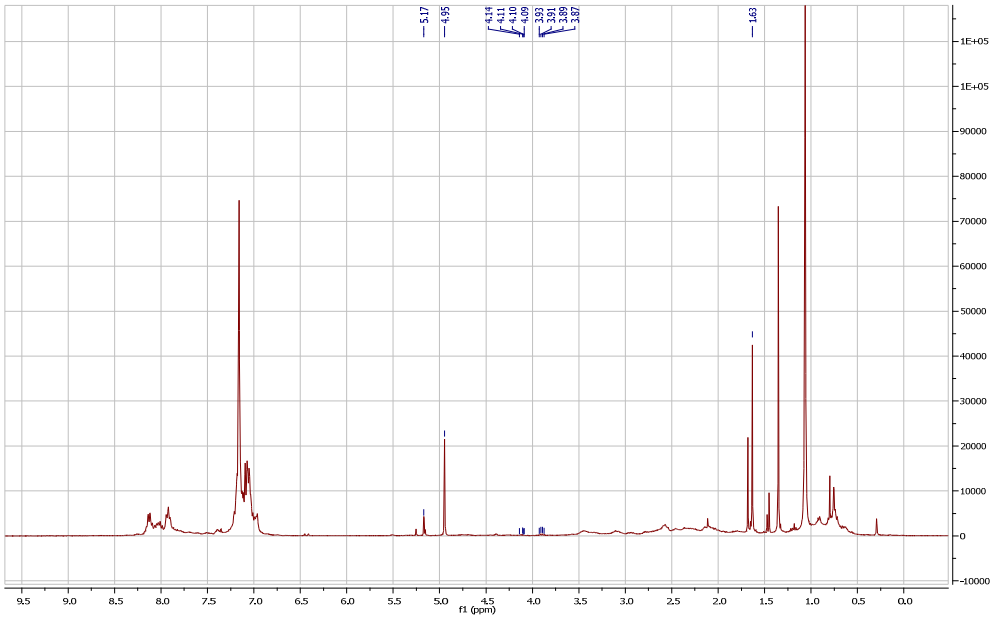

Figure S19. ^{1}H NMR of **3** with 0.5 equiv of benzyl acetate after 10 minutes of heating at 50 ^{o}C. 3.90ppm quartet ethyl acetate α CH_2 of ethanol; 4.1ppm quartet of ethyl benzoate α CH_2 of ethanol; 4.95ppm benzyl acetate α CH_2 of benzyl alcohol; 5.17ppm benzyl benzoate α CH_2 of benzyl alcohol.

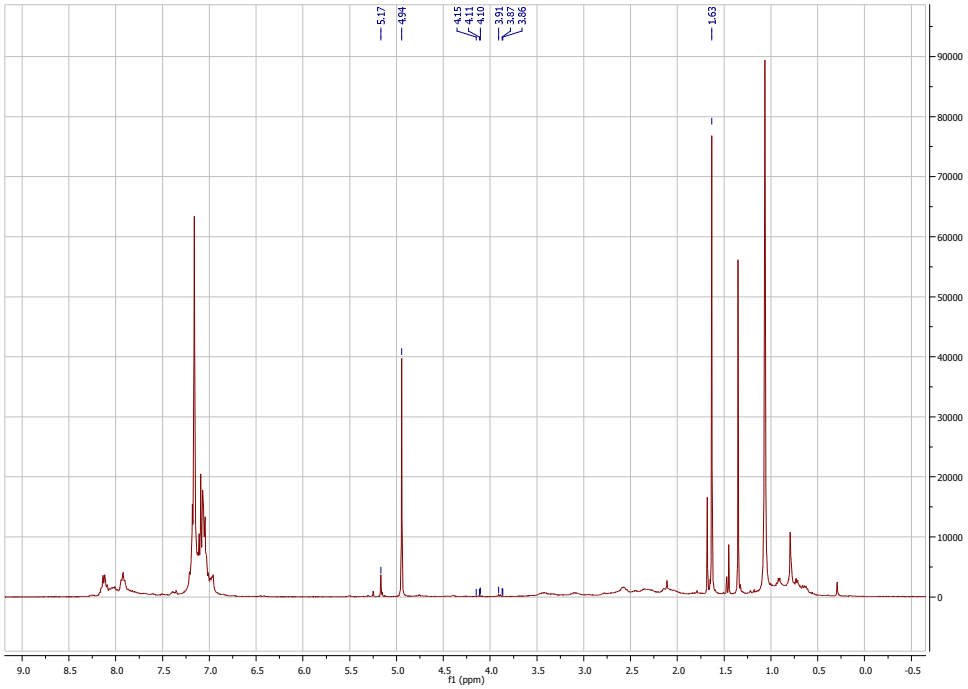

Figure S20. ^{1}H NMR of **3** with 1equiv of benzyl acetate after 10 minutes of heating at 50 ^{o}C. 3.90ppm quartet ethyl acetate α CH_2 of ethanol; 4.1ppm quartet of ethyl benzoate α CH_2 of ethanol; 4.95ppm benzyl acetate α CH_2 of benzyl alcohol; 5.17ppm benzyl benzoate α CH_2 of benzyl alcohol.

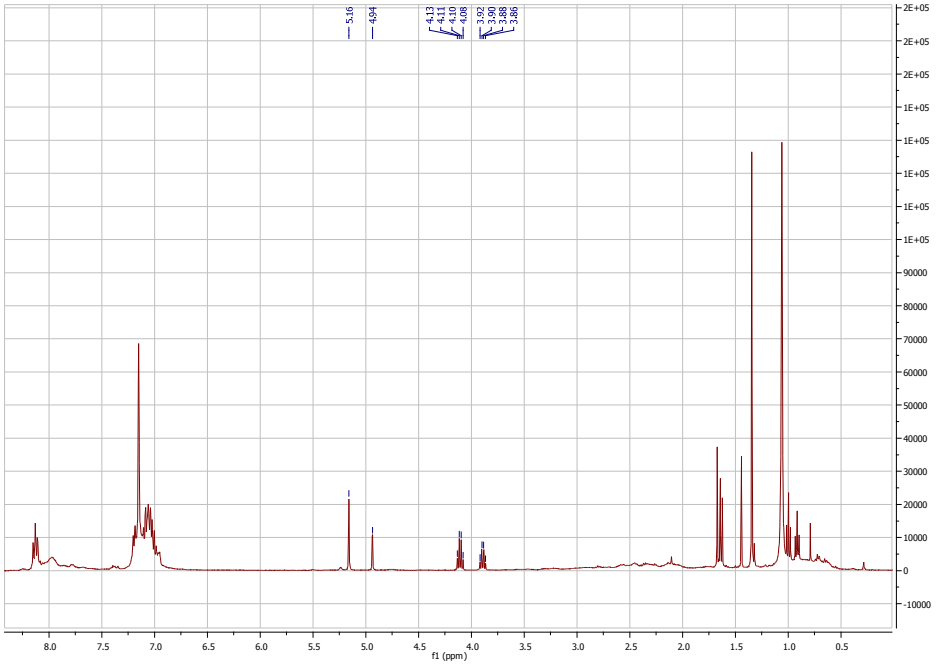

Figure S21. ^{1}H NMR of **3** with 1equiv of benzyl acetate after overnight at r.t. 3.90ppm quartet ethyl acetate α CH_2 of ethanol; 4.1ppm quartet of ethyl benzoate α CH_2 of ethanol; 4.95ppm benzyl acetate α CH_2 of benzyl alcohol; 5.17ppm benzyl benzoate α CH_2 of benzyl alcohol.

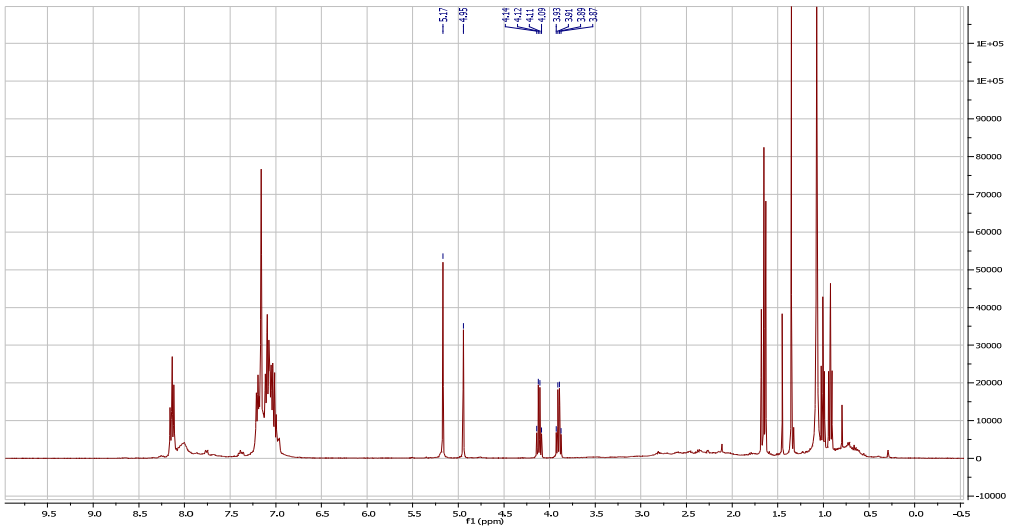

Figure S22. ^{1}H NMR solution from Figure S17 after adding 5 more equiv of benzyl acetate and leaving at r.t. for 3 hours. 3.90ppm quartet ethyl acetate α CH_2 of ethanol; 4.1ppm quartet of ethyl benzoate α CH_2 of ethanol; 4.95ppm benzyl acetate α CH_2 of benzyl alcohol; 5.17ppm benzyl benzoate α CH_2 of benzyl alcohol.

3) Reaction of activated **3** with ethyl benzoate **20**

In order to have one parallel reaction to the stoichiometric experiment carried out with **19**, Activated complex **3** (10 mg in 0.6 mL of C_6D_6 activated with 2 mg of KO^tBu) was used with 6 equiv. of **20** (13.6 μL). After 15 minutes at room temperature, only trace signals of metathesis products can be observed (Figure S23), with ethyl acetate α CH_2 signal being obscured by the carbon satellites of the starting material. After 4.5 hours of heating at 50 ^{o}C, metathesis is observed (Figure S24), however the amount of the products is a lot less than that observed in Figures S13-S16, where 250 equiv. of **20** were used and the corresponding concentration of the ester was a lot higher.

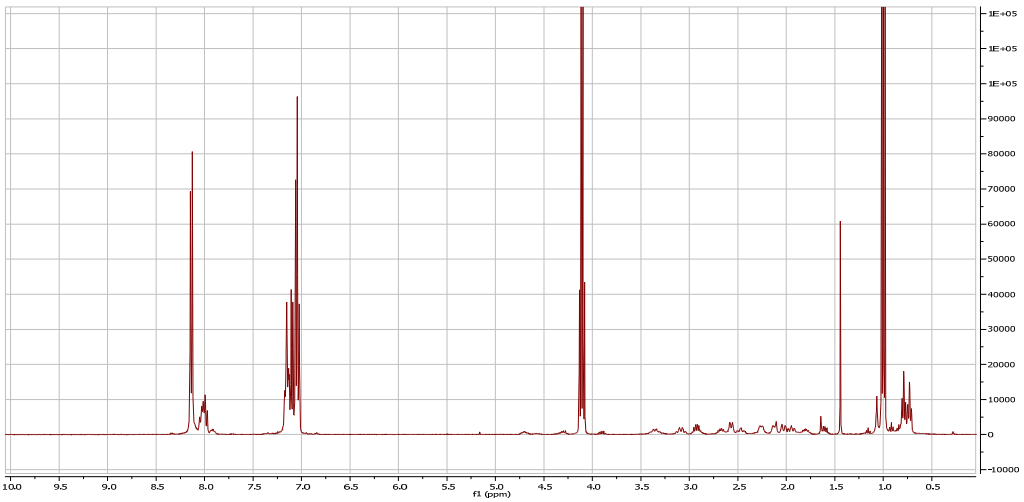

Figure S23. ^{1}H NMR of **3** with 6 equiv. of **20**, 15 minutes after mixing at r.t. 3.90ppm quartet ethyl acetate α CH_2 of ethanol obscured by carbon satellite of **20**; 4.1ppm quartet of ethyl benzoate α CH_2 of ethanol

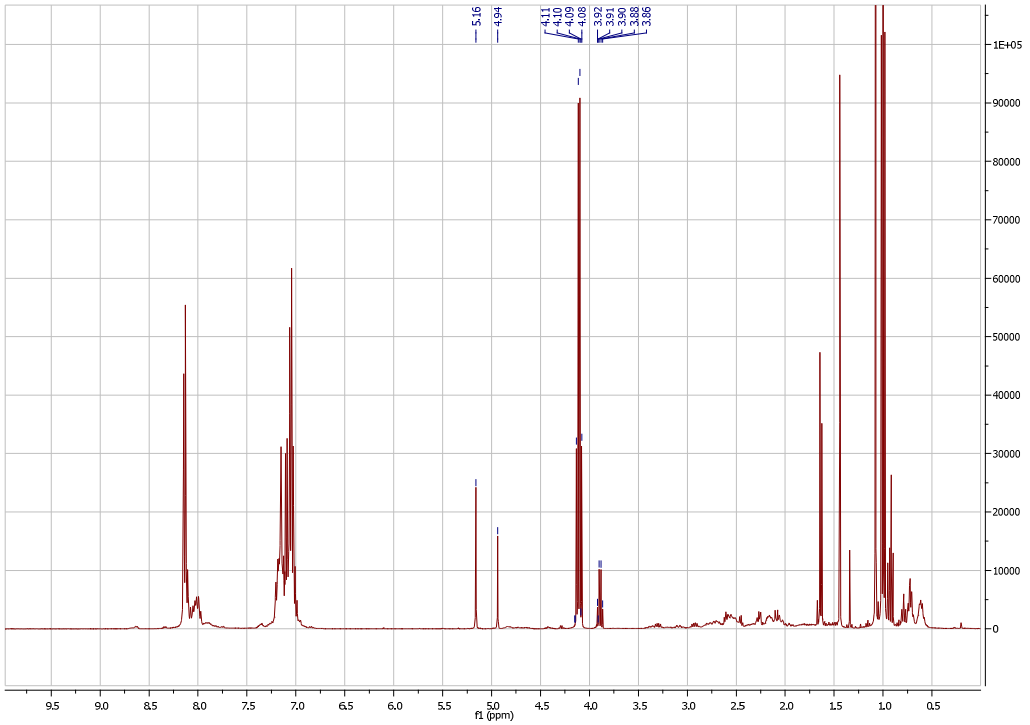

Figure S24. ^{1}H NMR of **3** with 6 equiv. of **20**, 4.5 hours after heating. 3.90ppm quartet ethyl acetate α CH_2 of ethanol; 4.1ppm quartet of ethyl benzoate α CH_2 of ethanol; 4.95ppm benzyl acetate α CH_2 of benzyl alcohol; 5.17ppm benzyl benzoate α CH_2 of benzyl alcohol.

4) Reaction of activated **3** with benzyl benzoate **18**

As in the above case with benzyl acetate, the symmetrical substrate benzyl benzoate was added in the same amounts of 0.5 equiv., another 0.5 equiv., and finally 5 equiv. The intervals between additions and the heating periods were the same as the reactions were done in parallel. The symmetrical substrate cannot show any metathesis and the reaction was done to confirm that the complex generates the same pattern of signals during the course of the reaction and that there is no significant decomposition from an interaction of the ester and the metal complex in order to generate a presumably active species. The intensity of the benzylic protons follows the order of addition when compared to C_6D_6 and is not degraded after heating periods.

Mechanistic Conclusions

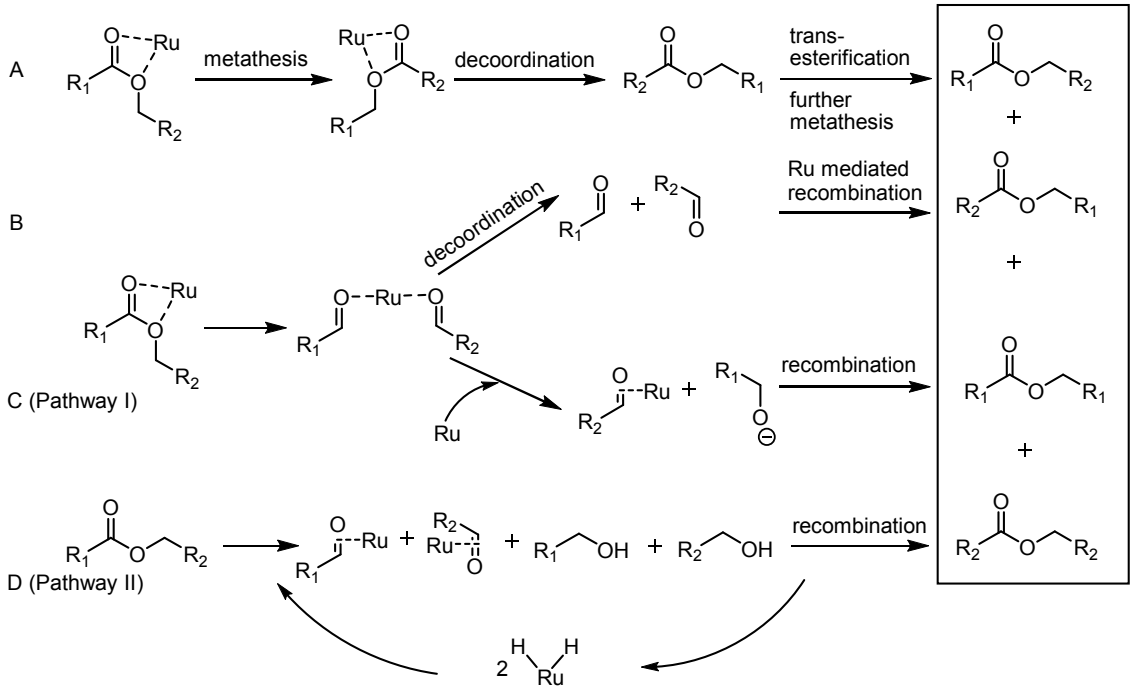

Deuteration Experiment

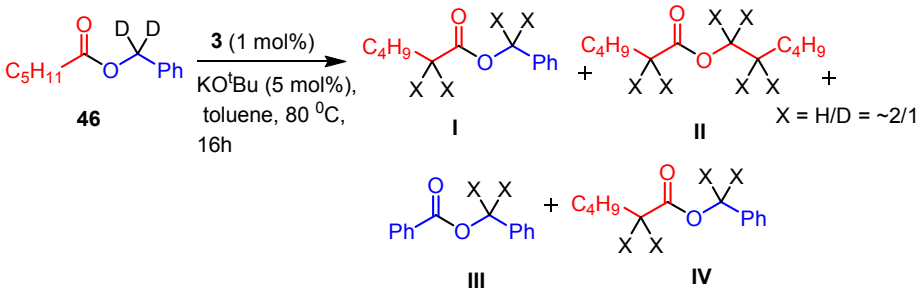

Pathway C that results in faster appearance of symmetrical products

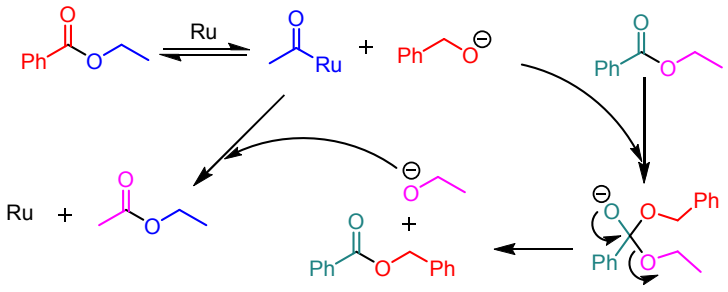

Figure S25. Mechanistic Figure from the main text with deuteration experiment included. Pathways C and D are I and II respectively in the main text.

The experiment on 2D-benzylhexanoate **46** gave deuteration in the β carbon position of the hexyl moiety to an equal extent with all the α carbons. It is known that this scrambling can occur in aldehydes via the intermediacy of keto-enol tautomerism, which can be catalyzed by bases, though an ester enolate cannot be ruled out as the mechanism for scrambling the label into the β position. The presence of an intermediate aldehyde that can be captured by another reactant has been assumed in the synthesis of olefins from alcohols.[4,5] The evidence suggests the intermediacy of aldehyde or alcohol-like species that are either free in solution or are bound to the complex, and rules out the one-center pathway A. Although pathway A can also be ruled out via the kinetic experiments, as the unsymettrical product should appear much more rapidly than the symmetrical esters and this is not the case.

Path B involves the separation of the ester into component parts: free aldehydes in solution which are then reformed, resulting in the appearance of the products. However, free aldehydes are not detected as trace species via ^{1}H NMR or by sampling the reaction mixture by GC/MS. A previous mechanistic report with the Milstein catalyst system also showed that free aldehyde will coordinate rapidly to the activated Ru species, and the resulting complexes are believed to be intermediates in catalytic alcohol dehydrogenative coupling.[6] Also, all products should form in equal rates if pathway B is followed, but this is not the case.

We could not differentiate between pathways B and C (pathway I in the main text) by stoichiometric experiments as we do not observe changes in the complex organometallic mixture when reacting activated complex **3** and **1** or **20**. Either free aldehyde or alcohol cannot be ruled out, but they were not present in sufficient amounts to be observed by NMR, although metathesis is observed. However, the kinetic experiments lead us to propose pathway C as the active mechanism. As mentioned above in ruling out pathways A and B, when reacting **3** and **19**, we can see that the two symmetrical products ethyl acetate and benzyl benzoate appear at equal rates following pseudo first-order kinetics, much more rapidly than the unsymmetrical product **20**, which has an infective 'induction period' before starting to appear in the reaction.

Pathway C is involves one part of the ester remaining coordinated to the Ru complex, while the other is released as an alkoxy species. **20** is more stable than **19** by ~1.8 kcal/mol and is ~1.0kcal/mol more stable than the two symmetrical species (see SI for gas phase DFT results). After long reaction times, **20** is the major species present in the reaction mixture as expected from thermodynamics. Moreover, when the reverse reaction is performed, with **20** as the starting material, the symmetric products also appear at the same rate and faster than unsymmetrical product **19**. While the reverse reaction now does follows the thermodynamic profile, it is also the exact mirror of the reaction with **19**, which does not.

Initial rates in catalyst found that the rate is complex and rises slowly until ~0.4mol% of catalyst, after which it begins to decrease. Most dramatically, a reaction with 18mol% of catalyst and **20** showed significantly slower activity (~30% metathesis efficiency after 4.5 hours at 80^{o}C) than a reaction set up with only 0.4mol% catalyst (full metathesis after 4.5 hours at 50^{o}C). The same decrease of activity was observed when performing the reaction with **19** as the starting ester. A pictorial explanation for how symmetrical products might be preferred in pathway C, and why free ester accelerates the reaction, is presented in the bottom panel of Figure S25. Both the concentration of free ester and the amount of active catalyst are important in the reaction. As presented, if the first step is reversible, there is a maximum catalyst loading beyond which the rate should not increase.

Symmetrical products are formed initially according to this pathway, and the unsymmetrical product can be generated when the catalyst subsequently reacts with these symmetrical products. In the case of **20** as starting material, **19** can be generated after reaction between the catalyst and ethyl acetate. Importantly, an acyl Ru species that is suggested by the mechanism also helps explain the rapid deactivation of the catalyst when

methyl esters are involved, as this pathway would lead to covalently bound HCO-Ru that is easily converted to CO. It is unlikely that these types of organometallic species (RCO-Ru) would be tolerant of other functional groups as well.

It is also possible that a trace amounts of catalyst converted to a dihydride complex is active in the metathesis reaction by converting the ester into alcohol constituent parts (i.e. ester hydrogenation occurs, followed by dehydrogenative alcohol coupling) according to pathway D (pathway II in the main text). The trace dihydride species can be generated from dehydrogenation of ester; or from trace impurities. However, esters where dehydrogenation is highly unlikely, such as an aryl/aryl ester, and **19** or **20** (Table 3, entries 4-5) on which kinetic experiments were done, did not decompose to a detectable extent even at high catalyst concentration, and showed no interaction with the active catalyst even at stoichiometric loadings on the NMR timescale, suggesting that impurities or ester CH activation can be ruled out in the one component metathesis reaction.

On the other hand, in the hydrogenation reaction where ethanol or other alcohols are used, the dihydride complex can easily form from ethanol, even at -80^{o}C as reported by Milstein.[6] Adding one equivalent of benzyl alcohol to activated catalyst **3** at room temperature does lead to what is apparently a coordinated aldehyde complex with two broad peaks at 2.6 and 4.6ppm, but no benzyl benzoate product. Benzyl alcohol retards the rate of the metathesis reaction in comparison to an NMR reaction set up without benzyl alcohol. Adding 5 eq. of **19** to this mixture and heating for 50^{o}C for one hour leads a measurably slower rate of metathesis compared to a mixture with the same concentration of all reactants, but without benzyl alcohol. This result helps explain the experimental finding that hydrogenation with benzyl alcohol gives poorer results than hydrogenation with ethanol.

Even if a dihydride complex does not form upon the addition of ethanol, free hydrogen is released in the ethanol coupling reaction to form ethyl acetate, where the first turnover is observed even at low temperatures.[6] The presence of free H_2 from excess alcohol in the closed reaction system opens up an opportunity for Ru dihydride complex formation *in-situ*. An alternative pathway may thus be available for ester scrambling during the hydrogenation reaction. The activity of some substrates in hydrogenation that proved to be inactive in metathesis, as well the dramatic improvement in the activity of catalyst **4**, suggests that both pathways C and D can be active in transfer hydrogenation of esters, and it is likely that only pathway C is active in one-component ester metathesis.

A final note must be made on the trans-esterification reaction catalyzed by KO^{t}Bu where two esters react according to the following equation: $R_1COOR_2 + R_3COOR_4 \rightarrow R_1COOR_2 + R_3COOR_4 + R_1COOR_4 + R_3COOR_2$. This reaction has been described previously.[7] This is a completely different reaction from the one described by us as no reduction or oxidation of R1-R4 fragments takes place. It is true that rapid trans-esterification can facilitate scrambling once metathesis has occurred, and pathway C requires attack of a primary alkoxide on an ester to generate another primary alkoxide, which is immediately consumed by the Ru intermediate. There is an excess of a tertiary alkoxide in the reaction mixture, however under our reaction conditions this $^{-}$O^{t}Bu catalyzed transesterification is not as rapid as metathesis at 80^{o}C. This can be seen in the GC traces for the transfer hydrogenation of esters, for example Figure S46 in the SI, where significant amounts of hexyl ethanoate are detected in the presence of a large excess of ethanol and some extra equivalents of KO^{t}Bu. Most importantly, we found no change in the metathesis reaction outcome when using KHMDS, a very bulky base that is very unlikely to participate in trans-esterification, when compared to KO^{t}Bu.

DFT energies and optimized geometries (Cartesian coordinates)

Benzyl Acetate

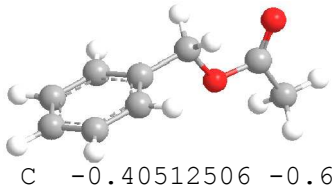

```
 C  -0.40512506 -0.60763873 -0.44748291
 C  0.91792360 0.10836580 -0.41067908
 H  0.85986648 1.10030188 -0.88106929
 O  1.30058547 0.28353672 0.99162179
 C  2.50604524 0.89236956 1.18459132
 C  -0.45786843 -2.01039917 -0.39257613
 C  -1.68669050 -2.67776999 -0.41742976
 C  -2.87914643 -1.94783975 -0.50209768
 H  1.70972287 -0.46451535 -0.91447642
 C  2.81059938 1.01555191 2.66110067
 O  3.22109690 1.27412522 0.27677648
 H  3.77940366 1.50729827 2.79236228
 H  2.82765128 0.01986795 3.12630964
 H  2.02277539 1.59646938 3.16103756
 C  -2.83701446 -0.54966423 -0.56054761
 C  -1.60597779 0.11502277 -0.53295612
 H  0.47160479 -2.58115466 -0.33090756
 H  -1.71436567 -3.76818422 -0.38060734
 H  -3.83814317 -2.46802111 -0.52990423
 H  -3.76307324 0.02334753 -0.63251080
 H  -1.57409232 1.20594920 -0.58140280
```

Benzyl Benzoate

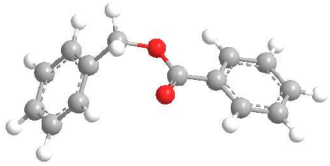

```
 C  1.08699144 -0.63256646 -0.97871969
 C  2.52743151 -0.80545030 -0.56194733
 H  3.18263070 -0.09371253 -1.08034616
 O  2.69737017 -0.62287970 0.88165637
 C  3.02441255 0.63371949 1.29753902
 C  0.21214396 -1.73169559 -0.97771871
 C  -1.12625759 -1.57653001 -1.35451124
 C  -1.60259893 -0.31696814 -1.73856363
 H  2.86900049 -1.83303230 -0.74164447
 C  3.16643624 0.71151855 2.78442480
 O  3.18689259 1.57964597 0.54169205
 C  3.50697583 1.95480235 3.34532070
 C  3.65453580 2.08295328 4.72803677
 C  3.46424996 0.97086437 5.55939347
 C  -0.73651772 0.78379946 -1.74548134
 C  0.60164540 0.62801855 -1.36812946
 H  0.58467660 -2.71590705 -0.68334502
 H  -1.79673375 -2.43779460 -1.35176401
 H  -2.64606131 -0.19432618 -2.03420464
 H  -1.10344210 1.76605120 -2.04864956
```

```
 H   1.27939917 1.48347750 -1.36421620
 C   3.12449114 -0.26963732 5.00420221
 C   2.97513333 -0.40297090 3.62072156
 H   3.64945136 2.80654376 2.67929936
 H   3.91795159 3.05013518 5.15904128
 H   3.58048902 1.07105213 6.64008311
 H   2.97454695 -1.13560422 5.65102346
 H   2.70939560 -1.36519046 3.18441930
```

Ethyl Acetate

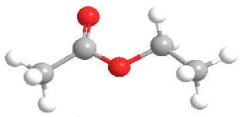

```
    14
 C   -0.61340347 -0.44730613 0.07378975
 C   0.61302004 0.43777972 0.05464133
 O   0.65776868 1.57755490 -0.36918082
 O   1.69294010 -0.22028842 0.56483431
 C   2.94012946 0.53170527 0.55870282
 H   -0.69023838 -0.99300803 1.02304863
 H   -0.53337417 -1.19257183 -0.73192322
 H   -1.50567582 0.16454872 -0.09292685
 C   4.01593409 -0.36087427 1.15114584
 H   2.79664411 1.45212920 1.14360709
 H   3.16802541 0.82380997 -0.47706794
 H   4.97511936 0.17691083 1.16039792
 H   4.14113460 -1.27698313 0.55734683
 H   3.77035397 -0.64434379 2.18404732
```

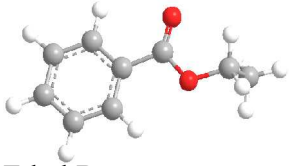

Ethyl Benzoate

```
 C   0.12167731 -0.29031154 -1.12638516
 C   0.46637712 0.39218966 0.19025819
 O   1.89470520 0.65827425 0.29260418
 C   2.65822223 -0.35575153 0.79014352
 C   4.10829793 0.00712038 0.84461914
 O   2.20446123 -1.43066217 1.15111676
 C   4.59105212 1.25776019 0.41897180
 C   5.95835169 1.53885434 0.49193092
 C   6.84917635 0.57794113 0.98749820
 C   6.37067582 -0.66870068 1.41259137
 C   5.00545626 -0.95395601 1.34230040
 H   0.46462789 0.30808274 -1.98200334
 H   -0.96974281 -0.40767113 -1.20384703
 H   0.57738268 -1.28766704 -1.18044722
 H   0.16063817 -0.21970356 1.04953432
 H   0.00373555 1.38548626 0.26240806
 H   3.89423110 2.00097310 0.03280460
 H   6.33028193 2.50976664 0.16051218
 H   7.91631309 0.80068311 1.04261461
 H   7.06310977 -1.41775686 1.80009318
 H   4.61009537 -1.91669527 1.66830932
```

number	Compound	ZPVE(kcal/mol)	E(Hartrees)	E(kcal/mol)	E0(Hartrees)	E0(kcal/mol)	G(kcal/mol)
A	ethyl acetate	71.7036	-59.53448	-37364.37546	-59.420214	-37292.66109	50.94
B	benzyl acetate	103.9837	-89.099852	-55919.86901	-88.934143	-55815.86855	79.7341
C	ethyl benzoate	104.6466	-89.103976	-55922.45727	-88.937212	-55817.79469	81.5611
D	benzyl benzoate	137.1105	-118.670021	-74478.37321	-118.451522	-74341.24127	110.2215

Computational details**.**

Theoretical calculations in this work have been performed using density functional theory (DFT) method,[8] specifically functional PBE,[9] implemented in an original program package "Priroda".[10,11] In PBE calculations relativistic Stevens-Basch-Krauss (SBK) effective core potentials (ECP)[12] optimized for DFT-calculations have been used. Basis set was 311-split for main group elements with one additional polarization *p*-function for hydrogen. Full geometry optimization has been performed without constraints on symmetry. For all species under investigation frequency analysis has been carried out. All minima have been checked for the absence of imaginary frequencies.

GC/FID spectra of metathesis and hydrogenation reactions

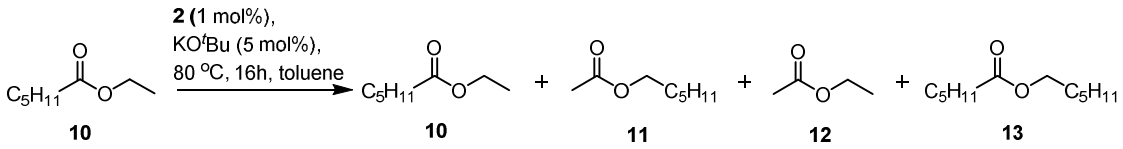

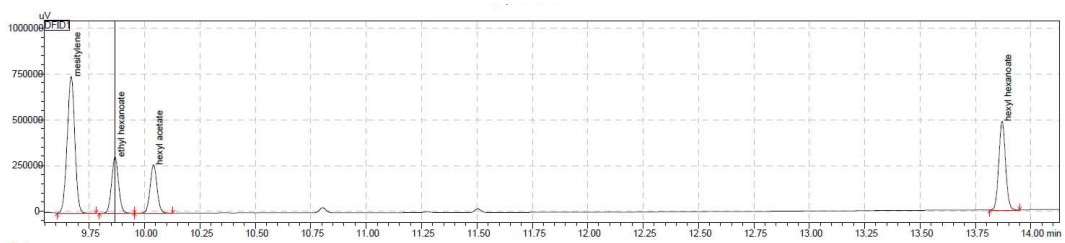

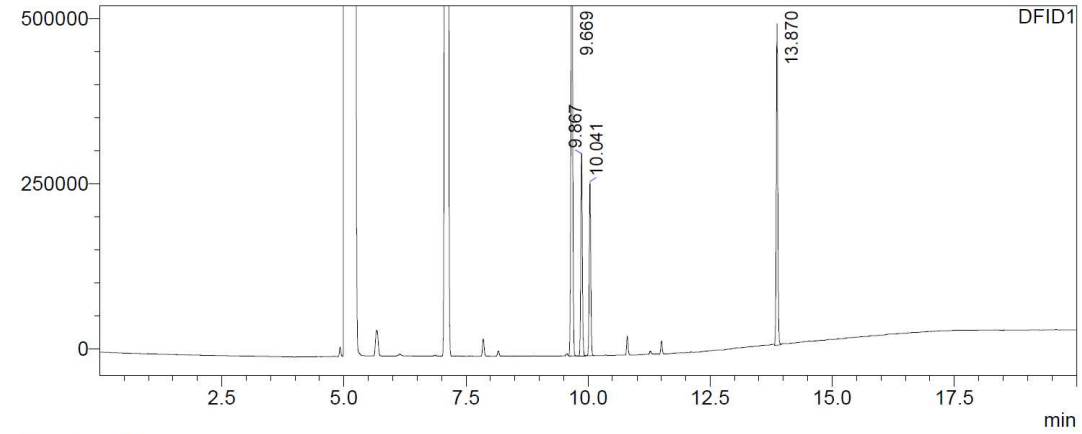

<Peak Table>

DFID1

Peak#	Ret. Time	Area	Height	Conc.	Unit	Mark	Name
1	9.669	1786215	740858	43.979	ppm	V	mesitylene
2	9.867	668937	302887	16.470	ppm		ethyl hexanoate
3	10.041	570336	262418	14.042	ppm	V	hexyl acetate
4	13.870	1036024	477682	25.508	ppm	V	hexyl hexanoate
Total		4061512	1783845				

% efficiency of metathesis calculated based on the difference between two esters **11** and **10** with respect to internal standard and conversion factor.

Figure S26. GC chromatograph (Table-1, entry-1)

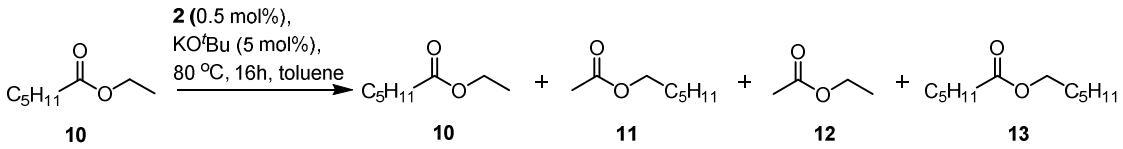

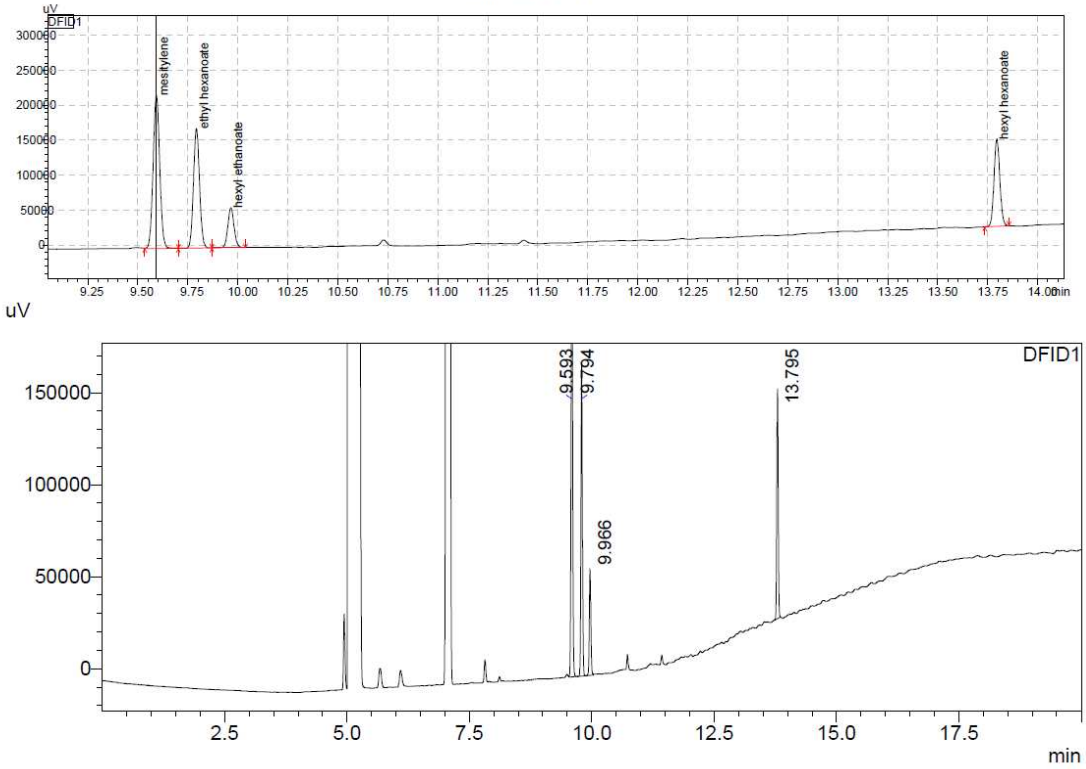

<Peak Table>

DFID1

Peak#	Ret. Time	Area	Height	Conc.	Unit	Mark	Name
1	9.593	504061	217959	40.498	ppm	V	mesitylene
2	9.794	361978	169915	29.083	ppm	V	ethyl hexanoate
3	9.966	125921	56995	10.117	ppm	V	hexyl ethanoate
4	13.795	252696	123029	20.302	ppm	M	hexyl hexanoate
Total		1244656	567899				

% efficiency of metathesis calculated based on the difference between two esters **11** and **10** with respect to internal standard and conversion factor.

Figure S27. GC chromatograph (Table-1, entry-2)

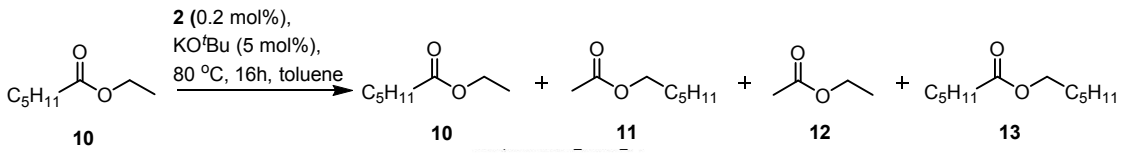

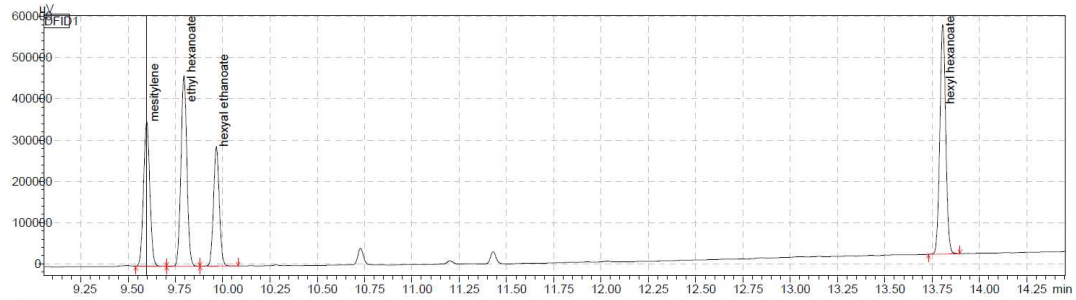

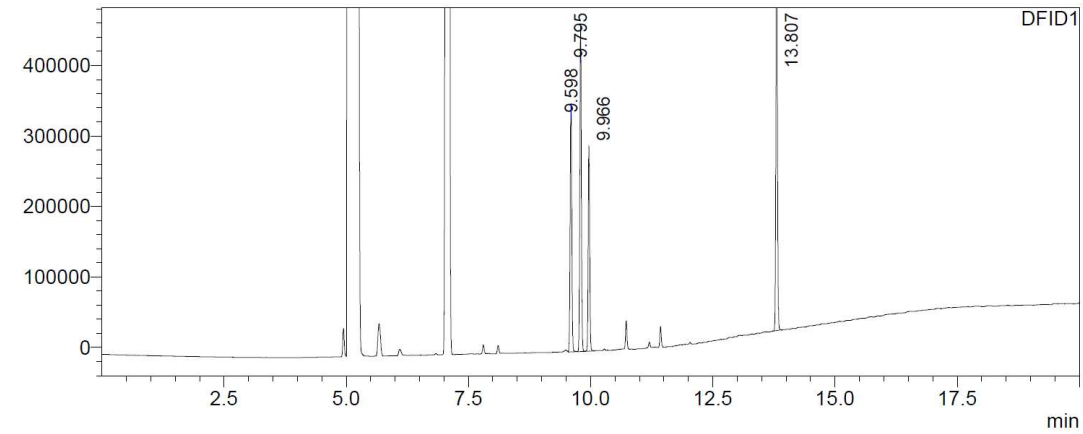

<Peak Table>

DFID1

Peak#	Ret. Time	Area	Height	Conc.	Unit	Mark	Name
1	9.598	815644	350076	22.411	ppm	V	mesitylene
2	9.795	1007874	458590	27.692	ppm	V	ethyl hexanoate
3	9.966	618364	288910	16.990	ppm	V	hexyal ethanoate
4	13.807	1197654	552137	32.907	ppm	M	hexyl hexanoate
Total		3639536	1649713				

% efficiency of metathesis calculated based on the difference between two esters **11** and **10** with respect to internal standard and conversion factor.

Figure S28. GC chromatograph (Table-1, entry-3)

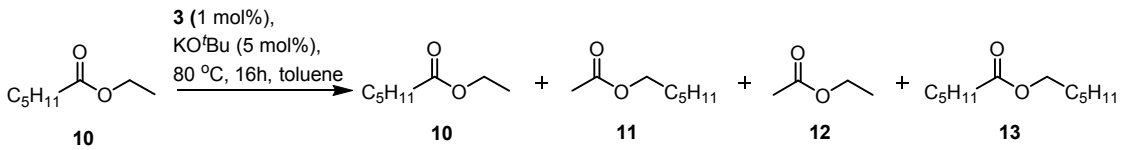

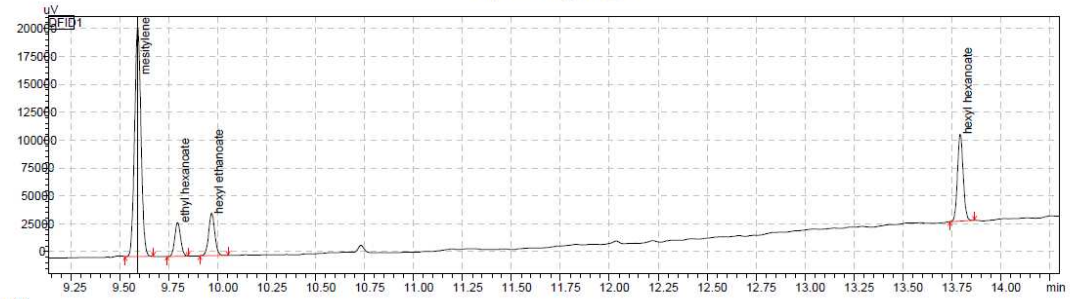

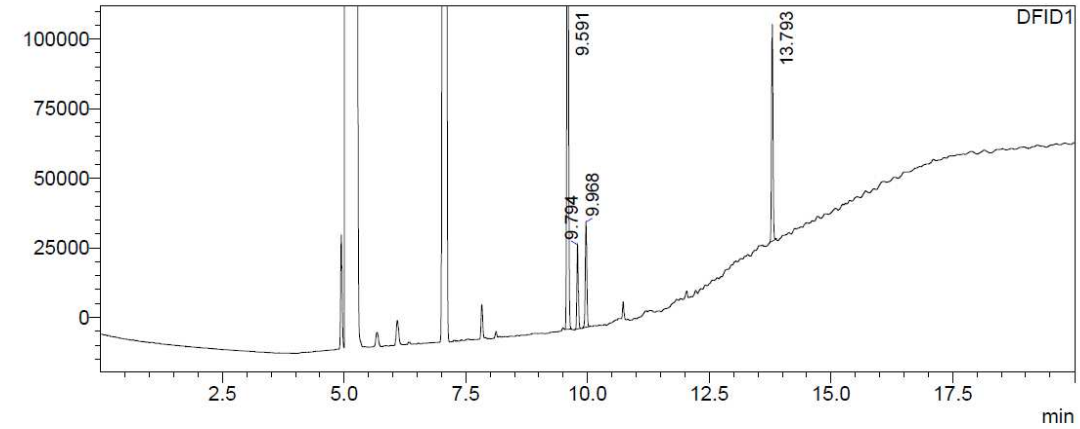

<Peak Table>

DFID1

Peak#	Ret. Time	Area	Height	Conc.	Unit	Mark	Name
1	9.591	468706	202787	60.696	ppm	M	mesitylene
2	9.794	63210	30151	8.186	ppm	M	ethyl hexanoate
3	9.968	82535	37458	10.688	ppm	M	hexyl ethanoate
4	13.793	157771	77333	20.431	ppm	M	hexyl hexanoate
Total		772222	347729				

As **11** is ≥ than starting material **10**, % efficiency is quantitative

Figure S29. GC chromatograph (Table-1, entry-4)

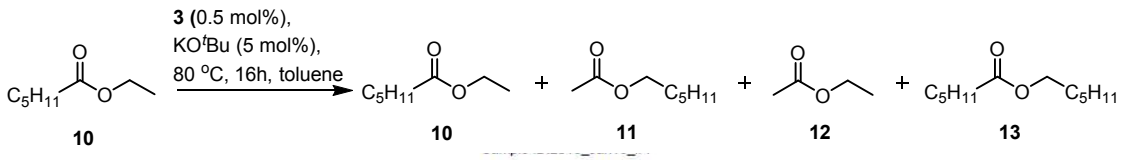

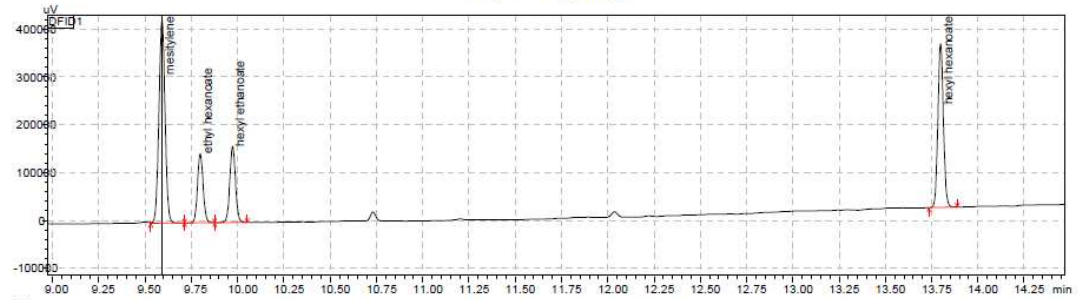

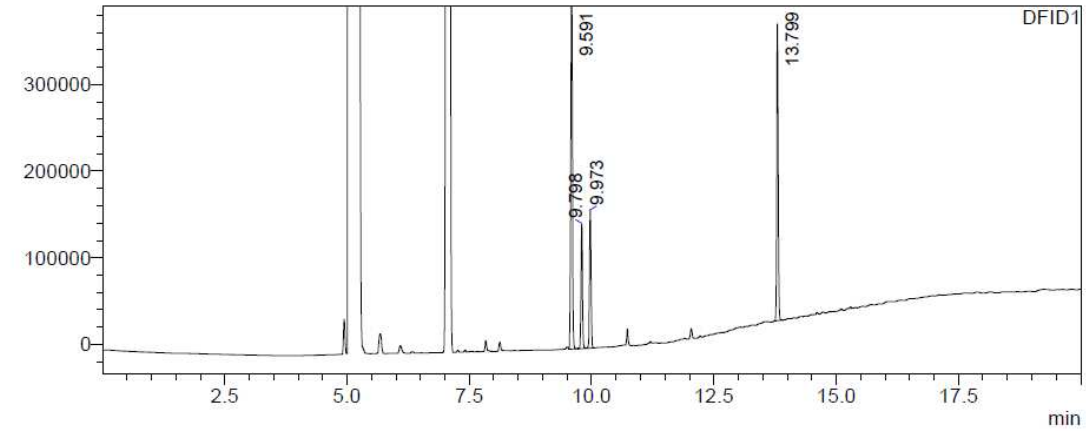

<Peak Table>

DFID1

Peak#	Ret. Time	Area	Height	Conc.	Unit	Mark	Name
1	9.591	971768	416046	41.753	ppm	V	mesitylene
2	9.798	304817	143410	13.097	ppm	V	ethyl hexanoate
3	9.973	342974	158467	14.736	ppm	V	hexyl ethanoate
4	13.799	707855	339842	30.414	ppm	M	hexyl hexanoate
Total		2327415	1057765				

As **11** is ≥ than starting material **10**, % efficiency is quantitative

Figure S30. GC chromatograph (Table-1, entry-5)

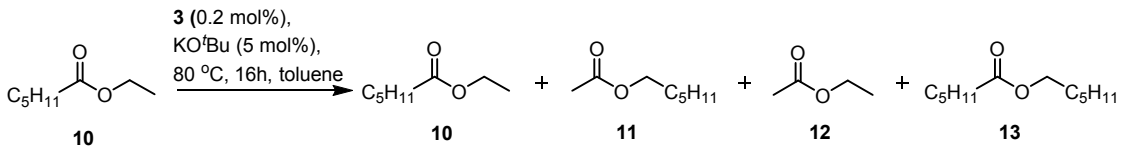

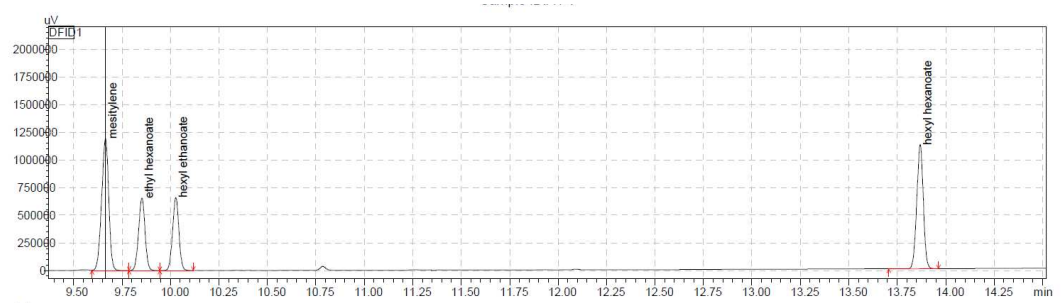

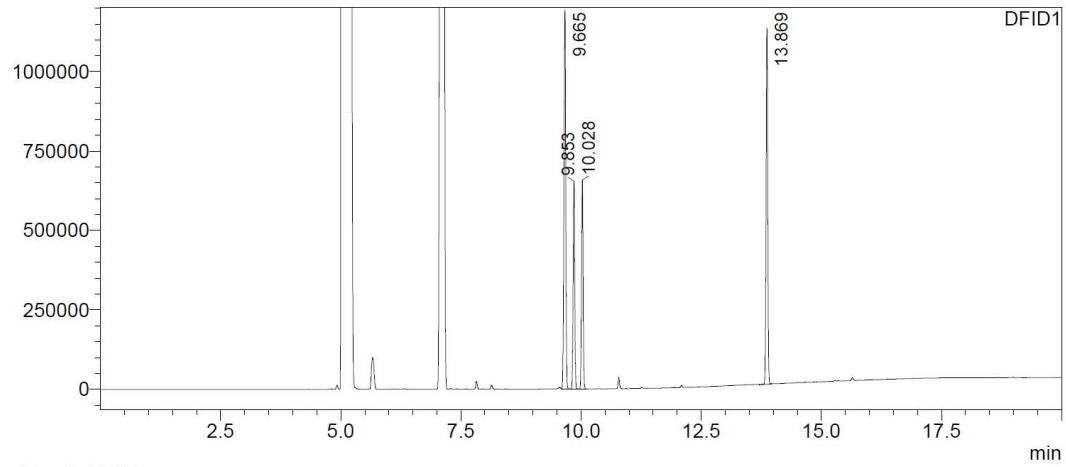

<Peak Table>

DFID1

Peak#	Ret. Time	Area	Height	Conc.	Unit	Mark	Name
1	9.665	3037546	1181817	34.998	ppm	V	mesitylene
2	9.853	1511539	650098	17.416	ppm		ethyl hexanoate
3	10.028	1486378	653908	17.126	ppm	V	hexyl ethanoate
4	13.869	2643616	1115234	30.460	ppm	V	hexyl hexanoate
Total		8679079	3601057				

% efficiency of metathesis calculated based on the difference between two esters **11** and **10** with respect to internal standard and conversion factor.

Figure S31. GC chromatograph (Table-1, entry-6)

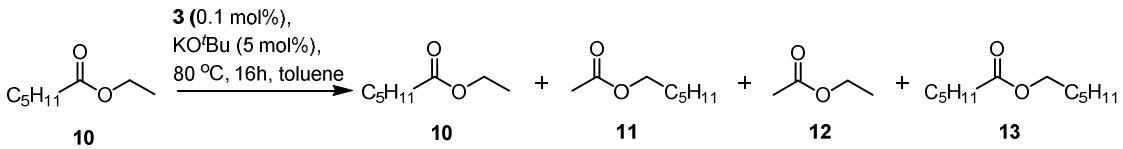

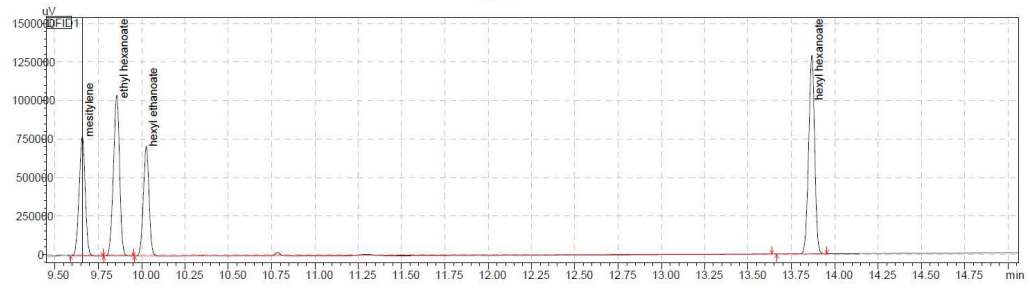

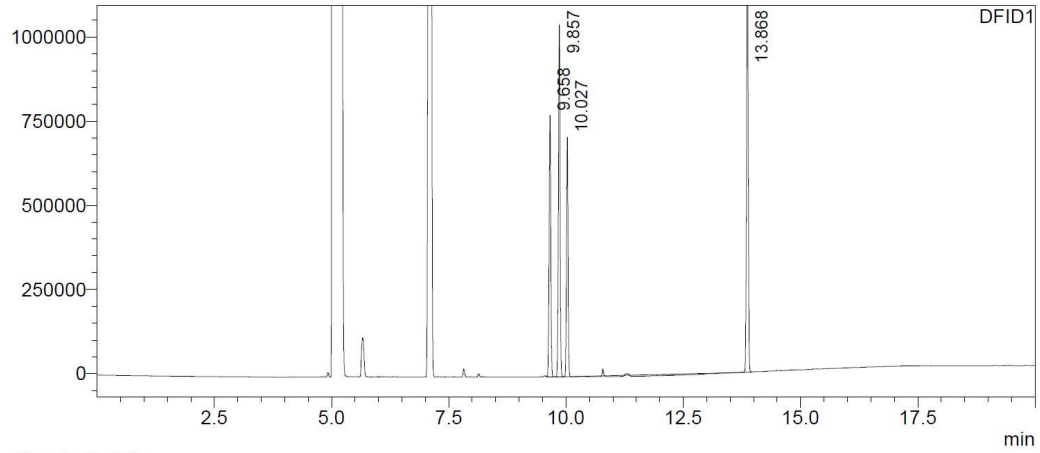

<Peak Table>

DFID1

Peak#	Ret. Time	Area	Height	Conc.	Unit	Mark	Name
1	9.658	1915128	772227	22.068	ppm	V	mesitylene
2	9.857	2577437	1031657	29.700	ppm		ethyl hexanoate
3	10.027	1058053	707888	12.192	ppm	S	hexyl ethanoate
4	13.868	3127592	1284281	36.040	ppm		hexyl hexanoate
Total		8678210	3796053				

% efficiency of metathesis calculated based on the difference between two esters **11** and **10** with respect to internal standard and conversion factor.

Figure S32. GC chromatograph (Table-1, entry-7)

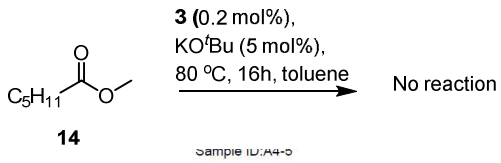

14

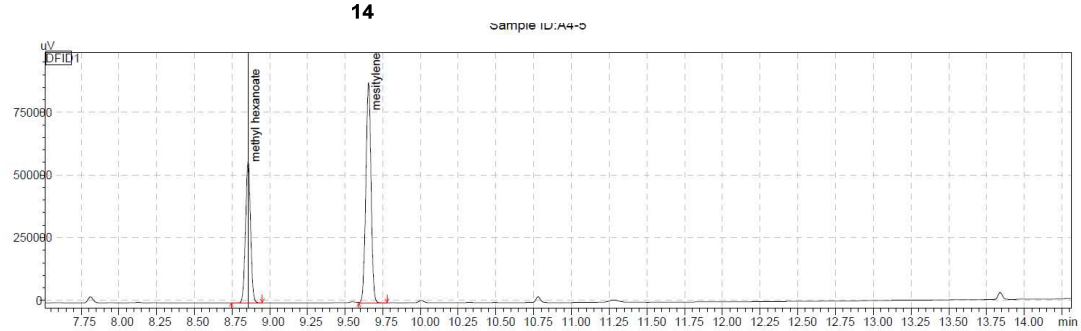

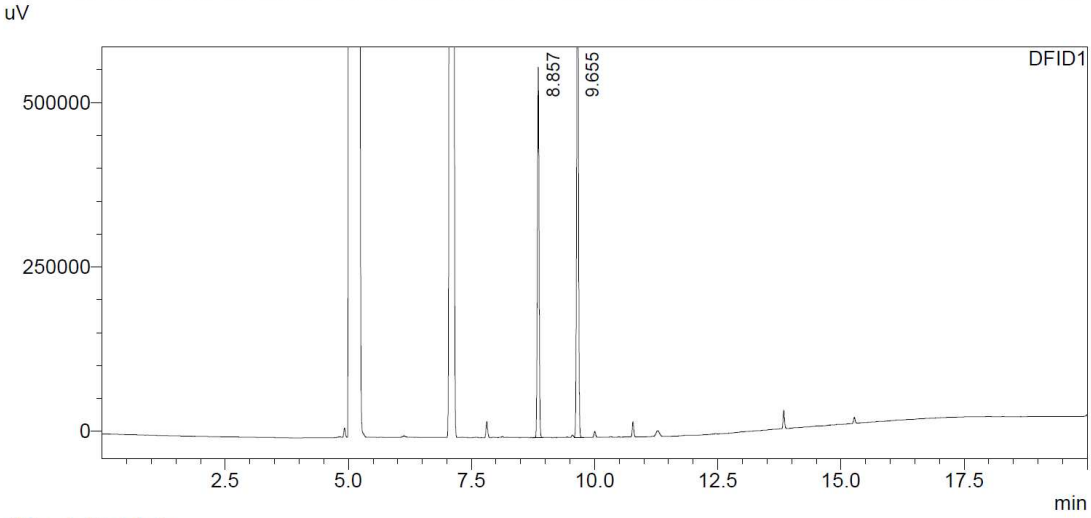

<Peak Table>

DFID1

Peak#	Ret. Time	Area	Height	Conc.	Unit	Mark	Name
1	8.857	1308622	557869	38.443	ppm	V	methyl hexanoate
2	9.655	2095453	872498	61.557	ppm	V	mesitylene
Total		3404075	1430367				

Figure S33. GC chromatograph (Table-2, Entry-1)

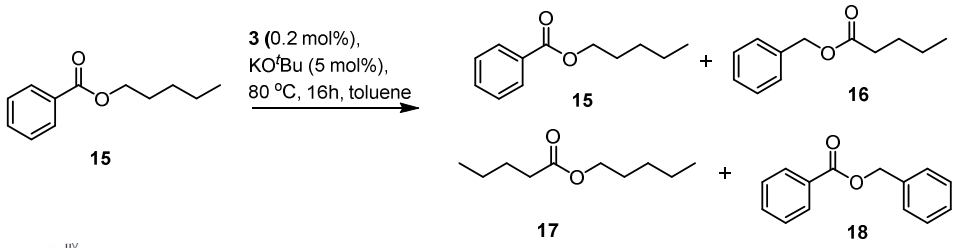

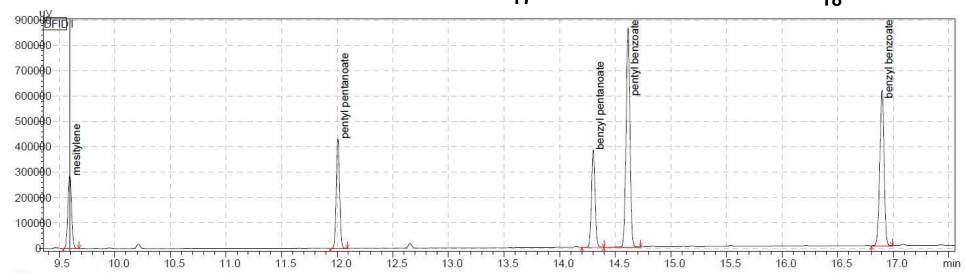

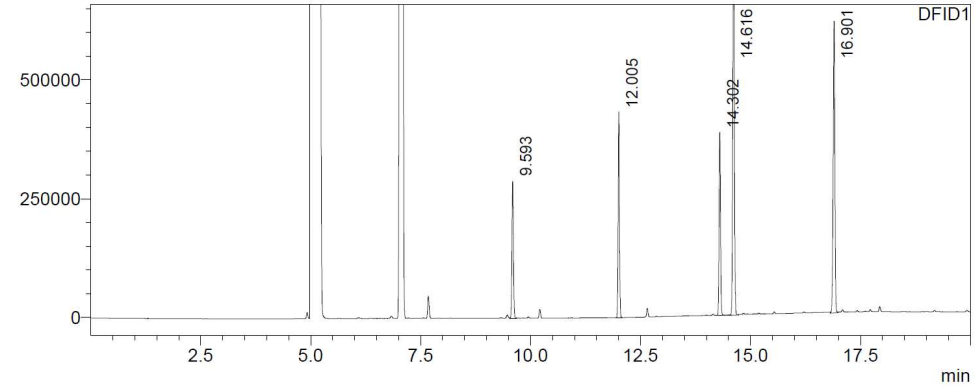

<Peak Table>

DFID1

Peak#	Ret. Time	Area	Height	Conc.	Unit	Mark	Name
1	9.593	670681	288175	10.800	ppm	V	mesitylene
2	12.005	911694	429928	14.681	ppm	V	pentyl pentanoate
3	14.302	867900	383100	13.976	ppm	V	benzyl pentanoate
4	14.616	2109713	857436	33.974	ppm	V	pentyl benzoate
5	16.901	1649879	612403	26.569	ppm	V	benzyl benzoate
Total		6209867	2571042				

Metathesis efficiency is 99% due to benzyl benzoate being ~26% (should be 25). Pentyl benzoate **15**, the starting material, is more stable than benzyl pentanoate **16**, so efficiency cannot be measured from taking the difference of the two mixed aryl/alkyl esters.

Figure S34. GC chromatograph (Table-2, Entry-3)

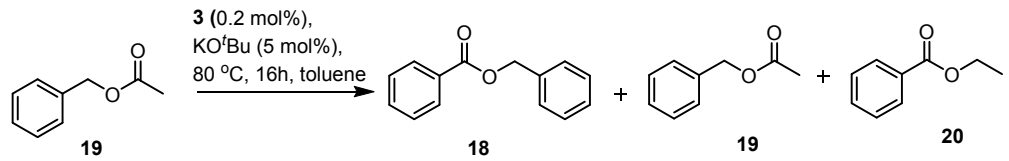

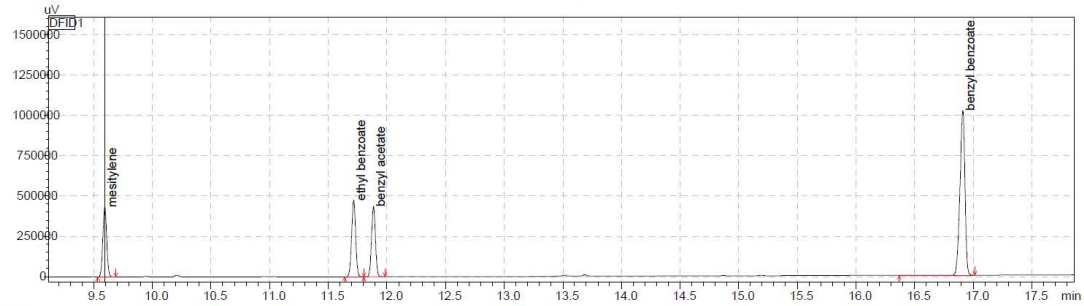

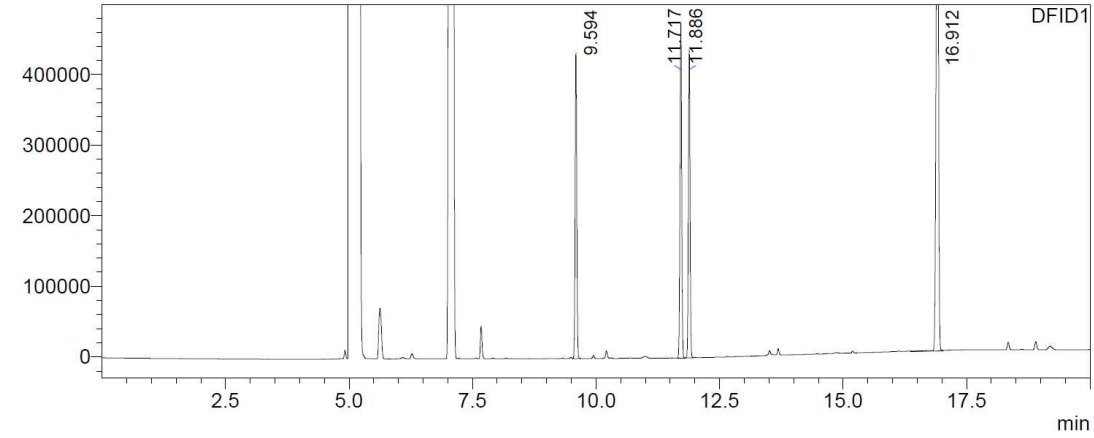

<Peak Table>

DFID1

Peak#	Ret. Time	Area	Height	Conc.	Unit	Mark	Name
1	9.594	1000568	432433	16.124	ppm	V	mesitylene
2	11.717	1133712	472329	18.269	ppm		ethyl benzoate
3	11.886	1007358	434539	16.233	ppm	V	benzyl acetate
4	16.912	3063891	1015804	49.374	ppm	V	benzyl benzoate
Total		6205529	2355105				

As **20** is ≥ than starting material **19**, % efficiency is quantitative

Figure S35. GC chromatograph (Table-2, Entry-4)

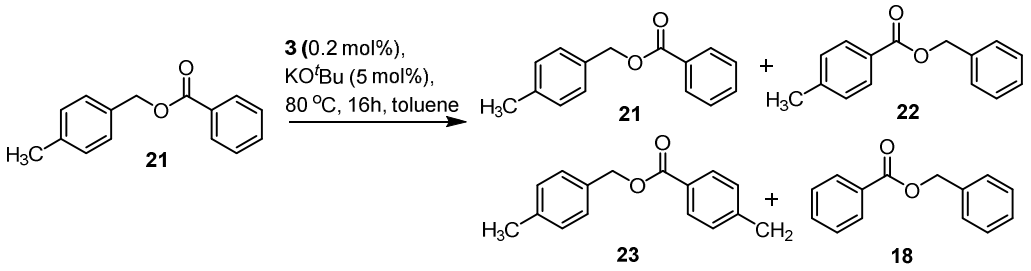

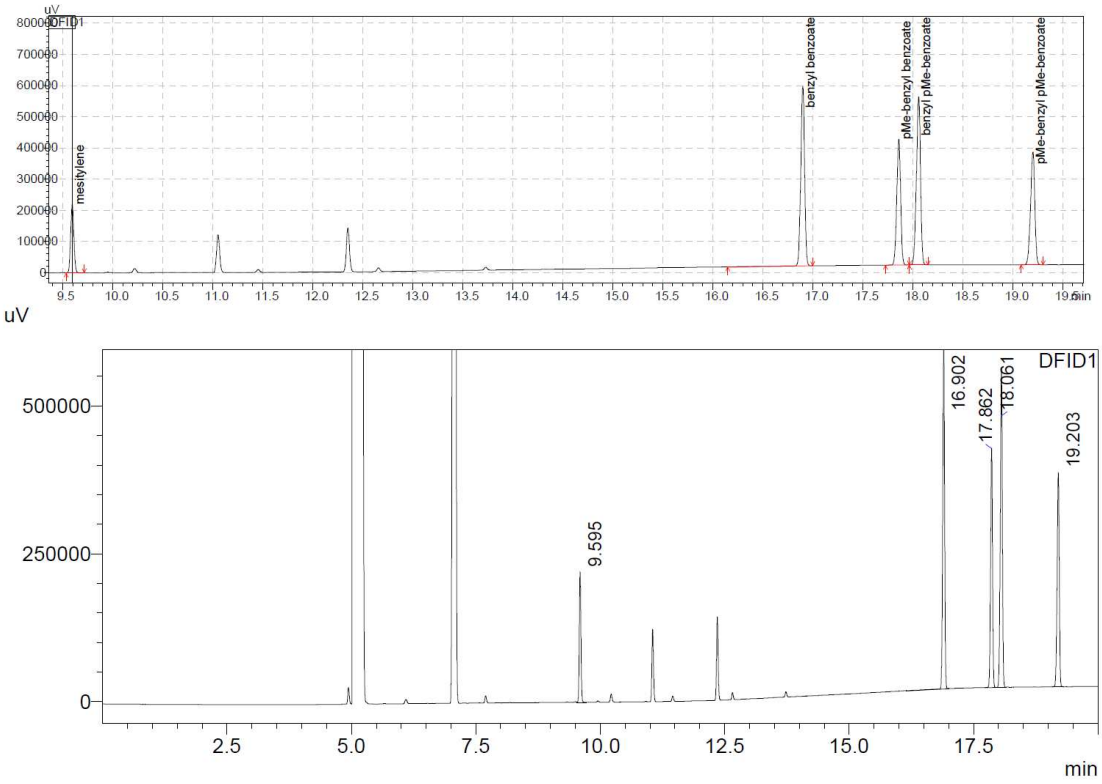

<Peak Table>

DFID1

Peak#	Ret. Time	Area	Height	Conc.	Unit	Mark	Name
1	9.595	499020	216941	8.704	ppm	V	mesitylene
2	16.902	1545912	574222	26.965	ppm	V	benzyl benzoate
3	17.862	1083863	402990	18.906	ppm		pMe-benzyl benzoate
4	18.061	1534721	536141	26.770	ppm	V	benzyl pMe-benzoate
5	19.203	1069478	359187	18.655	ppm		pMe-benzyl pMe-benzoate
Total		5732995	2089481				

As **22** is ≥ than starting material **21**, % efficiency is quantitative

Figure S36. GC chromatograph (Table-2, Entry-5)

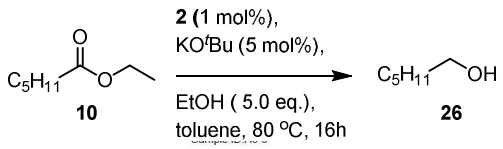

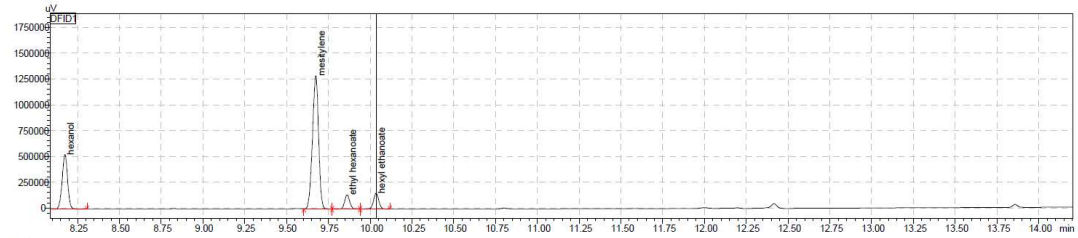

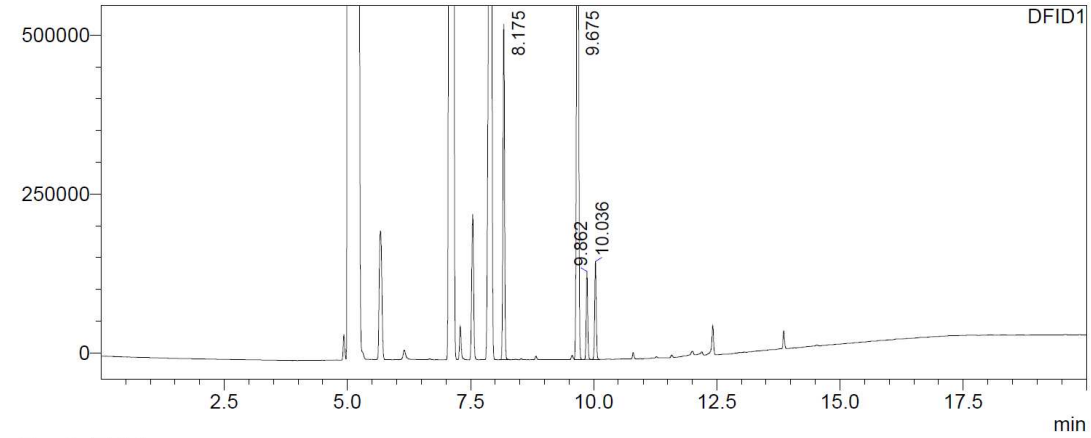

<Peak Table>

DFID1

Peak#	Ret. Time	Area	Height	Conc.	Unit	Mark	Name
1	8.175	1204771	525389	23.520	ppm		hexanol
2	9.675	3287751	1279433	64.184	ppm	V	mesitylene
3	9.862	290504	136971	5.671	ppm		ethyl hexanoate
4	10.036	339392	153253	6.626	ppm	V	hexyl ethanoate
Total		5122419	2095045				

Conversion factor for hexanol **26** with respect to mesitylene is 0.65

Figure S37. GC chromatograph (Table-3, Entry-1)

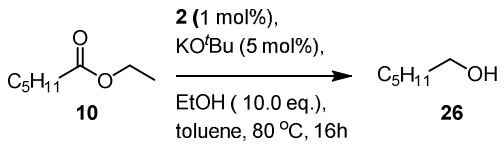

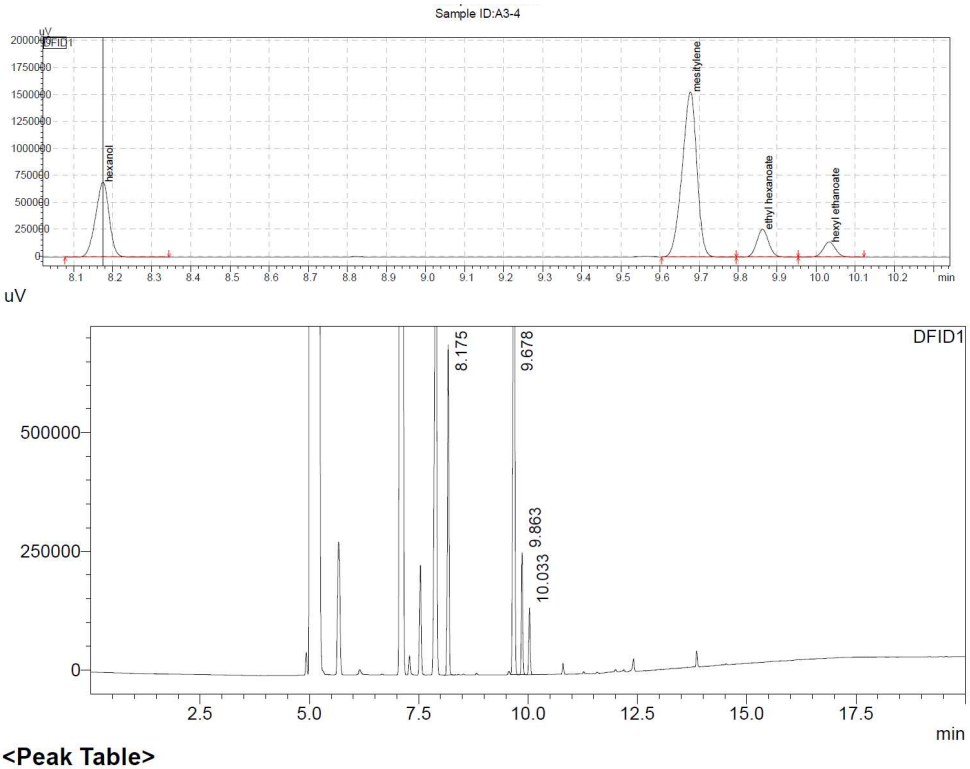

<Peak Table>

DFID1

Peak#	Ret. Time	Area	Height	Conc.	Unit	Mark	Name
1	8.175	1689331	692498	25.731	ppm	M	hexanol
2	9.678	4016219	1523652	61.174	ppm	V	mesitylene
3	9.863	548282	256030	8.351	ppm		ethyl hexanoate
4	10.033	311419	138738	4.743	ppm	V	hexyl ethanoate
Total		6565251	2610918				

Figure S38. GC chromatograph (Table-3, Entry-2)

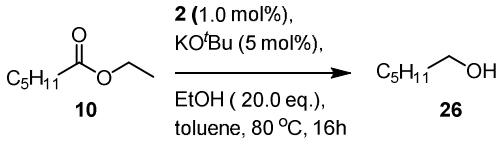

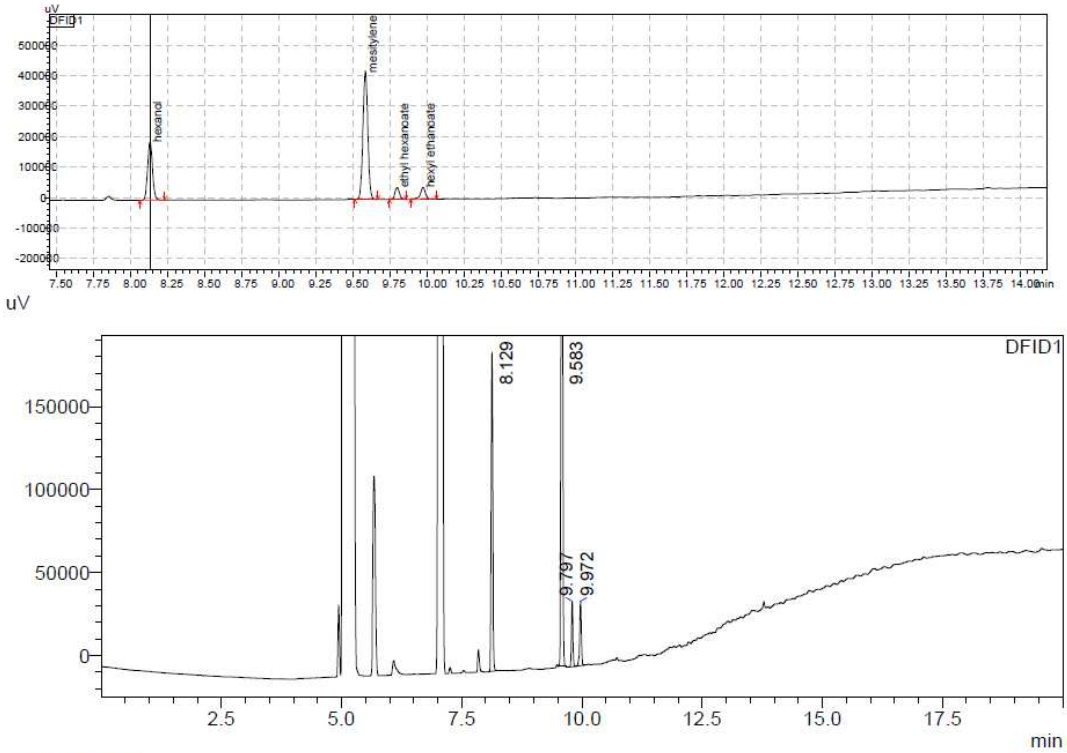

<Peak Table>

DFID1

Peak#	Ret. Time	Area	Height	Conc.	Unit	Mark	Name
1	8.129	440428	189722	27.940	ppm	M	hexanol
2	9.583	962072	418104	61.032	ppm	M	mesitylene
3	9.797	82509	38793	5.234	ppm	M	ethyl hexanoate
4	9.972	91330	38654	5.794	ppm	M	hexyl ethanoate
Total		1576339	685273				

Figure S39. GC chromatograph (Table-3, Entry-3)

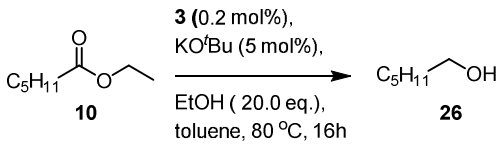

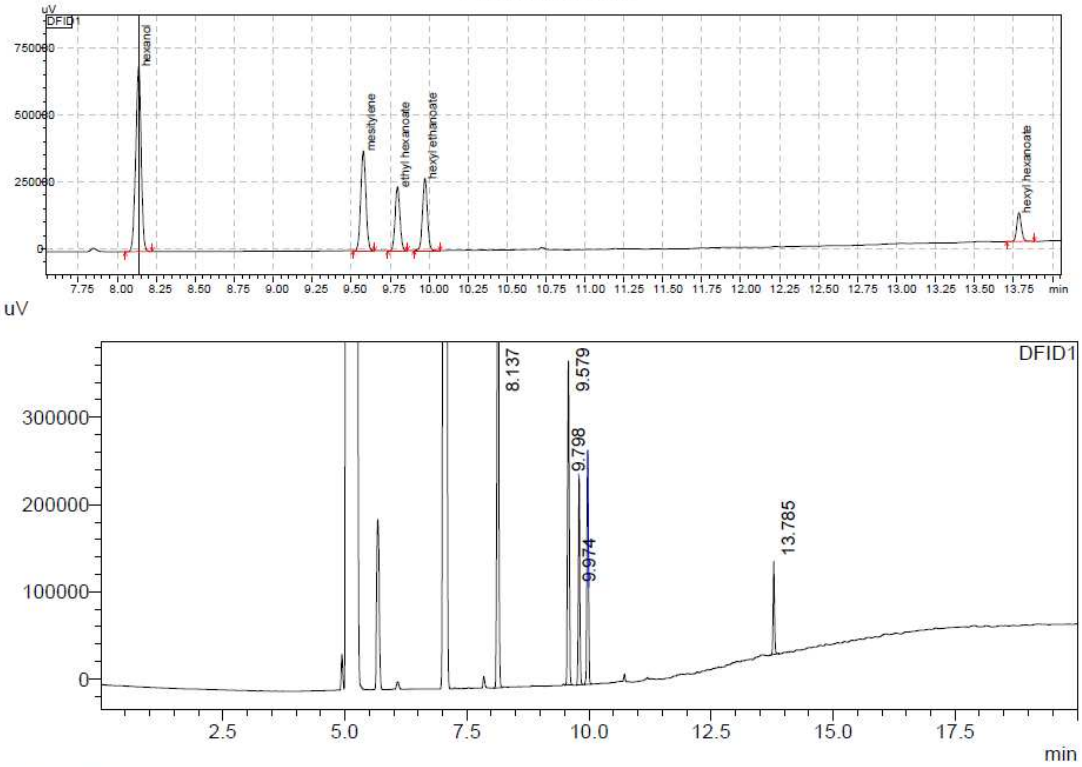

<Peak Table>

DFID1

Peak#	Ret. Time	Area	Height	Conc.	Unit	Mark	Name
1	8.137	1671871	687199	43.613	ppm		hexanol
2	9.579	859456	370054	22.420	ppm	M	mesitylene
3	9.798	506374	236697	13.209	ppm	M	ethyl hexanoate
4	9.974	576599	263554	15.041	ppm	M	hexyl ethanoate
5	13.785	219130	106149	5.716	ppm	M	hexyl hexanoate
Total		3833429	1663654				

Figure S40. GC chromatograph (Table-3, Entry-4)

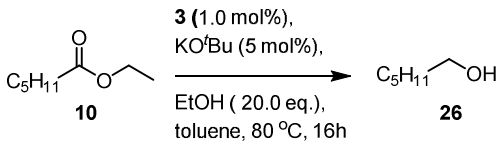

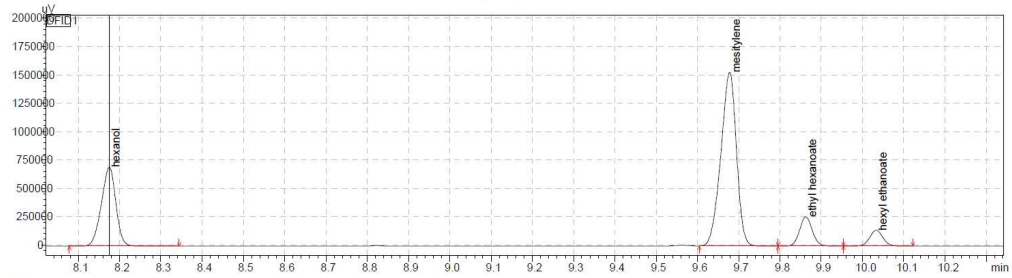

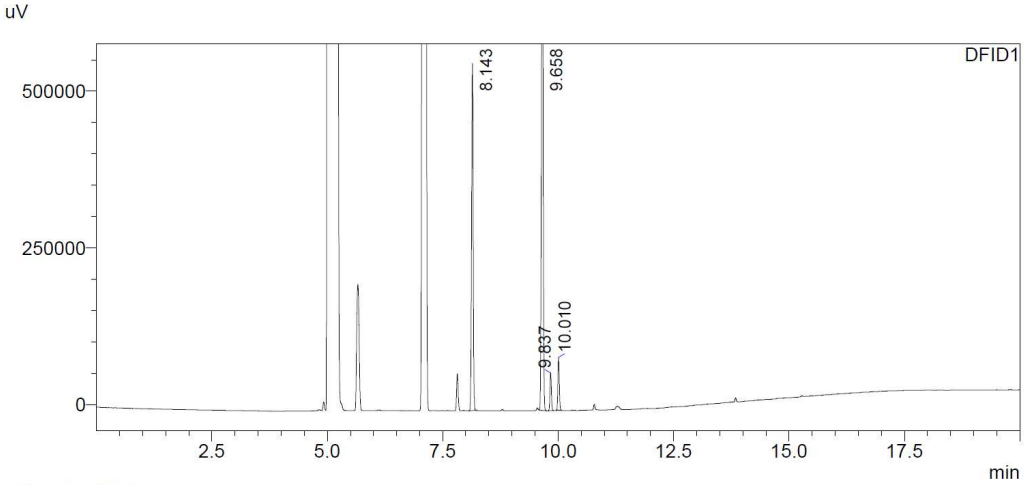

<Peak Table>

DFID1

Peak#	Ret. Time	Area	Height	Conc.	Unit	Mark	Name
1	8.143	1324306	547305	33.708	ppm	M	hexanol
2	9.658	2298225	949926	58.498	ppm		mesitylene
3	9.837	127602	59275	3.248	ppm	M	ethyl hexanoate
4	10.010	178588	83234	4.546	ppm	M	hexyl ethanoate
Total		3928720	1639740				

Figure S41. GC chromatograph (Table-3, Entry-5)

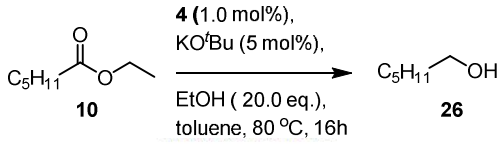

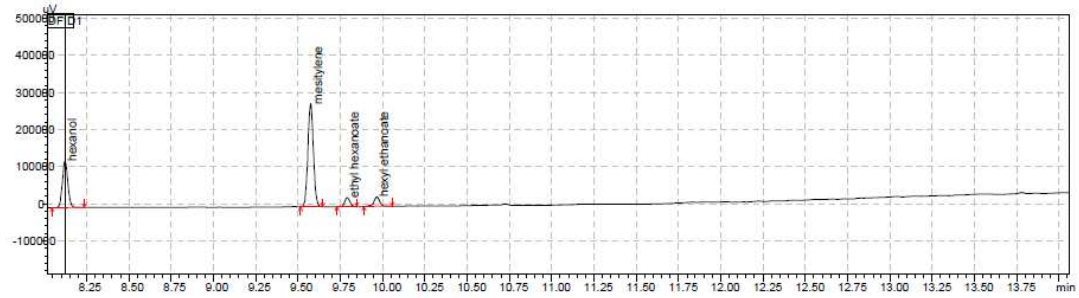

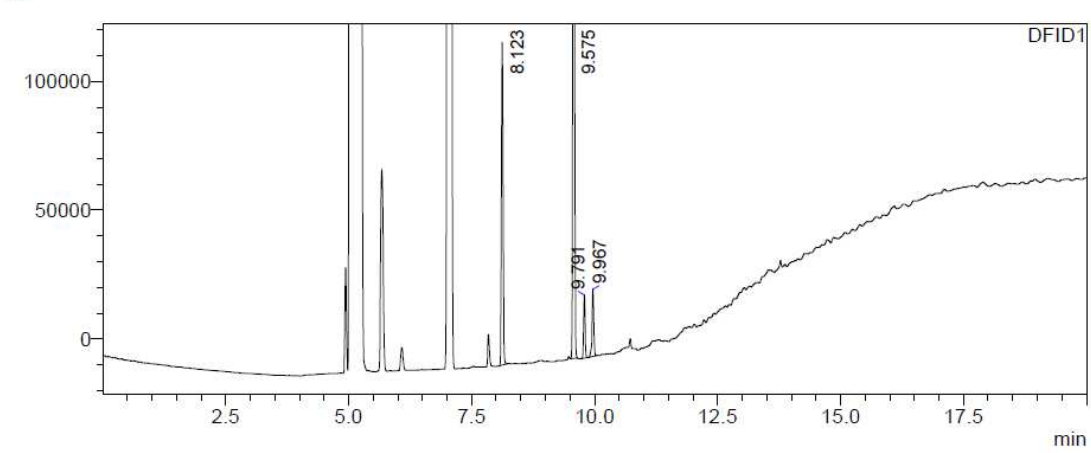

<Peak Table>

DFID1

Peak#	Ret. Time	Area	Height	Conc.	Unit	Mark	Name
1	8.123	285064	124639	27.758	ppm	M	hexanol
2	9.575	630027	276096	61.350	ppm	M	mesitylene
3	9.791	50654	24181	4.932	ppm	M	ethyl hexanoate
4	9.967	61202	25940	5.960	ppm	M	hexyl ethanoate
Total		1026946	450856				

Figure S42. GC chromatograph (Table-3, Entry-6)

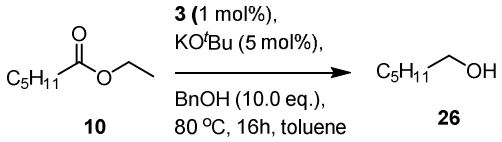

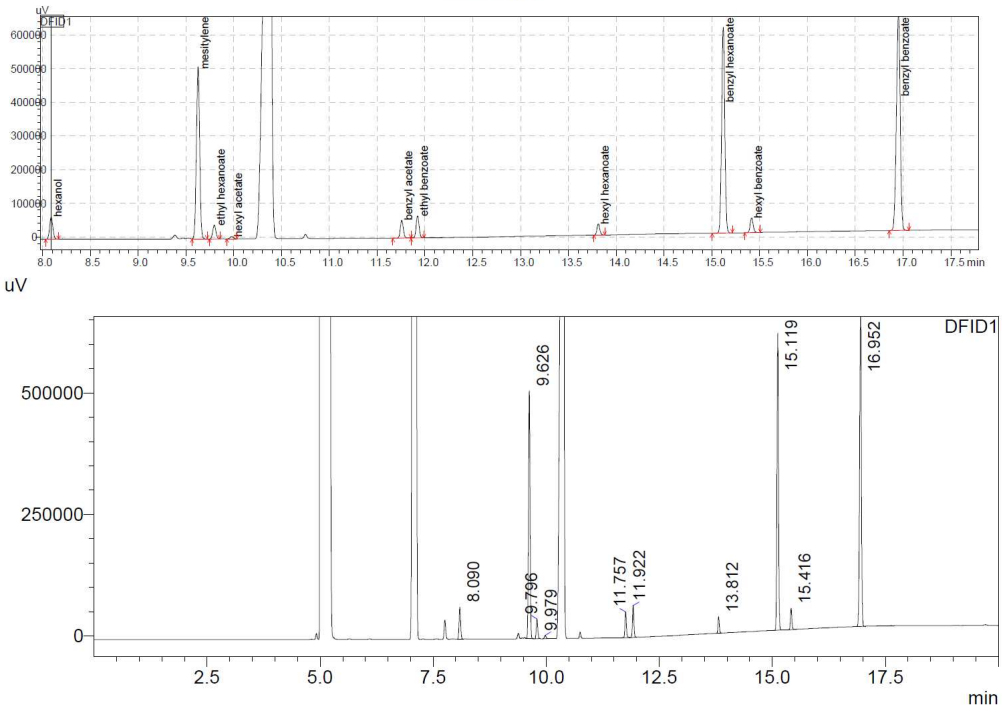

<Peak Table>

DFID1

Peak#	Ret. Time	Area	Height	Conc.	Unit	Mark	Name
1	8.090	156236	65514	3.083	ppm		hexanol
2	9.626	1214299	509089	23.960	ppm	V	mesitylene
3	9.796	93701	40184	1.849	ppm	M	ethyl hexanoate
4	9.979	16946	6870	0.334	ppm	M	hexyl acetate
5	11.757	116291	52502	2.295	ppm		benzyl acetate
6	11.922	143197	65437	2.826	ppm	V	ethyl benzoate
7	13.812	67327	33055	1.328	ppm	M	hexyl hexanoate
8	15.119	1408140	607414	27.785	ppm		benzyl hexanoate
9	15.416	94317	43209	1.861	ppm	M	hexyl benzoate
10	16.952	1757551	644027	34.679	ppm	M	benzyl benzoate
Total		5068005	2067302				

Figure S43. GC chromatograph (Table-3, Entry-7)

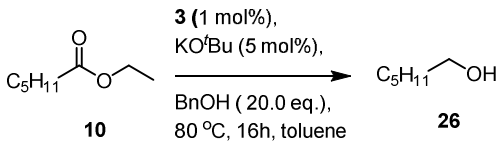

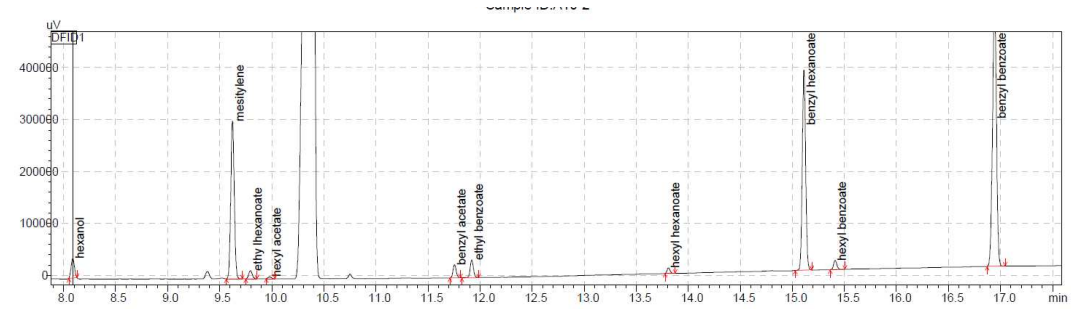

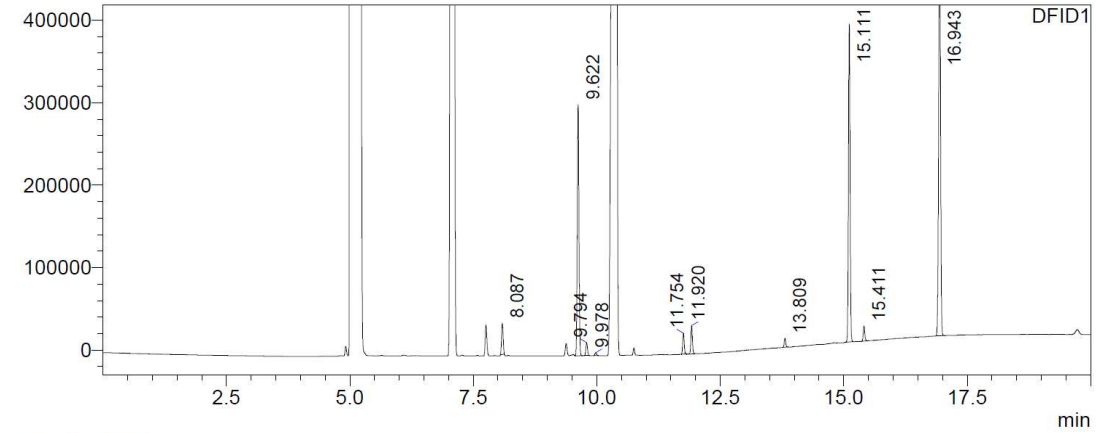

<Peak Table>

DFID1

Peak#	Ret. Time	Area	Height	Conc.	Unit	Mark	Name
1	8.087	84084	37214	2.590	ppm	M	hexanol
2	9.622	714672	303320	22.014	ppm	V	mesitylene
3	9.794	36958	15620	1.138	ppm	M	ethy lhexanoate
4	9.978	7483	3245	0.230	ppm	M	hexyl acetate
5	11.754	53359	25155	1.644	ppm	M	benzyl acetate
6	11.920	75416	33818	2.323	ppm		ethyl benzoate
7	13.809	21661	10632	0.667	ppm	M	hexyl hexanoate
8	15.111	869849	381046	26.794	ppm	M	benzyl hexanoate
9	15.411	39421	17832	1.214	ppm	M	hexyl benzoate
10	16.943	1343473	510964	41.384	ppm	M	benzyl benzoate
Total		3246376	1338846				

Figure S44. GC chromatograph (Table-3, Entry-8)

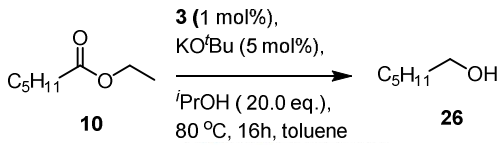

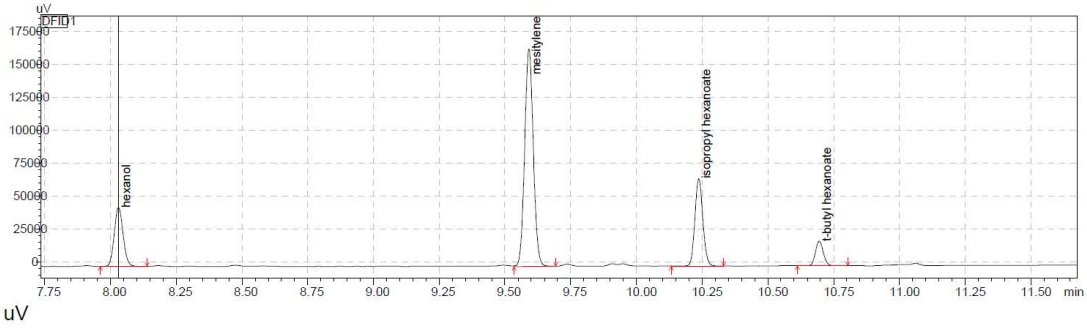

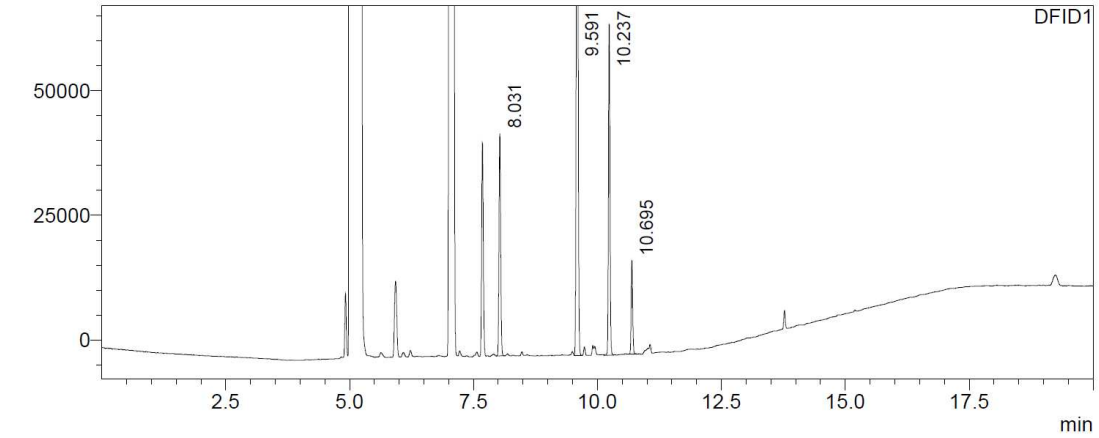

<Peak Table>

DFID1

Peak#	Ret. Time	Area	Height	Conc.	Unit	Mark	Name
1	8.031	104244	44391	15.808	ppm	M	hexanol
2	9.591	375227	162671	56.903	ppm	V	mesitylene
3	10.237	140645	66092	21.329	ppm	V	isopropyl hexanoate
4	10.695	39302	18662	5.960	ppm	M	t-butyl hexanoate
Total		659417	291816				

Figure S45. GC chromatograph (Table-3, Entry-9)

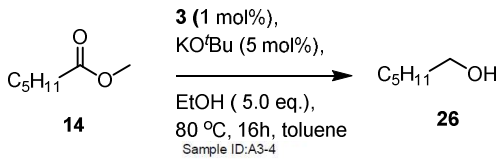

Sample ID:A3-4

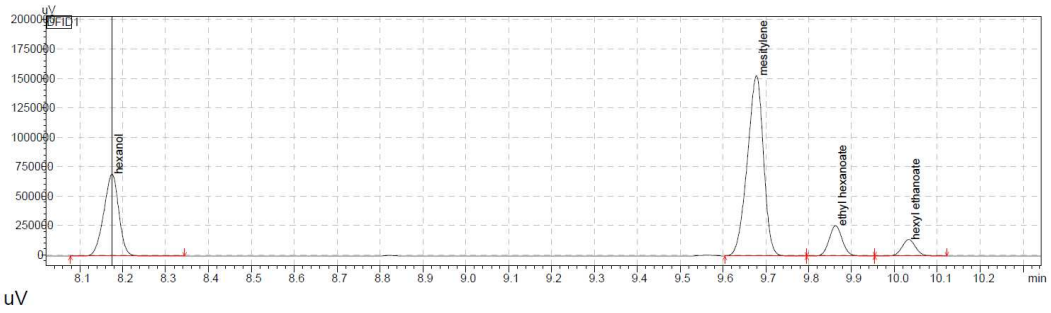

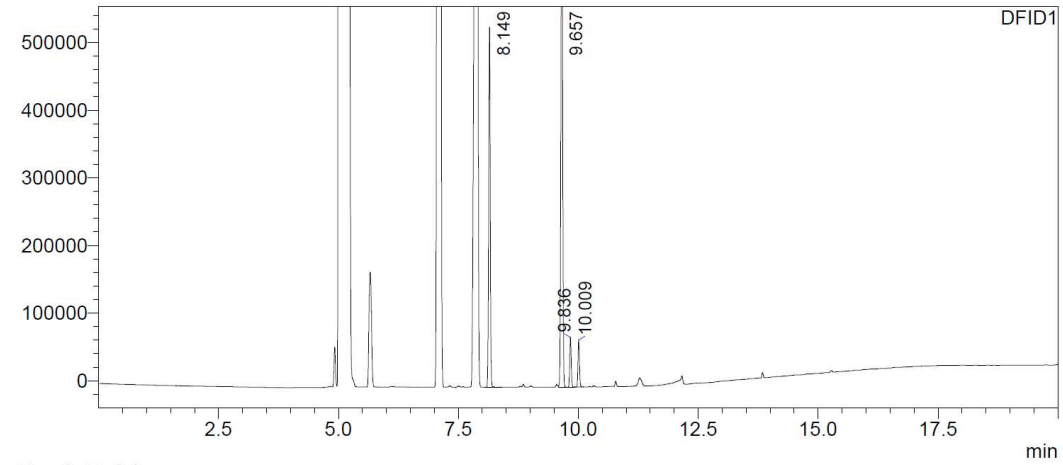

<Peak Table>

DFID1

Peak#	Ret. Time	Area	Height	Conc.	Unit	Mark	Name
1	8.149	1200587	526500	33.540	ppm	S	hexanol
2	9.657	2072929	853797	57.909	ppm	V	mesitylene
3	9.836	157848	73312	4.410	ppm		ethyl hexanoate
4	10.009	148243	69163	4.141	ppm	V	hexyl ethanoate
Total		3579607	1522771				

Conversion factor for hexanol **26** was determined to be 0.65

Figure S46. GC chromatograph (Table-4, Entry-1)

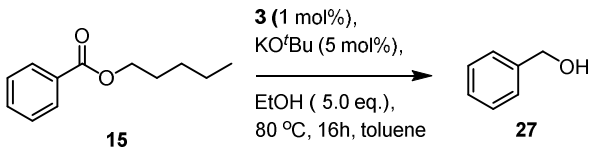

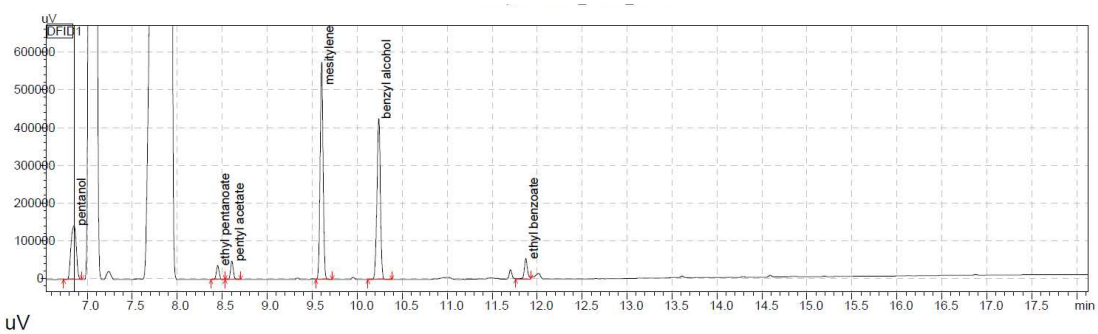

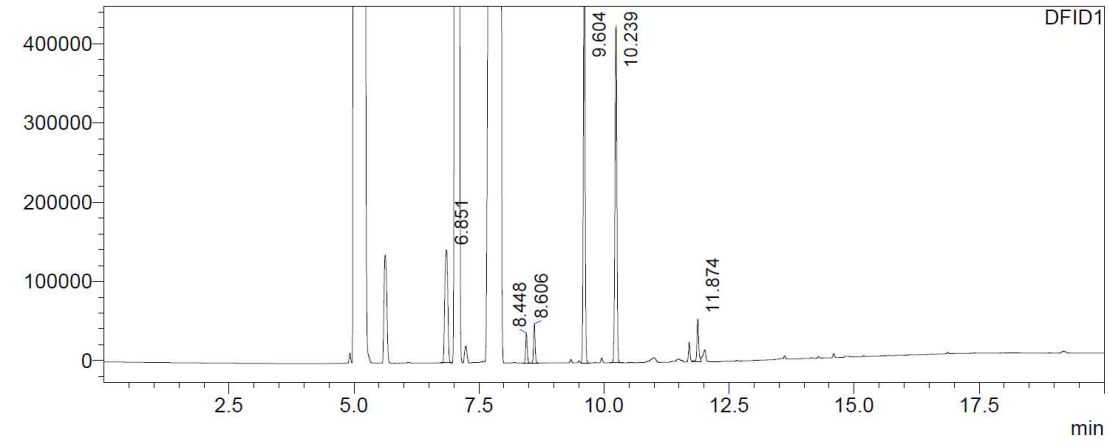

<Peak Table>

DFID1

Peak#	Ret. Time	Area	Height	Conc.	Unit	Mark	Name
1	6.851	588624	142662	17.587	ppm	M	pentanol
2	8.448	81367	37330	2.431	ppm	V	ethyl pentanoate
3	8.606	104350	48218	3.118	ppm	V	pentyl acetate
4	9.604	1313541	570927	39.247	ppm	V	mesitylene
5	10.239	1124616	421144	33.602	ppm	V	benzyl alcohol
6	11.874	134374	54204	4.015	ppm	V	ethyl benzoate
Total		3346871	1274485				

Conversion factor for benzyl alcohol **27** was determined to be 0.95

Figure S47. GC chromatograph (Table-4, Entry-2)

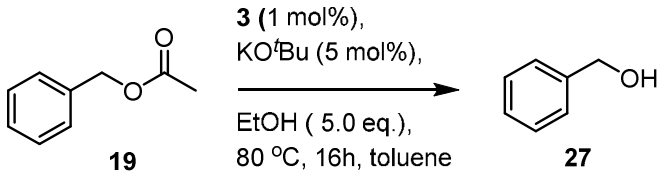

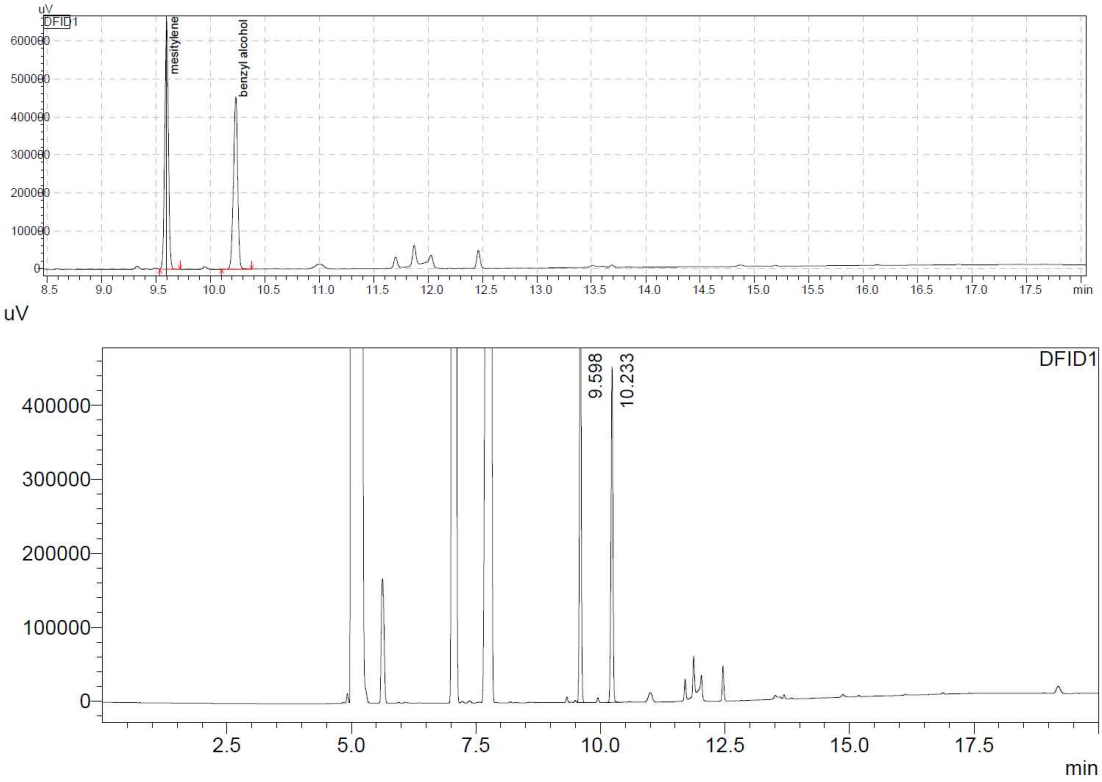

<Peak Table>

DFID1

Peak#	Ret. Time	Area	Height	Conc.	Unit	Mark	Name
1	9.598	1525485	652745	55.634	ppm	V	mesitylene
2	10.233	1216527	452003	44.366	ppm	V	benzyl alcohol
Total		2742012	1104748				

Figure S48. GC chromatograph (Table-4, Entry-3)

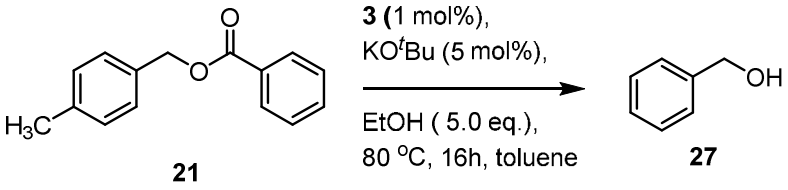

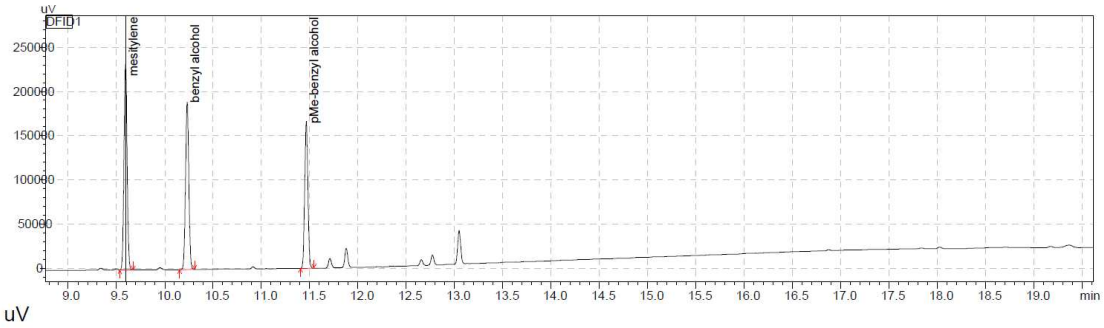

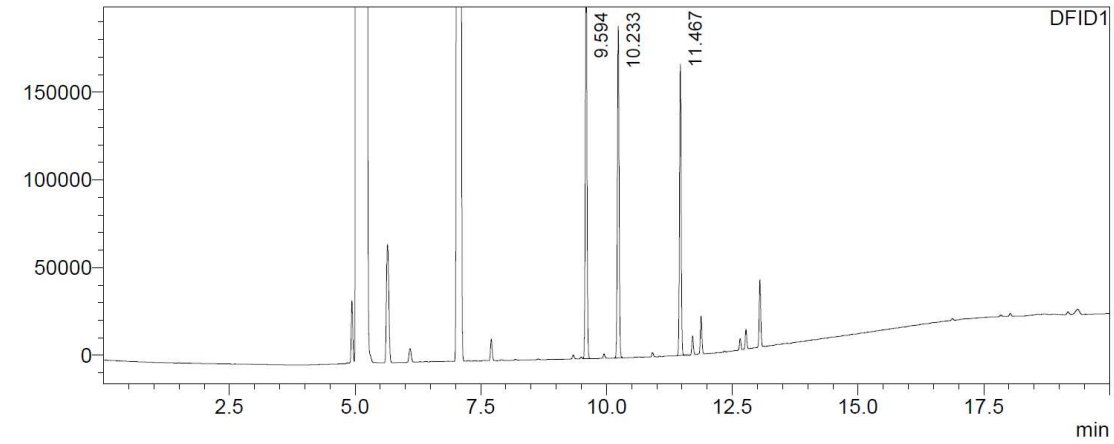

<Peak Table>

DFID1

Peak#	Ret. Time	Area	Height	Conc.	Unit	Mark	Name
1	9.594	524887	231209	38.838	ppm	M	mesitylene
2	10.233	445522	188601	32.966	ppm	M	benzyl alcohol
3	11.467	381065	164034	28.196	ppm	M	pMe-benzyl alcohol
Total		1351473	583844				

Figure S49. GC chromatograph (Table-4, Entry-4)

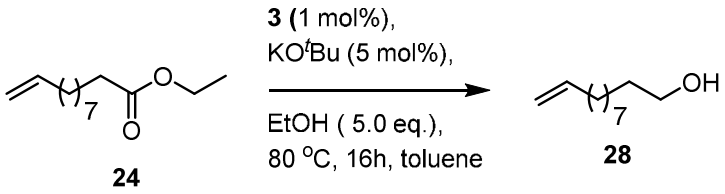

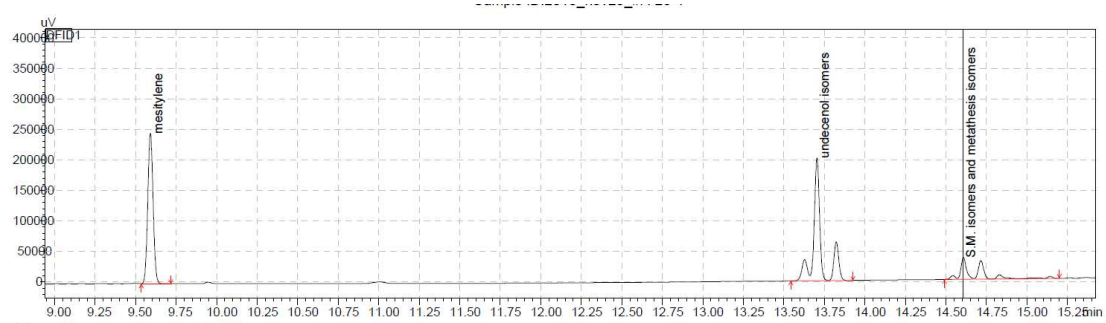

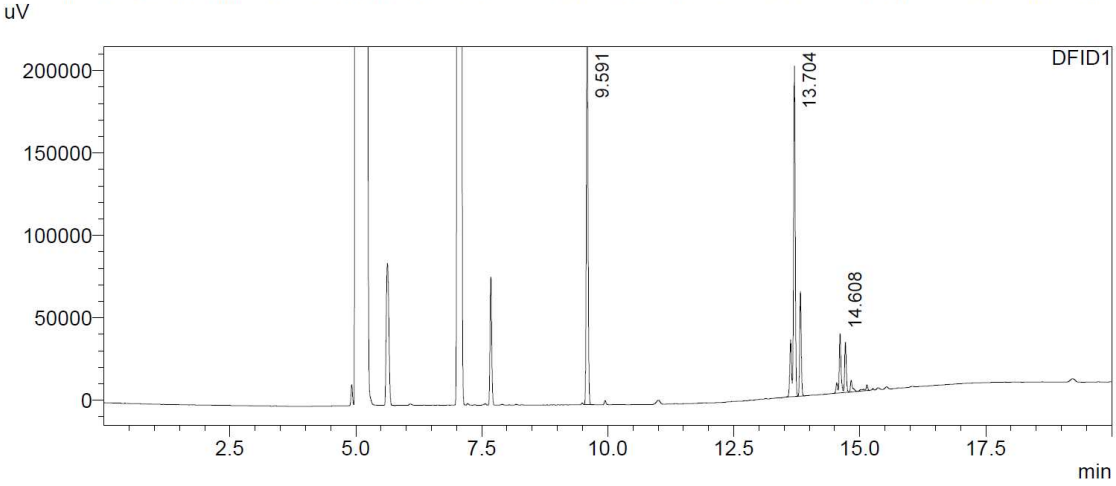

<Peak Table>

DFID1

Peak#	Ret. Time	Area	Height	Conc.	Unit	Mark	Name
1	9.591	561057	241769	0.000	ppm	V	mesitylene
2	13.704	659673	199898	0.000	ppm	M	undecenol isomers
3	14.608	198019	35504	0.000	ppm	M	S.M. isomers and metathesis is
Total		1418749	477172				

Conversion factor used for undecanol was hexanol conversion factor multiplied by 2.

Figure S50. GC chromatograph (Table-4, Entry-5)

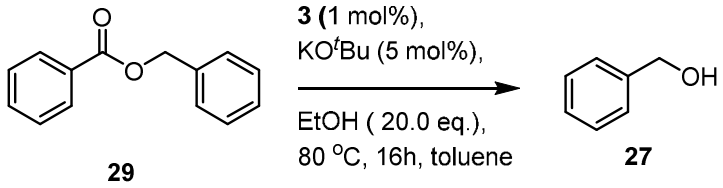

29 **27**

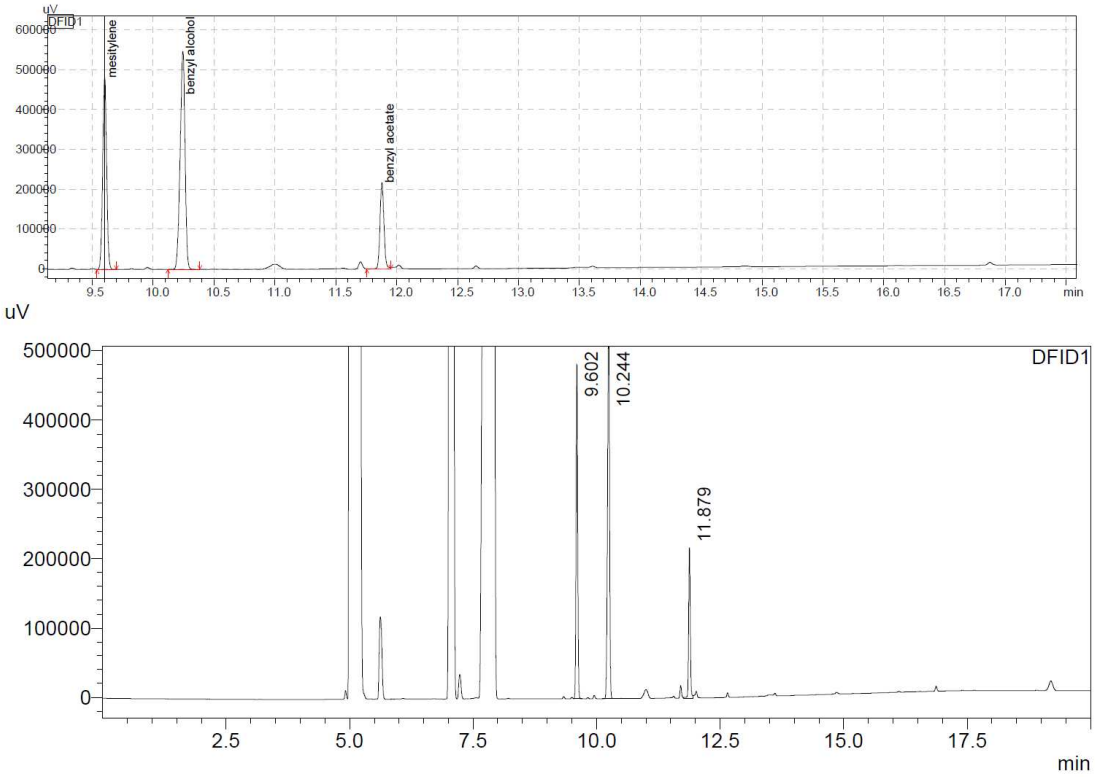

<Peak Table>

DFID1

Peak#	Ret. Time	Area	Height	Conc.	Unit	Mark	Name
1	9.602	1086323	479862	34.890	ppm	V	mesitylene
2	10.244	1530689	543752	49.162	ppm		benzyl alcohol
3	11.879	496534	216292	15.948	ppm	V	benzyl acetate
Total		3113546	1239906				

Conversion factor for benzyl alcohol was determined to be 0.95

Figure S51. GC chromatograph (Table-4, Entry-6)

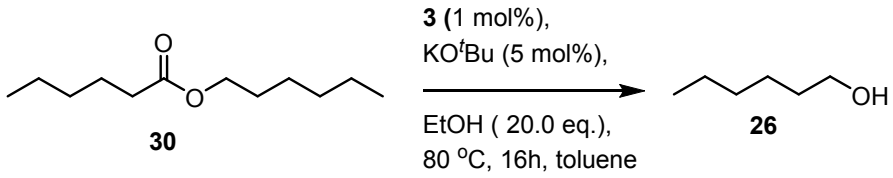

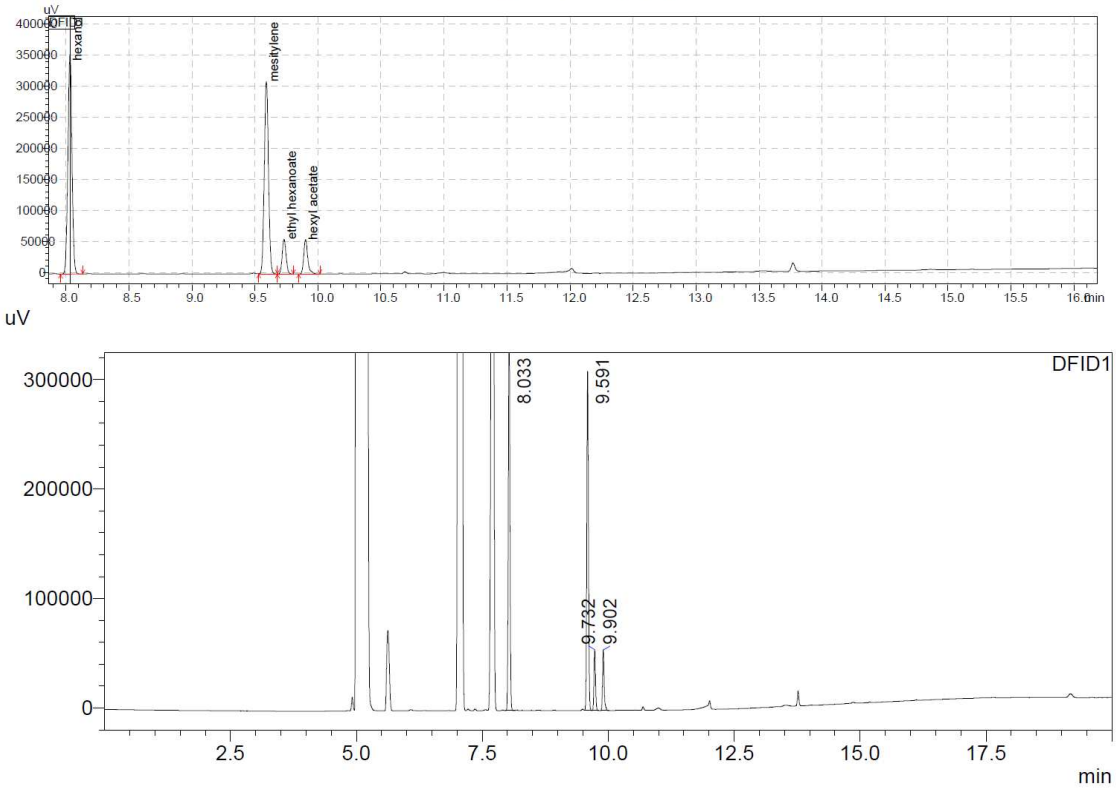

<Peak Table>

DFID1

Peak#	Ret. Time	Area	Height	Conc.	Unit	Mark	Name
1	8.033	796835	350651	45.420	ppm	M	hexanol
2	9.591	713831	305970	40.689	ppm	V	mesitylene
3	9.732	119337	55059	6.802	ppm	V	ethyl hexanoate
4	9.902	124360	55013	7.089	ppm		hexyl acetate
Total		1754363	766694				

Figure S52. GC chromatograph (Table-4, Entry-7)

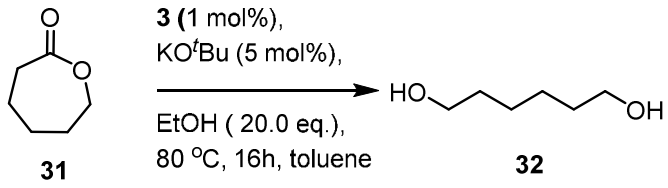

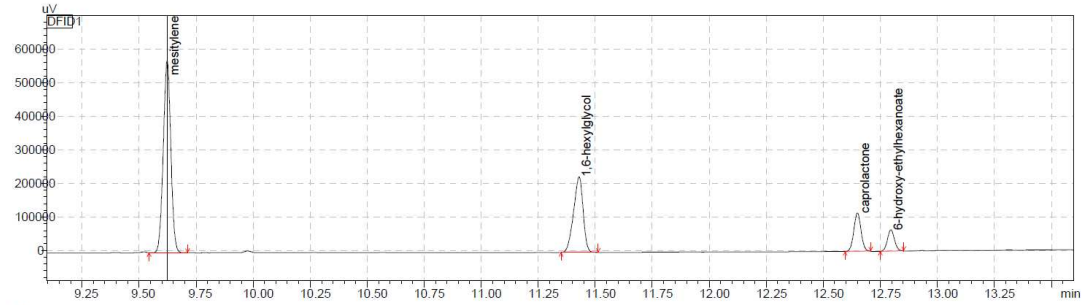

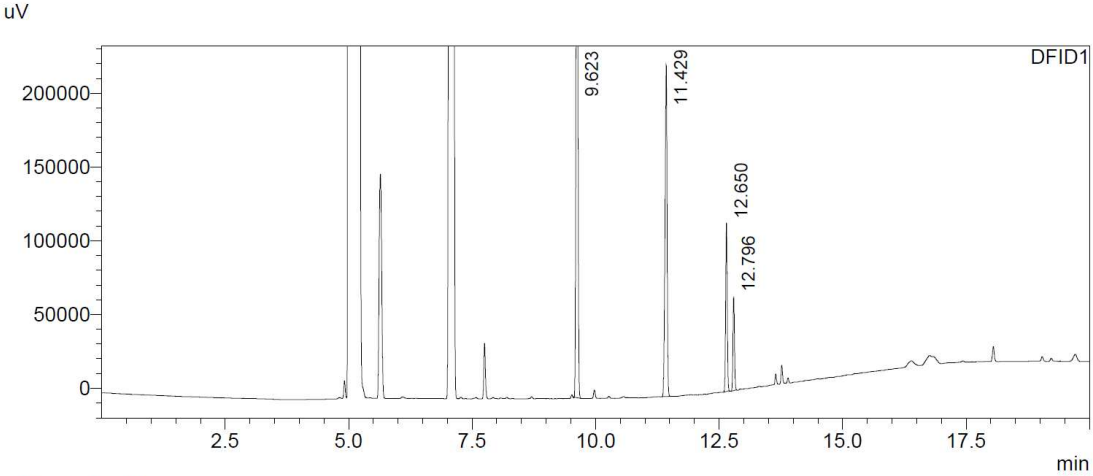

<Peak Table>

DFID1

Peak#	Ret. Time	Area	Height	Conc.	Unit	Mark	Name
1	9.623	1319492	565944	55.987	ppm	M	mesitylene
2	11.429	652136	223238	27.670	ppm	M	1,6-hexylglycol
3	12.650	250350	113473	10.622	ppm	M	caprolactone
4	12.796	134817	62959	5.720	ppm	M	6-hydroxy-ethylhexanoate
Total		2356795	965614				

Conversion factor for product diol **32** was determined to be 0.84.

Figure S53. GC chromatograph (Table-4, Entry-8)

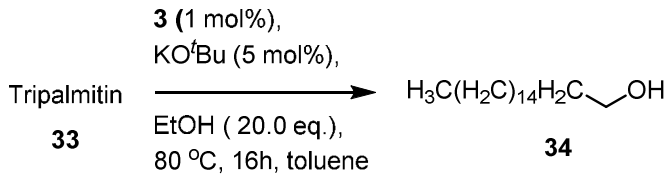

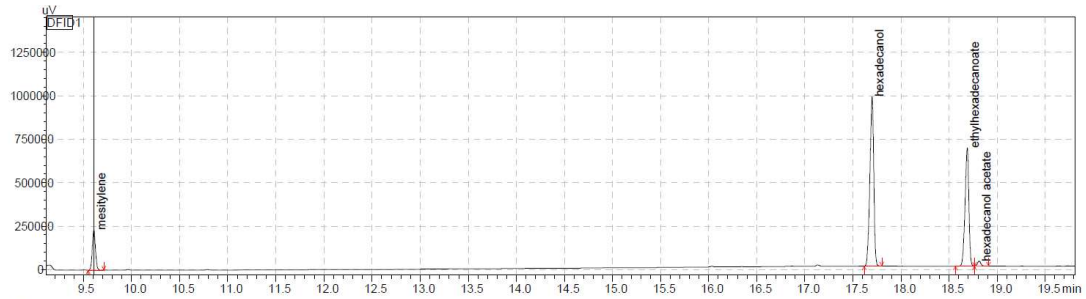

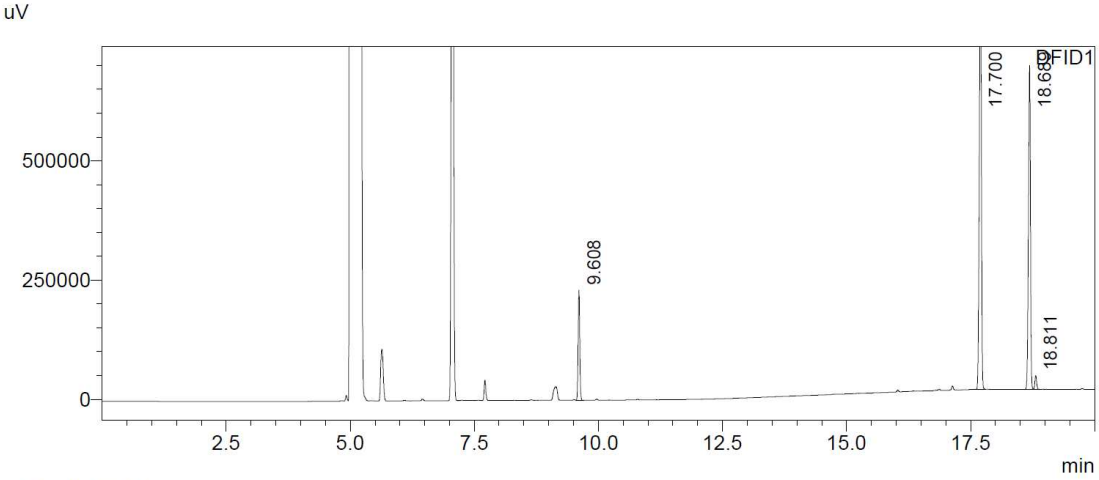

<Peak Table>

DFID1

Peak#	Ret. Time	Area	Height	Conc.	Unit	Mark	Name
1	9.608	526977	228530	10.156	ppm	V	mesitylene
2	17.700	2713436	968840	52.295	ppm	M	hexadecanol
3	18.689	1877327	677722	36.181	ppm		ethylhexadecanoate
4	18.811	70963	28774	1.368	ppm	V	hexadecanol acetate
Total		5188703	1903866				

Yield of hexadecanol divided by conversion factor 3.00 and further divided by 3 (triglyceride).

Figure S54. GC chromatograph (Table-4, Entry-9)

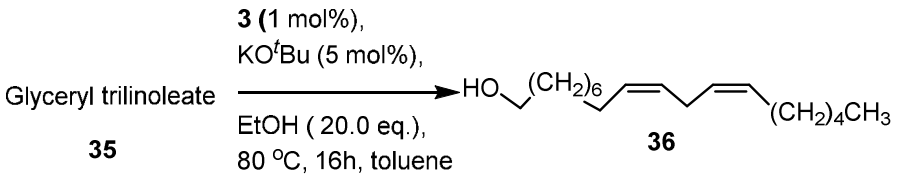

35 **36**

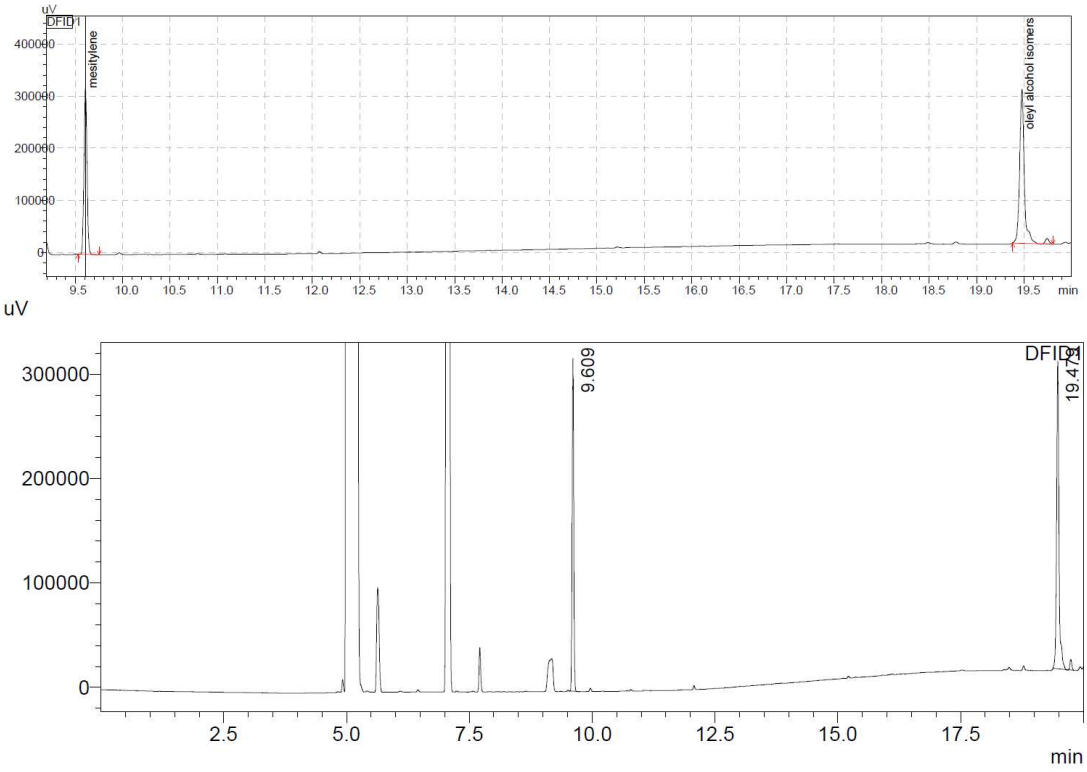

<Peak Table>

DFID1

Peak#	Ret. Time	Area	Height	Conc.	Unit	Mark	Name
1	9.609	719681	316513	41.603	ppm	M	mesitylene
2	19.479	1010198	293786	58.397	ppm	M	oleyl alcohol isomers
Total		1729879	610299				

Hexadecanol conversion factor 3.00 was used, and product was further divided by three (triglyceride)

Figure S55. GC chromatograph (Table-4, Entry-10)

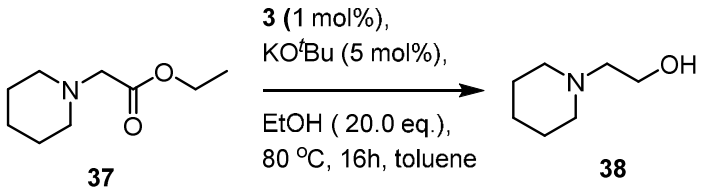

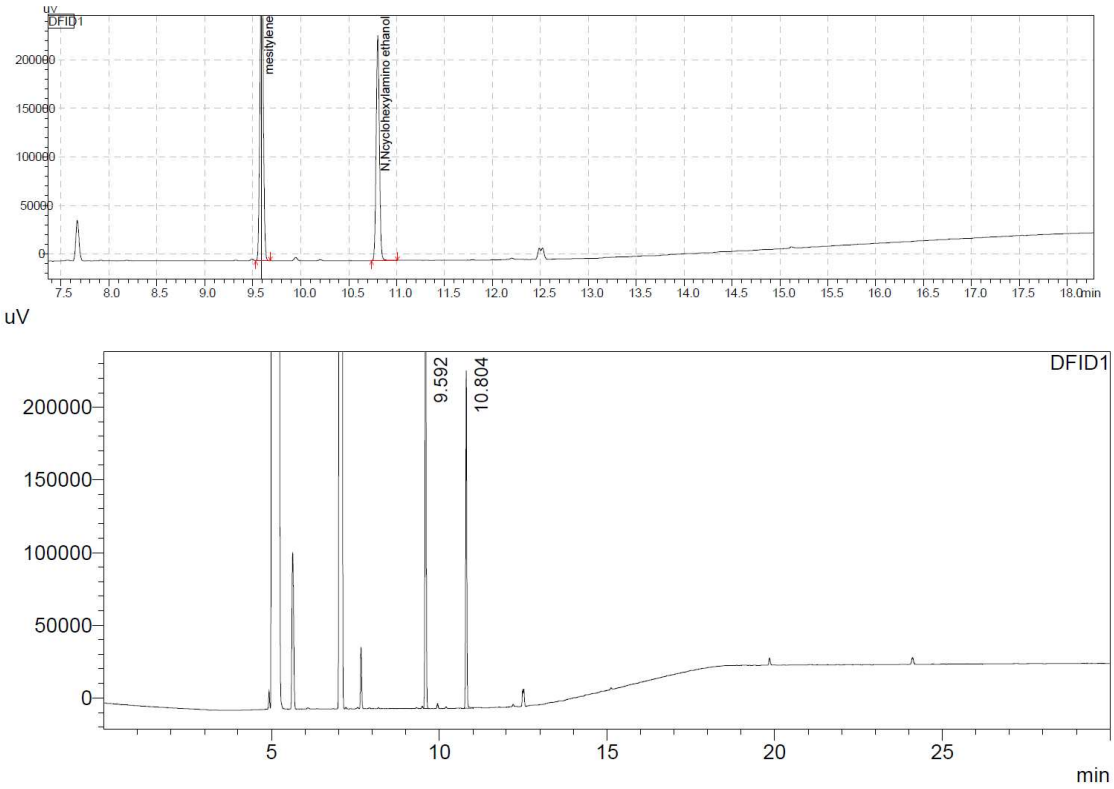

<Peak Table>

DFID1

Peak#	Ret. Time	Area	Height	Conc.	Unit	Mark	Name
1	9.592	807043	348794	59.699	ppm	V	mesitylene
2	10.804	544807	229159	40.301	ppm	V	N,Ncyclohexylamino ethanol
Total		1351850	577953				

Conversion factor used was based on ethyl-3N,N-dimethylamino propionate (0.67). Only trace starting material observed

Figure S56. GC chromatograph (Table-4, Entry-11)

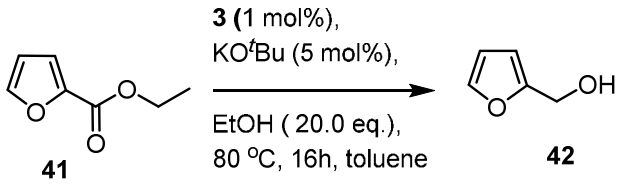

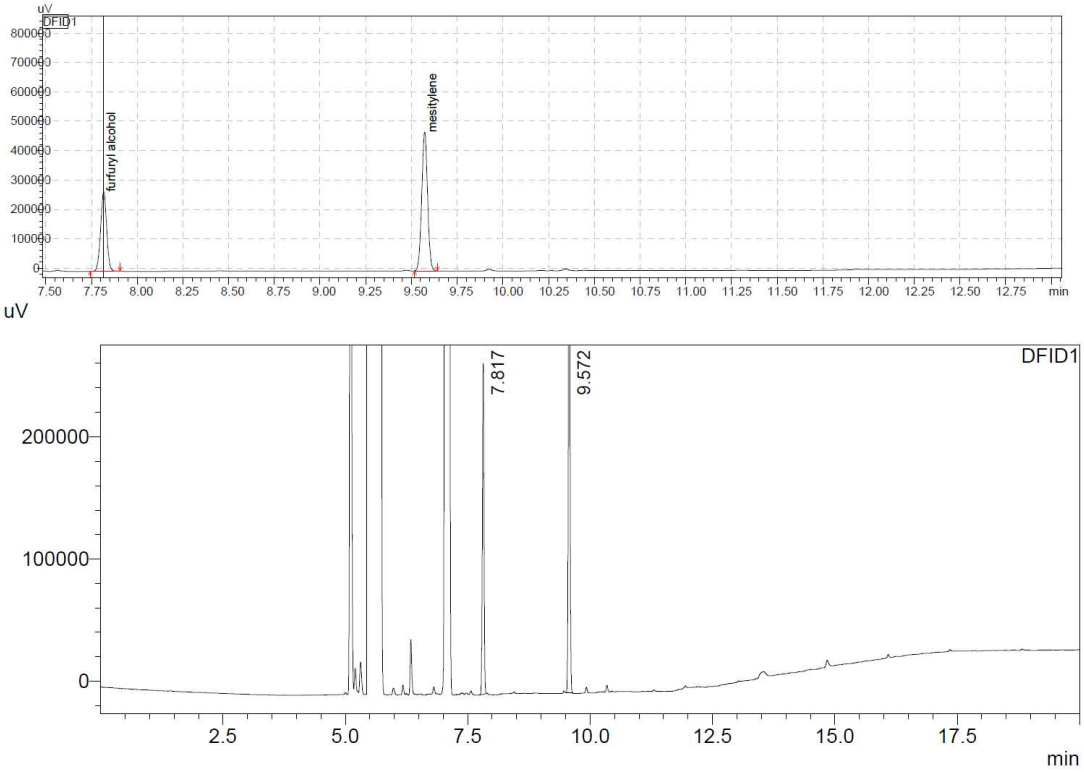

<Peak Table>

DFID1

Peak#	Ret. Time	Area	Height	Conc.	Unit	Mark	Name
1	7.817	618877	267525	36.994	ppm	M	furfuryl alcohol
2	9.572	1054049	464422	63.006	ppm	M	mesitylene
Total		1672925	731946				

Conversion factor for furfuryl alcohol **42** is 0.62; only trace starting material is observed. Runs had to be performed in ethyl acetate as furfuryl alcohol retention time overlaps with acetone (solvent used for all other runs) homocoupling product.

Figure S57. GC chromatograph (Table-4, Entry-14)

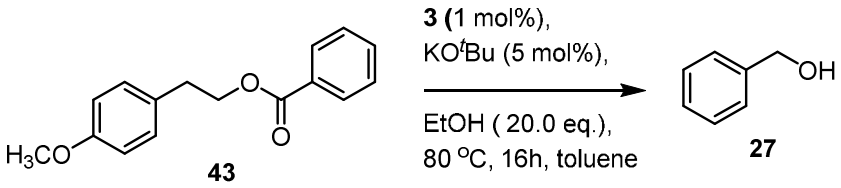

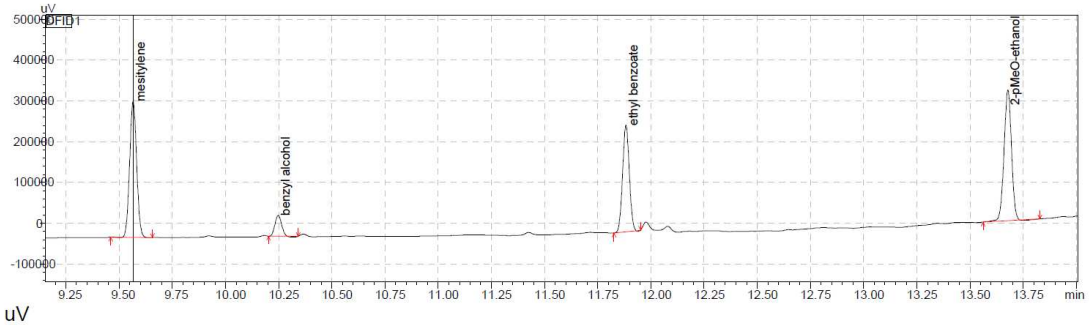

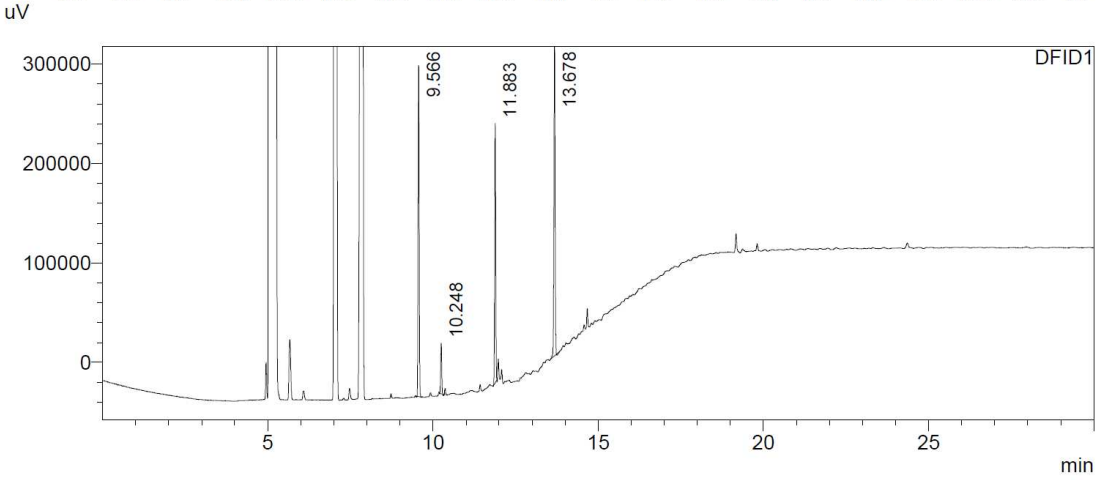

<Peak Table>

DFID1

Peak#	Ret. Time	Area	Height	Conc.	Unit	Mark	Name
1	9.566	761652	332196	34.346	ppm	M	mesitylene
2	10.248	107939	50706	4.867	ppm	M	benzyl alcohol
3	11.883	570914	258021	25.745	ppm	M	ethyl benzoate
4	13.678	777107	317713	35.043	ppm	M	2-pMeO-ethanol
Total		2217611	958636				

Figure S58. GC chromatograph (Table-4, Entry-15)

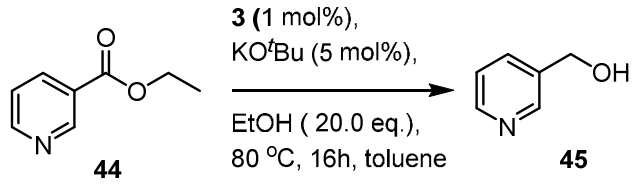

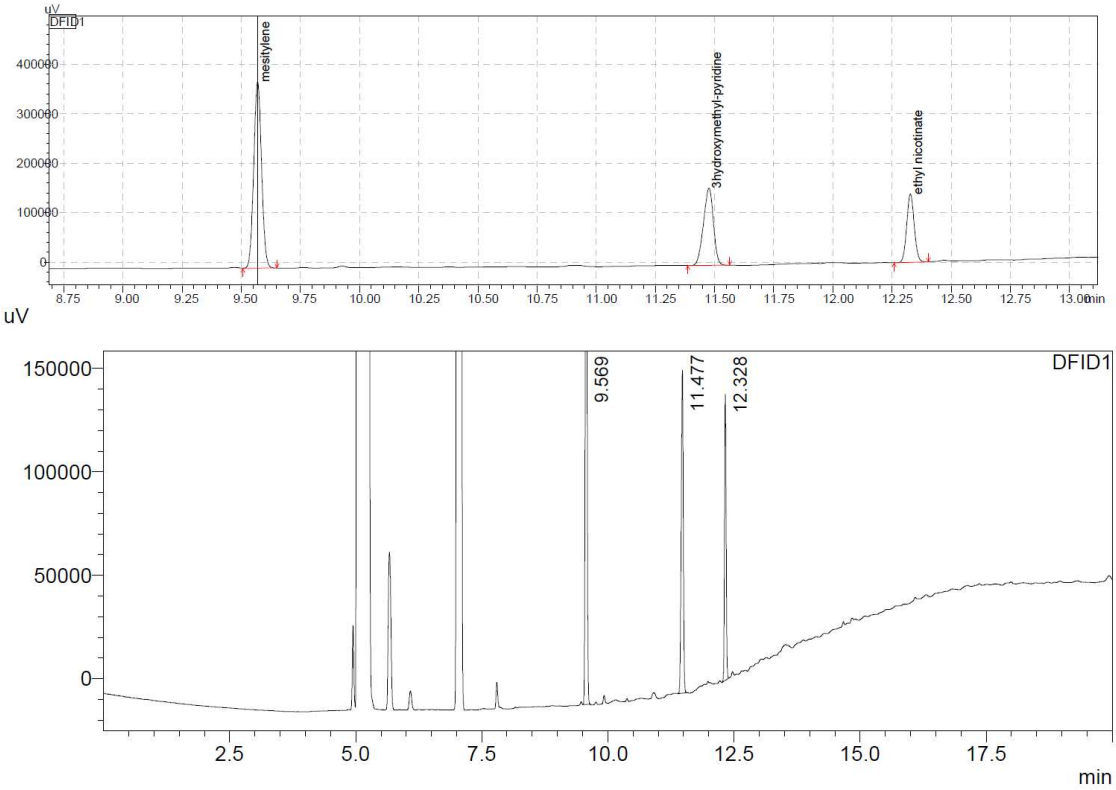

<Peak Table>

DFID1

Peak#	Ret. Time	Area	Height	Conc.	Unit	Mark	Name
1	9.569	866099	375919	53.193	ppm	M	mesitylene
2	11.477	457667	155613	28.108	ppm	M	3hydroxymethyl-pyridine
3	12.328	304461	137579	18.699	ppm	M	ethyl nicotinate
Total		1628227	669110				

Conversion factor for product was determined to be 0.73

Figure S59. GC chromatograph (Table-4, Entry-16)

References

(1) Spasyuk, D.; Smith, S.; Gusev, D. G. *Angew. Chem. Int. Ed.* **2013**, *52*, 2538-2542.
(2) Khaskin, E.; Milstein. D. *ACS Catal.* **2013**, *3*, 448-452.
(3) Ochiai, M.; Yoshimura, A.; Hoque, M.; Okubo, T.; Saito, M.; Miyamoto, K. *Org. Lett.* **2011**, *13*, 5568-5571.
(4) Srimani, D.; Leitus, G.; Ben-David, Y.; Milstein, D. *Angew. Chem. Int. Ed*. **2014**, *53*, 11092-11095.
(5) Khaskin, E.; Milstein, D. *Chem. Comm*. **2015**, *51*, 9002-9005.
(6) Montag, M.; Zhang, J.; Milstein, D. *J. Am. Chem. Soc*. **2012**, *134*, 10325-10328.
(7) Stanton, M. G.; Gagne, M. R. *J. Am. Chem. Soc.* **1997**, *119*, 5075-5076.
(8) Parr R. G.; Yang W. In *Density-functional theory of atoms and molecules*; Oxford University Press: Oxford, **1989**.
(9) Perdew, J. P.; Burke, K.; Ernzerhof, M. *Phys. Rev. Lett.* **1996**, *77*, 3865-3868.
(10) Laikov, D. N. *Chem. Phys. Lett.* **1997**, *281*, 151-156.
(11) Laikov, D. N.; Ustynyuk; Yu. A. *Russ. Chem. Bull.* **2005**, *54*, 820-826.
(12) (a) Stevens, W. J.; Basch, H.; Krauss, M. *J. Chem. Phys.* **1984**, *81*, 6026-6033; (b) Stevens, W. J.; Basch, H.; Krauss, M.; Jaisen, P. *Can. J. Chem.* **1992**, *70*, 612-630; (c) Cundari, T. R.; Stevens, W. J. *J. Chem. Phys.* **1993**, *98*, 5555-5565.